Alma Mater Studiorum

Università degli Studi di Bologna

DOTTORATO DI RICERCA

IN

SCIENZE BIOMEDICHE

Ciclo XXIX

Settore Concorsuale di afferenza: 06/D3

Settore Scientifico disciplinare: MED/15

LEUKEMIC STEM/PROGENITOR CELLS AND THEIR MICROENVIRONMENT: THE ROLE OF CRUCIAL INFLAMMATORY FACTORS AND BONE MARROW-DERIVED MESENSPHERES

Presentata da:

Dott. **DORIAN FORTE**

Coordinatore Dottorato

Prof. **LUCIO ILDEBRANDO COCCO**

Relatore

Prof.ssa **LUCIA CATANI**

Correlatori

Dott. **ANTONIO CURTI**

Prof. **SIMON MENDEZ-FERRER**

Esame finale anno 201

CONTENTS

Introduction **3**

1. A mirror reflect: the hematopoietic stem cells and their microenvironment 4

2. Structure and Properties of the HSC Niche 6

2.1 Osteolineage cells and mesenchymal stem cells 6

2.2 The vascular system 7

2.3 External Innervation of the BM 8

2.4 Hematopoietic cells, immune cells in the hematopoietic stem cell niche 8

3. Modulation of the HSC niche by different stimuli 10

3.1 HSCs and stress-mediated responses 10

3.2 Hematopoietic Responses to Inflammation 10

4. **The Niche for Malignant Hematopoietic Cells** 13

4.1 Chemokines and growth factors 14

4.2 Niche cell population alterations and supports 15

Aims of the thesis **18**

Results Ia **21**

ABSTRACT 23

INTRODUCTION 24

RESULTS 26

DISCUSSION 39

MATERIALS AND METHODS 41

Results Ib **53**

ABSTRACT 55

INTRODUCTION 56

RESULTS 58

MATERIALS AND METHODS 64

Results II **66**
ABSTRACT 68
INTRODUCTION 69
RESULTS 71
DISCUSSION 85
MATERIALS AND METHODS 87

Results III **94**
INTRODUCTION 95
RESULTS 97
DISCUSSION 120
MATERIAL AND METHODS 126

Conclusion **132**
Bibliography **136**

– Introduction

1.
A mirror reflect: the hematopoietic stem cells and their microenvironment

Hematopoietic stem cells (HSCs) constitute a small population in the bone marrow (BM). They have two unique and peculiar properties: self-renewing capacity and multi-lineage differentiation capacity. Specifically, self-renewal of HSCs represents its ability to generate themselves, while differentiation capacity means the ability to produce all blood cells (red blood cells, platelets, myeloid lineage cells, as well as lymphoid lineage cells).[1]

Most adult HSCs are quiescent and their turnover is slowly, on a monthly time scale. However, highly proliferative downstream hematopoietic progenitor cells (HPCs) provide a daily hematopoietic production. All cellular behaviors of HSCs and their fate are tightly regulated in turn by both cell-intrinsic factors and cell-extrinsic factors.[2] Intrinsic mechanisms are related to cellular metabolism and transcriptional regulatory network factors (such as epigenetic machineries, Polycomb group proteins, Hox genes, DNA damage response and transcription factors).[3] Extrinsic mechanisms are dictated by niche such as cytokines, chemokines, growth factors, metabolites, and exogenous pathogen-derived molecules. Beyond the intrinsic and extrinsic factors, BM niche modulates HSPC activation and retention.

This cross-talks involve different populations and mechanisms that confirm the supportive roles of BM niche on HSPCs (**Figure A**). Among them, for example, BM stromal cells and macrophages support hematopoiesis by production of hematopoietic cytokines, such as thrombopoietin (TPO), stem cell factor (c-Kit ligand), and granulocyte-colony stimulating factor.[4] In addition, vascular endothelial growth factor (VEGF) signaling is important to assist HSC regeneration and the vasculature preservation is mediated by endothelial cells through the Tie2/angiopoietin-1 axis and angiopoietin-like proteins. Of note, the retention of HSPC in the niche is mediated via integrins and C–X–C chemokine receptor type 4 (CXCR4)/stromal-derived-factor-1 (SDF-1).[5]

Among all the regulatory factors, reactive oxygen species (ROS) are another essential and crucial aspects for HSPC activation and regulation. ROS are not just byproduct of oxidative stress but press HSPC to enter cell cycle for proliferation and differentiation.[6]

Therefore, the stability and architecture of BM niche could substantially modulate the fate of HSPC. Importantly, it could be attractive to understand how the BM niche fosters tumor growth and progression. It is therefore necessary to highlight where HSCs reside in order to hit them.

In line of this, targeting microenvironmental properties could be more likely to succeed therapeutically in overcoming common mechanisms of drug resistance. A specialized architecture of BM exists, where the majority of HSCs resides and interacts with an orchestra of different cells. Two types of niche exist in the BM and confirmed by several studies: endosteal niche and vascular/peri-sinusoidal niche.[7]

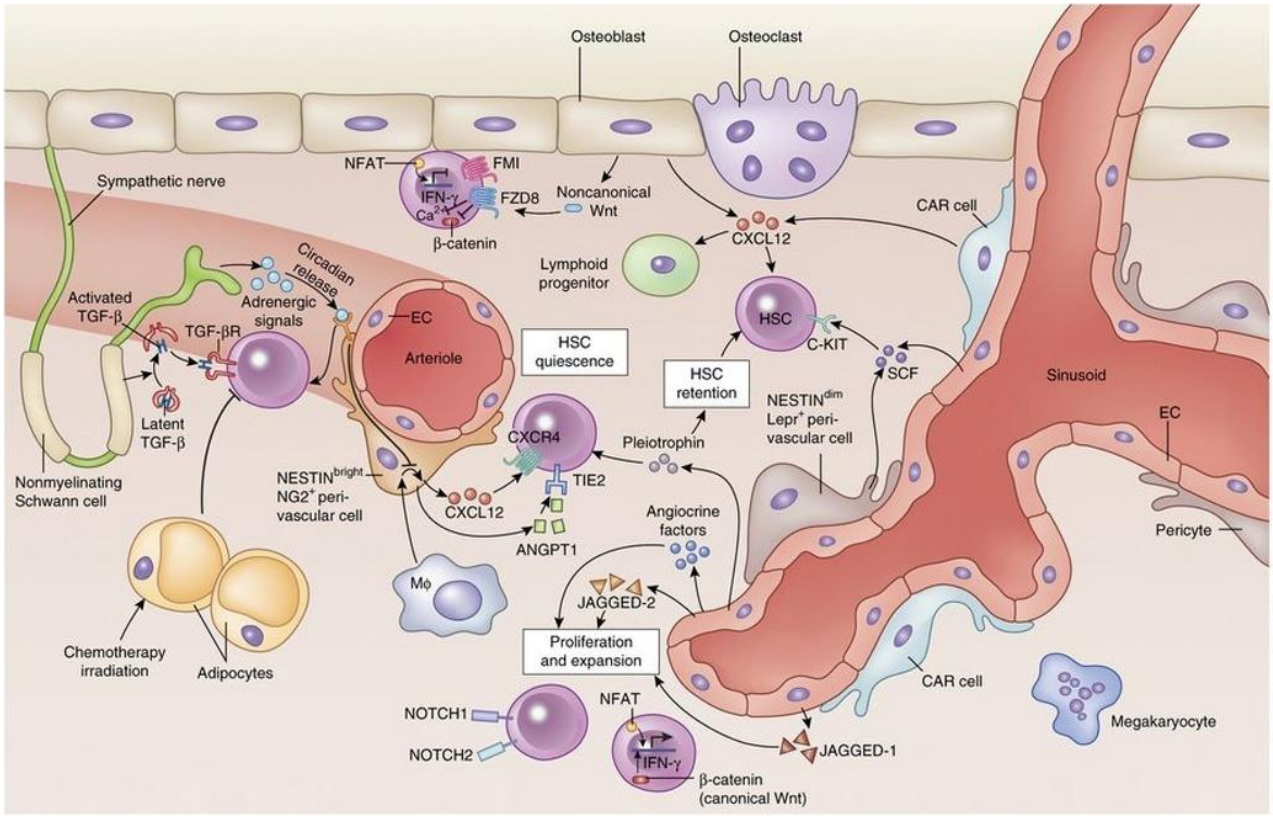

Figure A. The BM HSC niche in homeostasis *The cellular composition of the hematopoietic microenvironment. The bone marrow 'stroma' can initiate and maintain hematopoiesis.CXCL12 and SCF secreted by perivascular, endothelial, Schwann, and sympathetic neuronal cell, promoting the maintenance of HSCs. Dormant HSCs are found around arterioles, activated HSCs are located near sinusoidal niches. Macrophages or megakaryocytes can feed back to the niche to influence HSC migration or proliferation.*[8,9]

2.
Structure and Properties of the HSC Niche

2.1 Osteolineage cells and mesenchymal stem cells

Haematopoiesis is supported in all bones in mice, and on the contrary, is located within the axial skeleton in adult humans. In particular, the soft tissue of bone contains HSCs and is distributed throughout trabeculae that interconnecting bone rods or plates.[10] This provides a structural foundation for soft tissue, and the opposing actions of osteoblasts and osteoclasts shape it, regulating dynamically the bone matrix. Endosteum covers trabeculae that consists of osteoblasts, osteoprogenitor cells, and osteoclasts.[10] This is the "endosteal niche" that is created by mainly these osteolineage cells, located proximal to the endosteal.[11,12] The continuous remodeling of the bones and bone homeostasis involves a tiny balance between bone-forming osteoblasts (OBs) derived from multipotent mesenchymal stem cells (MSCs) and osteoclasts (OCs) that regulate bone resorption.[13] OBs have been proposed to regulate HSC maintenance in the endosteal niche, regulating its size and HSCs number.[10] Various soluble factors and cell adhesion molecules have been described to mediate HSCs and OBs interactions within their endosteal niche.[14] In mice, HSC expansion is permitted by increasing OB number with parathyroid hormone (PTH), involving Notch activation.[15] Moreover, bone morphogenetic protein (BMP) signaling increases the number of N-cadherin^{+} CD45^{-} osteoblastic cells with a subsequent correlation with an increased number of HSCs.[16] However, OBs could also negatively influence HSCs proliferation and induce a quiescent status. This is mediated by the interactions between Angiopoietin-1 (Ang-1) produced by OBs and its receptor, the Tie2 tyrosine kinase, expressed by HSCs.[7] However, *S. J. Morrison et al.*[17] reports that OBs are not able to directly support HSCs.

Mesenchymal stem cells (MSCs) are defined by their capacity to differentiate into osteoblastic, adipocytic, and chondrocytic lineages and osteolineage cells could develop from MSCs. These stromal cells are a key component of the BM microenvironment that regulates crucial niche functions. MSCs can be identified in mice through Nestin (Nes) promoter-driven GFP expression.[18] There are many relationship between Nes expression and MSCs and Nes is considered as a selective marker for BM-derived MSCs.[19] Previously described as a neural stem cells (NSCs) marker, Nes is an intermediate filament protein that appeared during development of the central nervous system (CNS). When Nes^{+} cells differentiate into neurons or glial cells its expression is downregulated.[20] Nes-expressing cells regulate long-term repopulating HSCs, linking MSCs to the endosteum and

HSC maintenance. Nes-expressing cells are distributed around vascular structures, associated with nerve fibers, or adjacent to bone. Due to their localization, MSCs can contribute to both endosteal and vascular niches.

2.2 The vascular system

The relationship with HSCs and blood vessels in the BM is determined by location, structure, and function. Some Long-term HSCs (LT-HSC) are associated with arterioles and the rapid access of HSCs to the bloodstream is provided by venous sinusoids.[10] Arterial vessels branch into smaller arterioles located near the endosteum and surrounded by layers of smooth muscle, pericytes, and non-myelinating Schwann cells. This vascular niche has been associated with quiescent HSCs.[21] However, sinusoidal blood vessels can promote presumably proliferation, differentiation, and mobilization of HSCs and this is provided by a more nutrient-rich microenvironment with higher concentrations of oxygen and growth factors.[22,23]

Endothelial cells support and regulate HSC activity through particular factors named angiocrine factors. One of most important function is provided by Notch signaling, because endothelial cells express the Notch ligands Jagged-1, Jagged-2, and Delta-like (DLL) -1 and -4, promoting in vitro self-renewal of LT-HSCs and in vivo reconstitution of the LT-HSC pool after myeloablation. Moreover, the increasing of endothelial and perivascular cell numbers promotes arterial formation by the Notch pathway.

In parallel to studies on Nes^{+} cells, several works have focused on the previously identified population of CXCL12-abundant reticular (CAR) cells. These CAR cells are adventitial reticular cells widely spread throughout the bone marrow and the loss of CAR cells coincides with a strong reduction in LT-HSC number in a mouse model.[24] In addition, LT-HSCs in CAR cell-depleted mice are smaller and more quiescent. Moreover short-term ablation of CAR cells *in vivo* severely impaired the adipogenic and osteogenic differentiation potential of BM cells, suggesting CAR cells contain adipo-osteogenic bipotential progenitors.[25] The HSCs have direct contact with CAR, which secrete higher levels of CXCL12 than OBs.[24]

In addition, the endosteal-vascular niche provides a hypoxic microenvironment that promotes quiescence of stem cells.[26] At low oxygen tensions, cells responds with an activate adaptive transcriptional program mediated by the hypoxia-inducible factor-1α (HIF-1α). HSC differentiation and cell cycle quiescence is regulated by hypoxic microenvironment.[27] Recently, works

demonstrate that to maintain hypoxia in the HSC niche is required by the integrity of blood vessels and the presence of densely-populated cells. Capillaries branching from arterioles fed sinusoids and are located around a central sinus that drains blood out of the bone marrow. Fenestrated sinusoids permit HSC and leukocyte mobilization[26] and direct contact with the HSC niche is necessary for LT-HSC maintenance. So that, long periods of mobilization is able to reduce the stemness potential of HSCs, promoting differentiation into mature cells.[28]

2.3 External Innervation of the BM

Myelinated and non-myelinated nerve fibers are found in the BM.[29] The stem cell niche and the migration of hematopoietic cells are regulated by the autonomic nervous system (ANS); HSC mobilization is influenced by the sympathetic nervous system (SNS).[30] This behaviour is direct dependent by rhythmic secretion of noradrenaline modulated by circadian oscillations of HSC numbers in peripheral blood. Notably, noradrenaline decreases CXCL12 expression, an essential chemokine for HSC localization to the niche in BM stromal cells. CXCR4-expressing HSCs egress from the niche after decreasing CXCL12 levels. Non-myelinating Schwann cells have also been oserved to localize close to HSCs and maintain HSC quiescence by activating transforming growth factor-β (TGF-β)-SMAD signaling.[29]

The nervous system regulation on HSC niche is dictated by circadian rhythmic and modulate HSC mobilization and quiescence.

2.4 Hematopoietic cells, immune cells in the hematopoietic stem cell niche

The migration of HSCs provides a tool for BM microenvironment to communicate on a systemic level. 1-5 % of the pool of HSCs enters the circulation and this generates a vacant niche spaces to accept HSCs to home back to the BM. Many studies showed the presence of HSCs in spleen, lung, liver and kidney, as proof of HSCs behaviour to enter in circulation and migrate through peripheral tissue.[31]

Neutrophils constitute the highly migratory myeloid cells and sensitive to tissue damage and infection or inflammation.[32] Also the release of neutrophils is modulated by BM niche, similar to

HSCs, according to circadian rhythm. In particular aged neutrophils express low levels of CD62 L and high levels of CXCR4, increasing homing to BM.

Interestingly, the $CD169^+$ macrophages in the BM engulf dying neutrophils. These $CD169^+$ macrophages with neutrophil engulfed inhibit CXCL12 production by niche stromal cells, with a subsequent realease of HSCs from the niche. On the contrary, the retention of HSCs is promoted by increasing CXCL12 production from Nes^+ MSCs. $CD169^+$ macrophages promote HSC retention by increasing CXCL12 production from Nes^+ MSCs. HSCs mobilization is linked to the circadian rhythm of neutrophil migration and the regulation of niche, modulated by the depletion of $CD169^+$ macropohages that reduce the ability of BM stromal cells to produce CXCL12.[33]

Infection or different stimuli entail cytotoxic $CD8^+$ T cells homing to the BM with a stimulation of MSC-mediated myelopoiesis.[34] CTLs secrete IFN-γ and MSCs, in turn, produce IL6 that promote myelopoiesis. This responce of CTLs in a peripheral organ can indirectly stimulate innate immune protection within the BM.[28]

3. Modulation of the HSC niche by different stimuli

3.1 HSCs and stress-mediated responses

HSCs sense their microenvironment and may be impaired by diverse sources of stress: including oxidation, radiation, hypoxia, chemotherapy and inflammation, hampering homeostasis and hindering regeneration.[35] Specifically, ionizing radiation and chemotherapy, used to treat hematopoietic malignancies and leukemia, lead to BM injury and alteration in cell composition.[8] The dynamics of BM cell production, maturation, trafficking and lifespan are all compromised by radiation and chemotherapy. HSCs reactions result in increasing apoptosis in a dose- and time-dependent manner, which can be attenuated by different mechanisms, such as VEGF-induced expression of myeloid cell leukemia-1 (MCL1) in hematopoietic progenitor cells.[36]

Importantly, the ability of hematopoietic tissues to maintain redox status is crucial to maintaining normal hematopoiesis. Indeed, an overabundance of cellular ROS emerges into oxidative stress. This derives by the partial reduction of oxygen or a defect in the antioxidant protection mechanisms. Free radicals and ROS produced by high doses of radiation alter HSC repopulating ability and damage the BM vasculature.[37] ROS can activate DNA damage response pathways (e.g. mediated by p53, ATM, 53BP1 (TP53BP1), CHK2 and FOXO3a), promoting loss of stem cell functionand senescence.[38] Accordingly, therapeutic approaches aimed at reducing excessive ROS accumulation may also provide a recovery after stress induced.

3.2 Hematopoietic Responses to Inflammation

'Wounds that do not heal': this is the inflammation. Infection and tissue injury/damage could explode in an inflammatory response that is defined as a protective immune response.[1] Endogenous and exogenous factors can induce local or systemic inflammation. Inflammatory cytokines appear to stimulate HSCs to proliferate in the short-term; however, little is known about HSC identification becomes substantially more complex in the contest of inflammatory signaling. IFNs and TNF-α induce the expression of the canonical stem cell marker Sca-1 in hematopoietic cells. In addition, when HSCs are stimulated to proliferate after 5-fluorouracil treatment, the c-Kit marker is downregulated and Mac-1, one of the lineage markers, is upregulated.[39] HSPCs can themselves home to sites of inflammatory microenvironment and this provides a direct contribute to inflammatory processes. In particular, HSPC express Toll-like receptors (TLRs), which are

important for the recognition of microbial moieties by innate immune cells.[40] HSPCs home to various inflammatory non-hematopoietic sites or ectopic sites and are capable to rapidly produce cells that are essential for the immune response. After migration, HSPCs can differentiate in situ and also colonize extramedullary hematopoietic sites, such as spleen and liver, to rapidly produce effector innate immune cells.[24] To survive in a toxic environment of inflamed tissues, evidences suggest the phagocytic activity of macrophages increases in the presence of pro-inflammatory molecules, and this response would be beneficial to clear offending pathogens during infection.

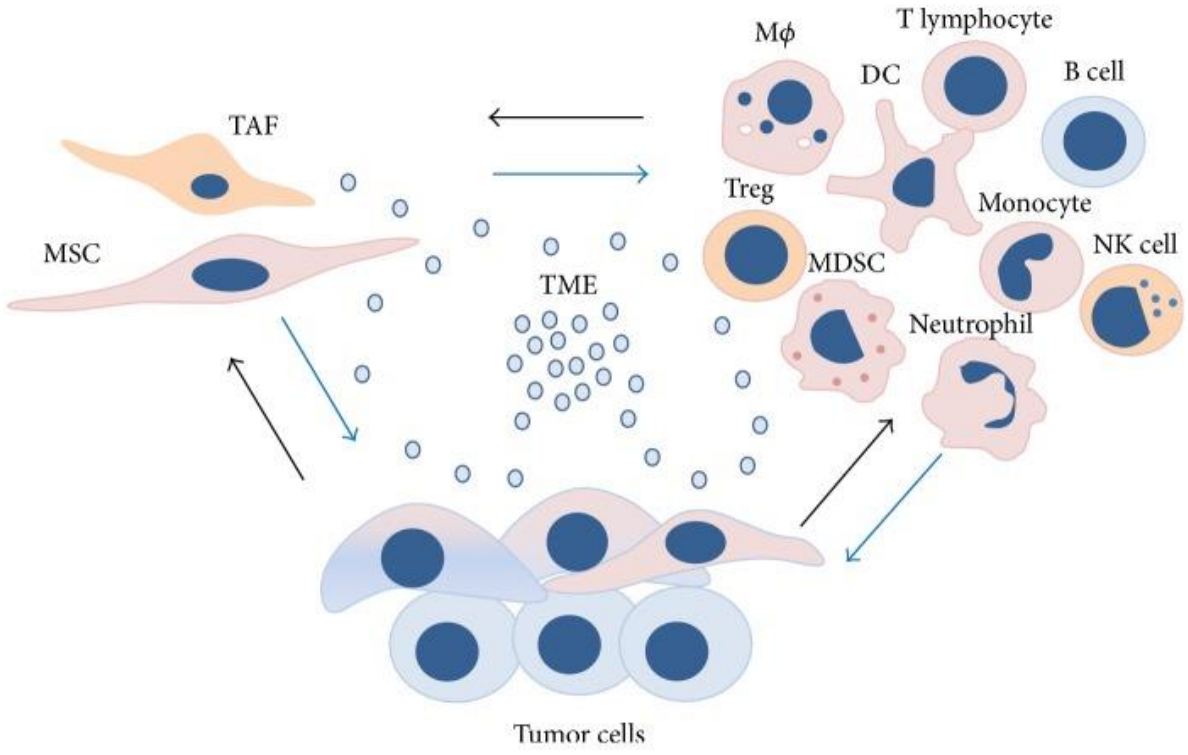

Figure B. Tumor microenvironment (TME) as a fertile soil for dynamic cell phenotype and function.
Composition of TME includes mesenchymal stromal/stem cells (MSCs), tumor-associated fibroblasts (TAFs); immune cells: macrophages (MΦ), regulatory T cells (Treg), myeloid-derived suppressor cells (MDSCs), natural killer (NK) cells, dendritic cells (DCs), monocytes, neutrophils, T lymphocytes, B cells, and heterogenic population of tumor cells. Reciprocal cross-talk within cellular compartment and complex network.[44]

In addition, MSCs could adopt tumor-inhibiting phenotypes by means the activation of various surface receptors.[41] MSCs help tumor cells in maintenance of permissive tumor microenvironment and suppression of antitumor immune response. They act as "ambulatory cells" home sites of inflammation, manifesting immunosuppressive properties, and differentiating into various cell types.[42] MSCs are involved in different step of tumor development, such as evasion of immune

surveillance, promotion of tumor angiogenesis, resistance to chemotherapeutics, invasion and metastasis.[43] Surprisingly, it was demonstrated that tumor-associated inflammation has been converted by tumor cells to their advantage as normal response to injury and infection. The activity of stromal cells in tumors appears to be subordinated by tumor microenvironment (TME) influences.[44]

One mechanism is due to the suppression of the immune response with a MSCs-mediated direct or paracrine communication with immune cells (**Figure B**).[45] For this reason, BM MSCs have been tested into the clinical settings. Consistent with macrophages differentiation, it has been proposed the existence of two functional phenotypes of MSCs, M1 (proinflammatory) and M2 (anti-inflammatory).[46] TNF-α, interferon (IFN)-γ, IL-6, IL-1, and TGF-β, as pro-inflammatory cytokines, can regulate immune activities of MSCs. Also, the activation of NF-κB by MSCs alters the macrophages polarization toward M1 or M2 phenotype.[47] Thus, it seems that MSCs can behave like immune cells, responding to inflammatory stimuli of microenvironment and modifying their secretory and activity profile toward immunosuppression.

4.
The Niche for Malignant Hematopoietic Cells

Myeloid malignancies define clonal diseases of hematopoietic stem or progenitor cells with an alteration of proliferation, abnormal self-renewal and/or differentiation defects. Different genetic and epigenetic causes changes in HSCs and these functional changes in BM niche cells includes myeloid malignancies such as myeloproliferative neoplasms (MPN), myelodysplastic syndrome (MDS) and acute myeloid leukaemia (AML).[48]

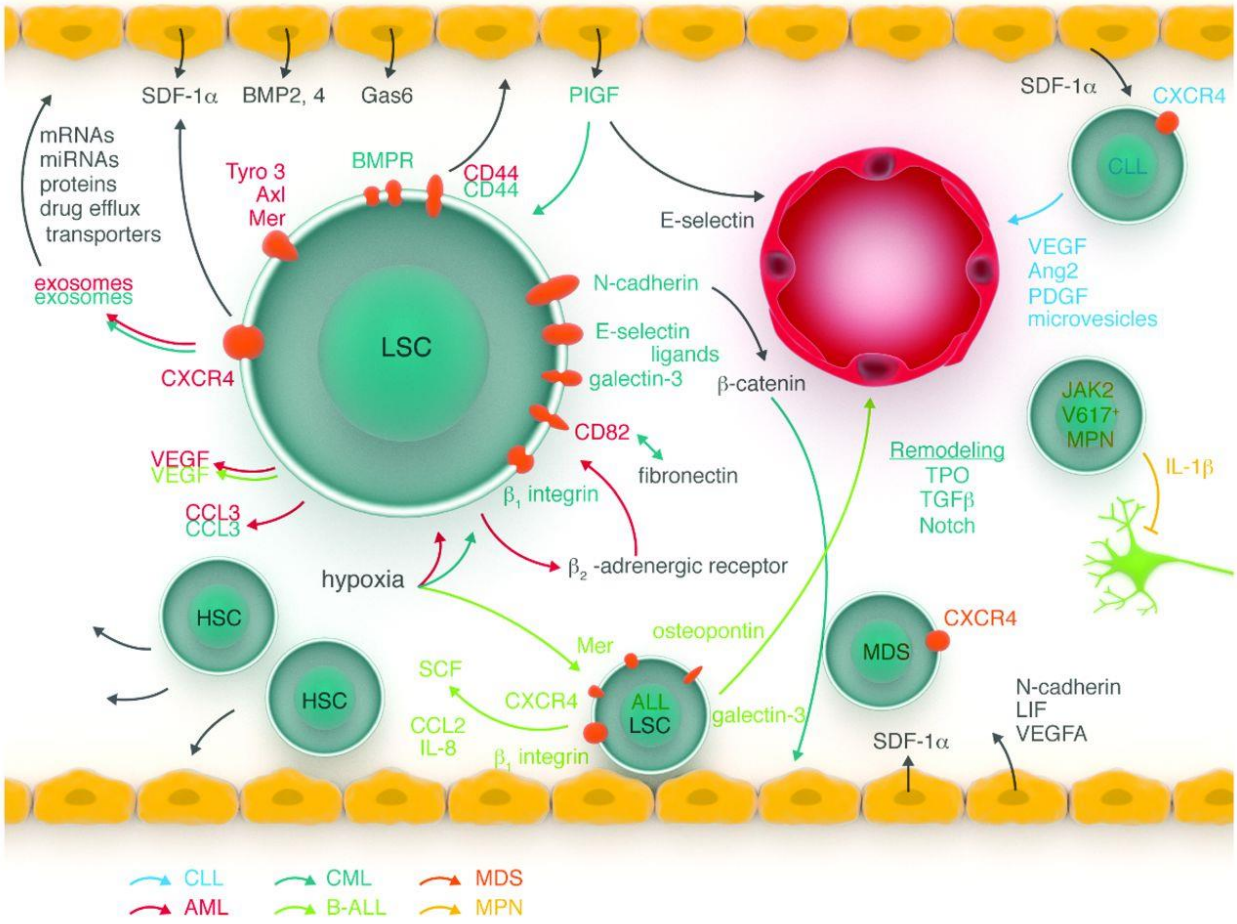

Figure C.The leukemic stem-like cell (LSC) niche in the bone marrow (BM). *Specific pathways of LSCs in acute myeloid leukemia (AML; red), chronic myelogenous leukemia (CML; dark blue), B-cell acute lymphoblastic leukemia (B-ALL; green), chronic lymphocytic leukemia (CLL; pale blue), myelodysplastic syndrome (MDS; orange) and JAK2 V617F positive myeloproliferative neoplasia (MPN; yellow) microenvironment-mediated. SDF-1α: stromal-derived factor 1α; BMP: bone morphogenetic protein; BMPR: bone morphogenetic protein receptor; Gas6: growth-arrest-specific-gene 6; VEGF (A): vascular endothelial growth factor (A); SCF: stem cell factor; IL-8: interleukin-8; PlGF: placental growth factor; TPO: thrombopoietin; LIF: leukemia-inhibitory factor; PDGF: platelet-derived growth factor; Ang2: angiopoietin2; TGFβ: transforming growth factor β.*[49]

Driver mutations in MPN patients involve *JAK2*, *Calreticulin* and *MPL* genes.[50] Irrespective of mutations, all patients show constutive activation of the JAK-STAT pathway.Specifically, *JAK2* mutation results in constitutive kinase activity and uncontrolled cell expansion. Moreover, both MPN patients and mice expressing the human $JAK2^{V617F}$ mutation in the HSCs showed a reduction of both sympathetic nerve fibers and Nes-GFP^{+} MSCs in the BM.[51] Concomitantly, *in vivo* MPN progression is accelerated by depletion of Nes^{+} cells, whereas administration of neuroprotective or sympathico-mimetic drugsreduces the myelofibrosis associated with this disease. This supports the idea that mutated HSCs have the potential to damage their own niche in MPN and initiate disease.

BM mesenchymal stromal cells (BMSCs) could be altered by genetic and epigenetic modifications.[52] A coordinated signaling network regulates the BM microenvironment and supports HSCs (**Figure C**). Likely, multiple different cell populations alter number, location, proliferation, self-renewal, and differentiation of the LSC.[53] Thus, an alteration in the microenvironment can serve as the initiating event in hematologic neoplasia.[49] BM includes HSCs, stromal cells, vascular cells, osteolineage cells, neuronal cells and the extracellular matrix in which these cells reside. HSCs lose quiescence and their stemness whether they cannot home to the niche.[9] HSCs, as source of all hematopoietic lineages, are tightly linked to the HSC niche. Importantly, the niche dynamically determines the balance of stem cells quiescence, renewal, differentiation and mobilization or homing.[54] We can hypothesize the presence of a bi-directional mirror effect where a change in stem cell activity reflects a change in the microenvironment.
Determining how a tumor influences the regulatory HSC niche could help to minimize tumor-associated immune suppression, thereby enhancing anti-tumor immune therapies.

4.1 Chemokines and growth factors

One of most crucial factor in HSC niche is CXCL12 and its interactions. In AML it has been shown CXCL12 deficiencies in HSC niche.[10] Changes in Nes^{+} $CD51^{+}$ $PDGFR\alpha^{+}$ mesenchymal stem and progenitor cells (MSPCs) induced by a MLL-AF9 AML model reveal a downregulation in the expression of HSC genes, linked to retention and maintenance (such as CXCL12, SCF, Vcam1, and Angpt1). As consequence, the frequency of LT-HSCs decreased and HSCs were mobilized from the BM to the periphery.[55] Further study shows a decreased level of CXCL12 in BM plasma of AML patientsor in the culture supernatants of AML MSC, associated to an elevated intracellular CXCL12 concentration.[56]

Pro-angiogenic factors such as bFGF and HGF are upregulated in AML, chronic myeloid leukemia (CML), and Myelodysplastic syndrome (MDS). Similarly, TNF-α, IL-6, and IL-1β are increased when AML blasts are co-cultured with ECs.[48] Thereby, leukemic cell expansion is promoted by these cytokines that, in turn, stimulate EC proliferation and G-CSF and GM-CSF production.[57] Moreover, secretion of TNF-α and IL-1β by AML blasts upregulates endothelial adhesion receptors(VCAM-1 and ICAM-1), promoting vascular adhesion and proliferation.[48] The proinflammatory environment promotes EC activation, compromising vascular integrity and favoring thrombosis.

As previuos described, proinflammatory cytokines produced by $JAK2^{V617F}$ hematopoietic cells, such as IL-1β, can cause local neuropathy and microenvironmental damage leading to disease manifestation.[51]

Regarding a CML model, CXCL12 downregulation is concurrently associated with an upregulation in BM of macrophage inflammatory protein-1α (MIP-1α), MIP-1β, IL-1α, IL-1β, TNF-α, IL-6, and G-CSF suggesting a new HSC niche that favors the development of leukemia.[58]

Considering other factors released in leukemic BM, G-CSF and granulocyte macrophage-colony stimulating factor (GM-CSF) were inducible from endothelial cells cultured in medium conditioned by patient-derived AML.

BCR/Abl positive CML can induce placental growth factor (PIGF) produced by BMSCs.[59] Interestingly, this upregulation was dependent on NF-κB, suggesting a role for inflammatory related cytokines in the progression of leukemia.

4.2 Niche cell population alterations and supports

The homeostasis of mesenchymal niche can be altered by leukemia. This finding was confirmed by different mouse model. BM niche can actively participate in leukemic initiation and progression.[9,49,56,60] Regarding studies about alteration of the mesenchymal niche, it has been previously described a transgenic model of CML that exhibit defective retention of HSCs and homing in the niche as consequence of decreased CXCL12 in BM MSCs. Concomitantly, in the BM of animals with leukemia there is an alteration of MSCs or osteoblastic cells induced by BCR-Abl.[61] Only recently, studies emerged about niche remodeling in human AML patients.[62] We and others found a permissive MSC niche for leukemogenesis as compared with the normal counterparts.[63,64] Specifically, Kim et al.[62] revealed that human BMs of AML patient's exhibit alteration in mesenchymal niche, such as extensive transcriptional reprogramming in MSCs along

with loss of MSCs proliferation and loss of mesenchymal progenitors ($CD146^+$, primitive subsets of MSCs). Moreover, they showed a distinctive regulation of normal and malignant hematopoietic progenitors by differential expression of cross-talk molecules (Jagged-1 or CXCL12). By means of these mechanisms, the reprogramming of mesenchymal niche selectively suppresses normal HSCs, sparing the leukemogenic activity of leukemia cells. Thus, the clonal dominance of leukemic cells over normal hematopoietic pool is preserved by mesenchymal niche alteration. In addition, they found that most BMs in AML patients who maintained complete remission showed low levels of mesenchymal components. This finding suggests that stromal pattern at initial diagnosis may be considered as a biomarker to predict the clinical course of AML, identifying high-risk patients. Accordingly, the individual microenvironment-based approaches should be considered as a new therapeutic planning.

On the other side, hematologic malignancies can alter the stromal compartments of the BM and subsequently the HSC niche. BM stromal cells of CML and AML patients are altered in the osteoblastic, neural, and endothelial compartments. It has been described an increased number of osteoblastic cells in the BM of CML and AML patients.[65] Interestingly, there is a skewing to the osteoblastic lineage of MSC in CML induced by BCR/Abl; this finding was also confirmed in an MLL-AF9 AML model.[55] Despite these differences, a significant upregulation of MIP-1α was observed in the mouse model and AML patients suggesting that MIP-1α may be an important mediator of the inhibitory effect on OBC.

Of note, also neurons, that innervate the BM, are also altered during the pathogenesis of hematopoietic malignancies. Indeed, treatment with β3 adrenergic agonists restored Nes^+ MSCs with a reduction of leukemia stem cells in the BM using a mouse model with HSCs that expressed the mutant JAK2.[51] Concomitantly, in an AML model MLL-AF9 the depletion of adrenergic nerves increased leukemic infiltration in the BM, accelerating leukemogenesis and diminishing survival.[55] In particular, in association with SNS denervation in leukemic BM there is a reduction of endothelial cells and perivascular mesenchymal stem and progenitor cells (MSPCs), which exhibit a block in differentiation to mature osteoblast cells, with potential damage of healthy HSCs.

Intriguingly, the link between microenvironment and cancer metabolism has been explored in the last decade. For example, BM stroma has been shown to have protective activity for chronic lymphocytic leukemia (CLL) cells by modulating oxidative stress. Particularly, the uptake of cystine is mediated by stromal cells with the conversion of cystine to cysteine and its release to the microenvironment. The uptake of cysteine by CLL cells for glutathione (GSH) synthesis, which is involved against oxidative damage, enhances the leukemia cell survival and drug

resistance.[66] Moreover, these results are also extended to ALL to maintain the redox state in leukemia cells that generate more ROS than non-malignant cells.[67] Further, recently, *Iwamoto et al.*[68] showed a high level of asparagine synthetase by MSCs as mechanism to protect acute lymphoblastic leukemia (ALL) cells from asparaginase cytotoxity. Again, it has been described that alterations of the immune microenvironment by AML blasts occur via release of arginase II, which suppresses T cell proliferation and the polarization of monocytes into a suppressive M2-like phenotype.[69]

In conclusion, only through a deeper knowledge of these intricate systems we can learn how to strive haematopoietic malignancies.

– Aims of the thesis

This thesis is based on the study of three different projects focusing on the role of inflammation in Acute Myeloid Leukemia, in Myelofibrosis (MF), and, particularly, on the contribution of BM-MSCs to the development of AML.

The specific aims were the followings:

1. To analyze the role of inflammation on the functional behaviour of circulating $CD34^+$ cells from patients with MF. It has been hypothesized that the sustained inflammatory microenvironment of MF can alter crucial biological processes, leading to genomic instability and cancer progression. In my thesis, we tested the *in vitro* functional effects of pivotal players of the inflammatory microenvironment: the extracellular ATP nucleotide and selected cytokines, such as Interleukin (IL)-1β, Tumor Necrosis Factor (TNF)-α or the Tissue Inhibitor of Metalloproteinases-1 (TIMP-1)) on the circulating $CD34^+$ cells from MF patients. Specifically, we analyzed the effects of these selected inflammatory mediators on the proliferative activity, clonogenic potential and migration capability of $CD34^+$ cells from $JAK2^{V617F}$ and calreticulin (CALR) mutated patients.

2. To investigate the novel function of the Tissue inhibitor of Metalloproteinases (TIMP-1) within the leukemic microenvironment. Here, in the attempt to provide further evidence for the critical role of inflammation in leukemic microenvironment, we investigated the role of TIMP-1 in leukemic blasts from patients with AML, at diagnosis. We dissected the molecular pathways TIMP-1's cytokine-like functions and signaling pathway in leukemic blasts underlying the cross-talk between inflammation and normal/leukemic microenvironment. Moreover, we explored the interplay of leukemic blasts and MSCs from donor o AML patients in co-cultures systems, showing TIMP-1 as a "bad actor" in a "bad soil" (leukemic microenvironment).

3. To explore the crosstalk of BMSC with leukemic cells. We set up a novel co-culture system with BMSCs and leukemic blasts from a MLL-AF9 model mouse (doxycycline-inducible rtTA;MLL-AF9 mouse strain),[70] investigating ROS-mediated signaling, lipid peroxidation and drug resistance mechanisms. BMSCs can be propagated as non-adherent '*mesenspheres*' allowing them to self-renew and expand, mimicking their properties in vivo and increasing their therapeutic potential. For these reasons, the aim of the project was to study the role of BM mesenspheres in controlling leukemic fate in AML. The hypothesis behind this proposal is that BM mesenspheres

may regulate leukemic blast survival, metabolic adaptation and chemo-resistance through ROS signaling and mitochondria exchanges. The goals of the final part of my thesis were:

A) to investigate whether murine mesenspheres affect *in vitro* survival of murine leukemic blasts;

B) to elucidate the specific signalling pathway by which mesenspheres controls *in vitro* cell survival including modulation of ROS levels or lipid peroxidation by mitochondrial transfer;

C) to highlight *in vitro* the drug resistance mechanisms of leukemic blasts in the presence of mesenspheres after treatment with cytosine arabinoside (AraC).

– Results Ia

Published in

Oncotarget. 2016 Jul 12; 7(28): 43974–43988.

Published online 2016 Jun 11. doi: 10.18632/oncotarget.9949

CRUCIAL FACTORS OF THE INFLAMMATORY MICROENVIRONMENT (IL-1β/TNF-α/TIMP-1) PROMOTE THE MAINTENANCE OF THE MALIGNANT HEMOPOIETIC CLONE OF MYELOFIBROSIS: AN IN VITRO STUDY

D. Sollazzo*, D. Forte*, N. Polverelli, M. Romano, M. Perricone, L. Rossi, E. Ottaviani, S. Luatti, G. Martinelli, N. Vianelli, M. Cavo, F. Palandri§, L. Catani§

(* or §:equally contributed)

Department of Experimental, Diagnostic and Specialty Medicine, Institute of Hematology "L. e A. Seràgnoli", University of Bologna, Bologna, Italy.

Key words: Circulating CD34$^+$ cells, Myelofibrosis, Inflammatory microenvironment, Migration, Survival

ABSTRACT

Along with molecular abnormalities (mutations in *JAK2*, *CALR* and *MPL* genes), chronic inflammation is the major hallmark of MF. Here, we investigated the *in vitro* effects of crucial factors of the inflammatory microenvironment (IL-1β, TNF-α, TIMP-1 and ATP) on the functional behaviour of MF-derived circulating $CD34^+$ cells.

We found that, regardless mutation status, IL-1β or TNF-α increase the survival of MF-derived $CD34^+$ cells. In addition, along with stimulation of cell cycle progression to the S-phase, IL-1β or TNF-α ± TIMP-1 significantly stimulate(s) the *in vitro* clonogenic ability of $CD34^+$ cells from $JAK2^{V617}$ mutated patients. Whereas in the $JAK2^{V617F}$mutated group, the addition of IL-1β or TNF-α + TIMP-1 decreased the erythroid compartment of the *CALR* mutated patients. Megakaryocyte progenitors were stimulated by IL-1β ($JAK2^{V617F}$mutated patients only) and inhibited by TNF-α. IL-1β + TNF-α + C-X-C motif chemokine 12 (CXCL12) ± TIMP-1 highly stimulates the *in vitro* migration of MF-derived $CD34^+$ cells. Interestingly, after migration toward IL-1β + TNF-α + CXCL12 ± TIMP-1, $CD34^+$ cells from $JAK2^{V617F}$ mutated patients show increased clonogenic ability.

Here we demonstrate that the interplay of these inflammatory factors promotes and selects the circulating MF-derived CD34+ cells with higher proliferative activity, clonogenic potential and migration ability. Targeting these micro-environmental interactions may be a clinically relevant approach.

INTRODUCTION

MF is a life-threatening chronic myeloproliferative neoplasia (MPN) of the hematopoietic stem/progenitor cell (HSPC) clinically characterized by progressive anemia, splenomegaly and constitutional symptoms and by an increased risk to develop acute leukemia (AL). It can arise de novo (primary MF; PMF) or can evolve from Polycythemia Vera (PV; PPV MF) or Essential Thrombocythemia (ET; PET MF).[71-73]

Approximately 50 to 60% of MF patients carry a mutation in the Janus kinase 2 (*JAK2*) gene, while 20-25% of patients show recurrent mutations in the *CALR* and an additional 5 to 10% have activating mutations in the myeloproliferative leukemia virus oncogene (MPL) gene. Around 10% of patients have non-mutated *JAK2*, *MPL* and *CALR* genes ("triple negative"). Regardless of molecular status, all patients have a deregulation in the JAK/STAT signalling.[74-79]

Besides molecular abnormalities, the inflammatory microenvironment has emerged in the last few years as a key-player in MF pathogenesis.[80] Abnormal expression and activity of several cytokines involved in inflammation and immunoregulation are associated with MF[81] and correlate with more severe marrow fibrosis,[82,83] worsening systemic symptoms and decreased survival.[84] Also, the constitutive mobilization of $CD34^+$ cells into the peripheral blood has been associated with profound alterations in the CXC chemokine receptor 4 (CXCR4)/ C-X-C motif chemokine 12 (CXCL12) axis.[85-87] Up-regulated production of proinflammatory cytokines by HSPCs and surrounding stromal cells generates a microenvironment that selects for the malignant clone.[81,88-92]

Interestingly, HSPCs actively sense pro-inflammatory factors.[24,93] However, the key players linking inflammation and cancer in MF are still to be defined. Particularly, the plasma levels of IL-1β, TNF-α and TIMP-1 are increased in MF patients,[75,84,94] but their contribution to disease pathogenesis in MF has been poorly[95] or never investigated. This is also true for the extracellular ATP nucleotide.[96] Under inflammatory conditions, IL-1β stimulates leukocytosis and thrombocytosis by inducing various cytokines (i.e. Granulocyte-Colony Stimulating Factor, IL-6) that are overexpressed in MF; also, IL-1β regulates the survival/proliferation of AL cells.[97,98] IL-1β has been recognized as the main trigger for neural damage and Schwann cell death caused by bone marrow mutant HSPC. Notably, mutant-HSPC-driven niche damage seems to critically contribute to MPN pathogenesis.[51] TNF-α promotes survival of human quiescent bone marrow-derived $CD34^+$ Burst Forming Unit-Erythrocyte (BFU-E) and facilitates the clonal expansion of $JAK2^{V617F}$-positive cells in MPNs.[95,99] TIMP-1, through receptor (CD63) binding, promotes cell survival, differentiation and migration; also, TIMP-1 displays cytokine-like features in the HSPC

compartment.[100-102] It was initially found to enhance the proliferation of erythroid cells;[103] also, we recently demonstrated that TIMP-1 increases the clonogenic efficiency of normal CB-derived progenitor cells.[104] Finally, extracellular nucleotides, mainly ATP, are important mediators in inflammation and modulation of cell proliferation, migration and death, including AL $CD34^+$ stem/progenitor cells.[104-109]

Here, we addressed the functional effects of these pro-inflammatory factors on the *in vitro* behaviour of HSPCs derived from MF patients, with the aim to investigate their putative role in disease pathogenesis.

RESULTS

Regardless of mutation status, the plasma levels of IL-1β, TNF-α and TIMP-1 are increased in MF patients

To evaluate the pro-inflammatory profile, selected plasma cytokines were measured. Compared with controls, IL-1β, TNF-α and TIMP-1 plasma levels were significantly increased in MF patients (regardless of IPSS risk stratification values) **(Figure 1 A, B, C).** We found a trend, albeit not statistically significant (*p=0.06*), toward increased IL-1β plasma levels in *CALR* mutated patients. Targeting TNF-α and TIMP-1, no significant differences were observed between *JAK2*^{V617F} and *CALR* mutated groups.

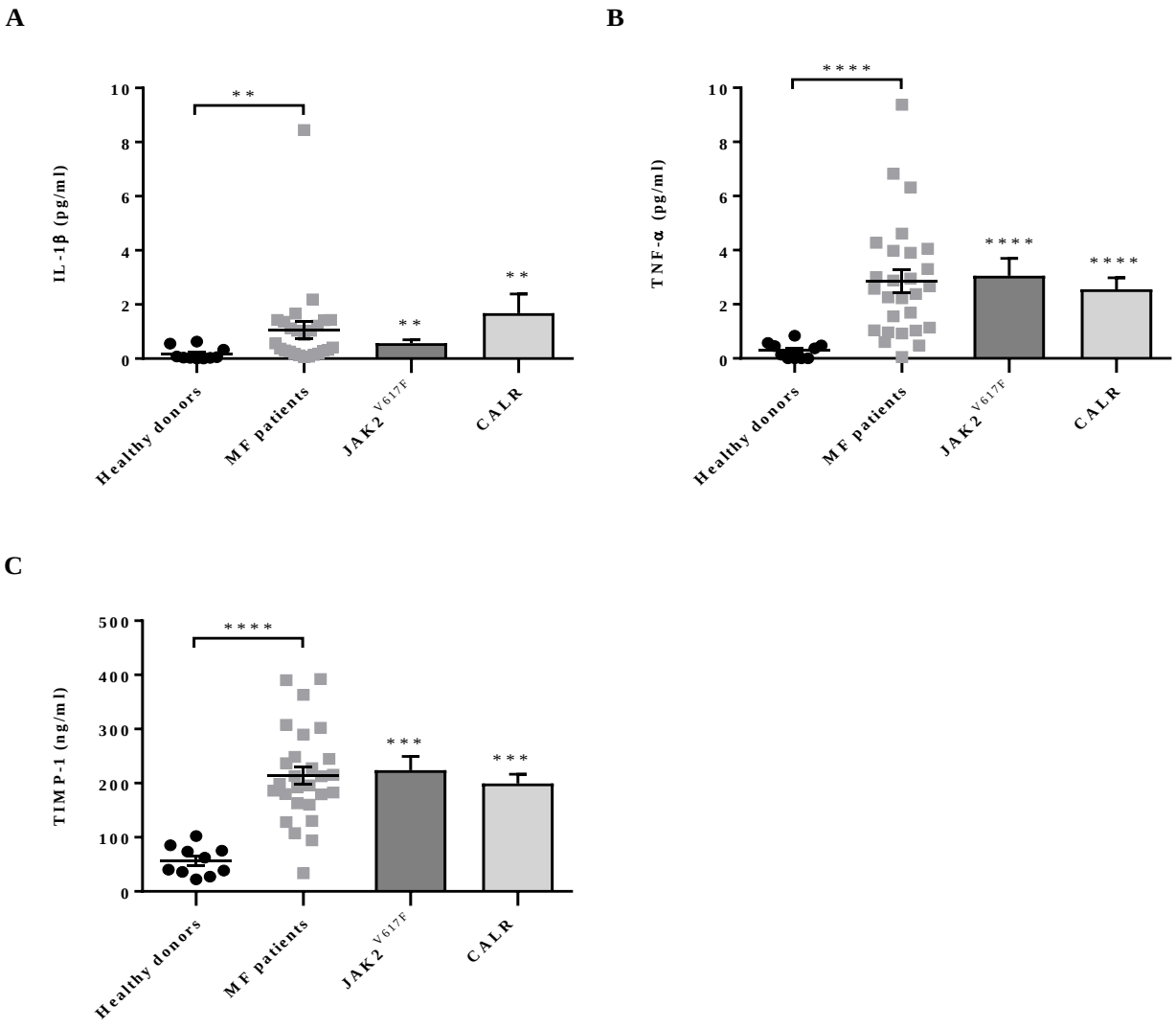

Figure 1

Regardless mutation status, the plasma levels of IL-1β, TNF-α and TIMP-1 are increased in MF patients

*IL-1β (A), TNF-α (B) and TIMP-1 (C) plasma levels were measured by ELISA in MF patients. (n = 26; JAK2^{V617F} positive n =16; CALR positive n = 10) and healthy controls (n = 15). Compared with controls, cytokines plasma levels were significantly increased in MF patients. Of note, there was no significant difference between JAK2^{V617F} or CALR mutated patients. All data are presented as mean ± SEM (**p ≤ 0.01; ***p ≤ 0.001; ****p ≤ 0.0001).*

Selected subsets of circulating HSPCs are expanded in MF patients

To determine the extent of the circulating HSPCs compartment according to mutations, we phenotypically analysed the whole blood of MF patients.

Irrespective of mutation status, the mean number of circulating CD34$^+$ cells was significantly higher in MF patients than in controls ($p \leq 0.0001$). No significant differences were observed between the two mutated groups (**Figure 2 A**). Of note, the number of CD34$^+$ cells correlated with IPSS risk in *JAK2^{V617F}* mutated patients (r=0.88; *p= 0.02*; data not shown).

Along with CD34$^+$CD38$^-$ and CD34$^+$CD133$^+$ cells (**Figure 2 B, C**), circulating CD34$^+$ cells co-expressing adhesion molecules (CD49d, CD47 and CD44; **Figure 2 D-F**) were also significantly increased in MF patients. Once again, no significant difference was observed between the two mutated groups.

The median number of circulating MF-derived CD34$^+$ cells co-expressing the TIMP-1 (CD63) or the CXCL12 receptor (CD184; CXCR4) was significantly higher (***p ≤ 0.001*** and ***p ≤ 0.01***,respectively) than the CB counterparts (**Figure 2 G, H**). *CALR* mutated patients showed increased number of circulating CD34$^+$CD63$^+$ and CD34$^+$CD184$^+$ cells compared to *JAK2^{V617F}* mutated patients (***p ≤ 0.01*** forCD34$^+$CD63$^+$) or the CB-counterparts (***p ≤ 0.01*** and ***p ≤ 0.05,*** respectively). CD34$^+$CD63$^+$ cells of *JAK2^{V617F}* mutated patients were also increased compared with the CB-derived cells ($p \leq 0.05$).

As shown in **Figure 2 I**, circulating megakaryocyte (MK) progenitors (CD34$^+$CD41$^+$) were also significantly increased ($p \leq 0.01$). *CALR* mutated patients showed increased number of CD34$^+$CD41$^+$ cells compared to *JAK2^{V617F}* mutated patients ($p \leq 0.01$) or the CB-counterparts ($p \leq 0.001$).

Of note, except of the decreased expression of CD184 in MF cells, the analysis of mean fluorescence intensity (MFI) of CD133, CD63,CD41, CD49d, CD44 and CD47 antigens on the CD34$^+$ cells did not reveal any difference between patients and controls or between the two mutated groups (data not shown).

These data demonstrate that in MF, irrespective of mutation status, there is an *in vivo* expansion of the HSPCs compartment. However, the *CALR* mutated patients show an increased number of circulating $CD34^+CD63^+$ and $CD34^+CD41^+$ cells compared to the $JAK2^{V617F}$ mutated counterparts.

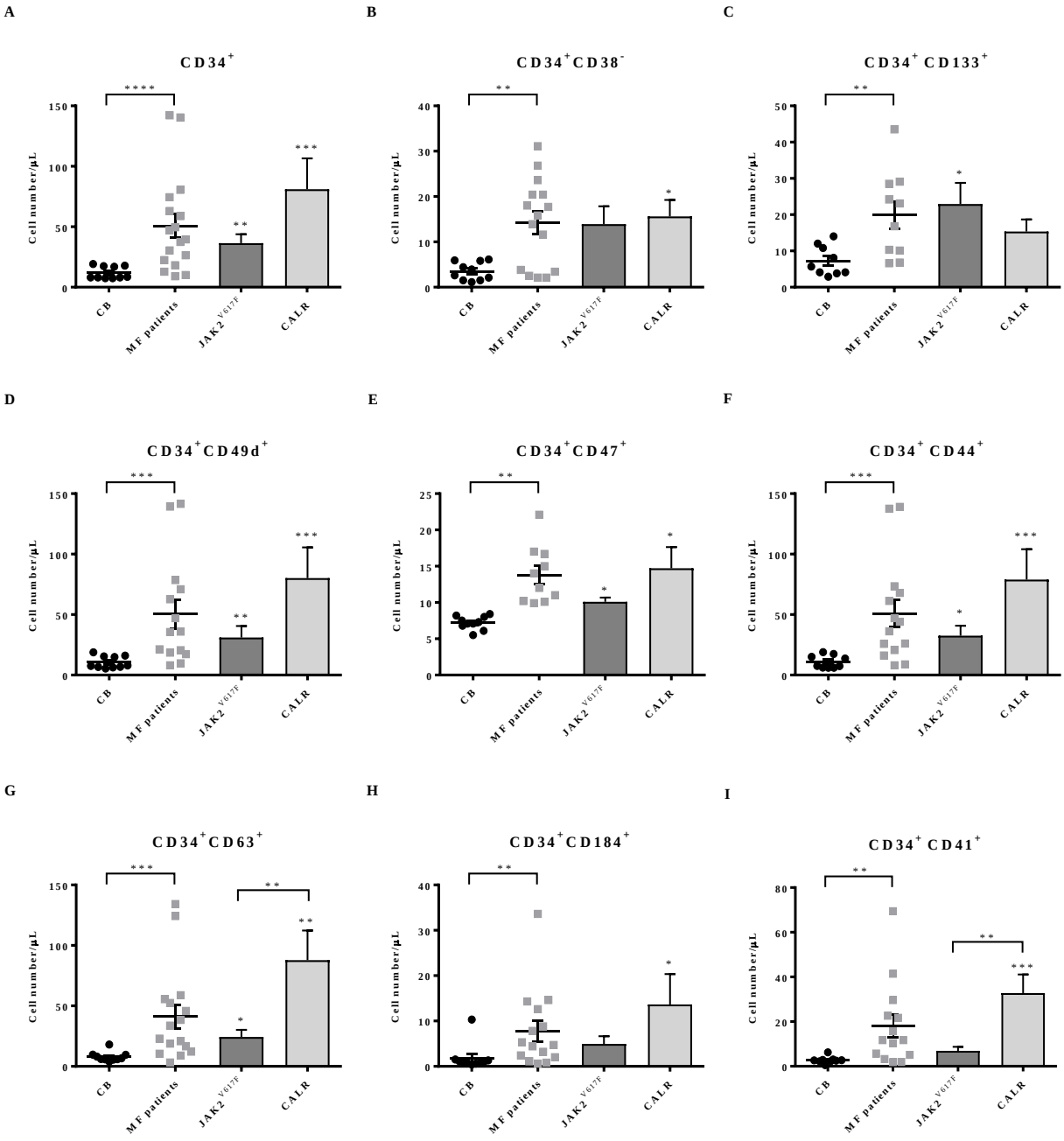

Figure 2

Selected subsets of circulating HSPCs are expanded in MF patients

*The circulating absolute number of MF (total (n = 30) and subdivided into JAK2V617F (n = 20) or CALR (n = 10) mutated groups) and CB (n = 10) $CD34^+$ cells coexpressing the CD133, CD49d, CD47, CD44, CD63, CD184 and CD41 antigens together with the $CD34^+$ $CD38^-$ subset are shown (A–I). All subsets were increased in MF patients as compared with the CB counterparts. No significant differences were observed between the two mutated groups, except the $CD34^+$ $CD63^+$ and the $CD34^+$ $CD41^+$ cells of CALR mutated patients which were significantly increased as compared with the JAK2V617F counterparts. All data are presented as mean ± SEM (*p ≤ 0.05; **p ≤ 0.01; ***p ≤ 0.001; ****p ≤ 0.0001).*

Survival of $CD34^+$ cells from MF patients is increased by IL-1β and TNF-α

To investigate whether inflammatory signals may regulate the survival of HSPCs, $CD34^+$ cells from MF patients or CB were *in vitro* cultured with the selected pro-inflammatory factors, alone or in combination, at concentrations previously shown to be effective in dose-response experiments (**Supplementary Figure 1**).

We firstly assessed the effects of factors alone on the *in vitro* survival of $CD34^+$ cells. As shown in **Figure 3 A**, the survival of $CD34^+$ cells from MF patients was significantly promoted by IL-1β or TNF-α as compared with the CB $CD34^+$ cells ($p \leq 0.01$ and $p \leq 0.05$, respectively) or with the untreated MF cells ($p \leq 0.001$ and $p \leq 0.01$, respectively). No significant differences in survival were observed between the two mutated groups in all tested conditions (data not shown).

As shown in **Supplementary Figure 2**, the combinations of factors two-by-two significantly promoted the MF-derived $CD34^+$ cells survival as compared with untreated cells. However, no significant differences in cell viability were observed as compared with factors alone. Interestingly, the two by two combined factors did not significantly enhance the survival of CB-derived $CD34^+$ cells, except for IL-1β + TNF-α ($p \leq 0.01$). Comparing MF vs CB-derived cells, the survival of MF $CD34^+$ cells was significantly enhanced by IL-1β + TIMP-1 ($p \leq 0.01$) and IL-1β + ATP ($p \leq 0.01$).

When multiple factors were combined no significant differences were observed between MF and CB-derived $CD34^+$ cells. Only TNF-α + TIMP-1 + ATP significantly promoted the survival of $JAK2^{V617F}CD34^+$ cells as compared with the *CALR* ($p \leq 0.01$) or CB counterparts ($p \leq 0.001$) (data not shown).

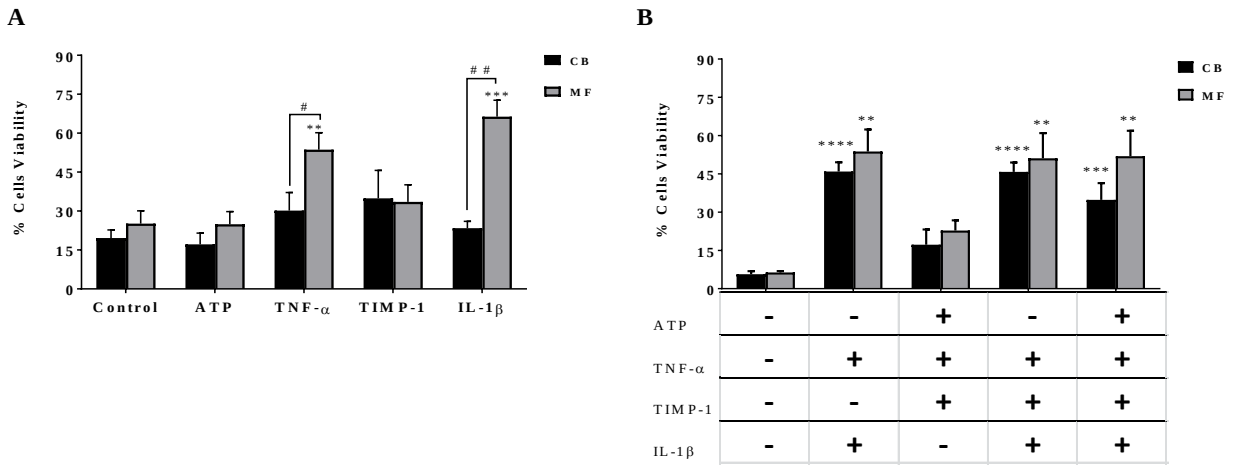

Figure 3

Survival of CD34$^+$ cells from MF patients is increased by IL-1β and TNF-α

*(**A**) CD34$^+$ cells from MF patients (n = 20) or CB (n = 8) were in vitro treated for 4 days with factors alone and the percentage of cell viability was assessed after Annexin V/PI staining, as described in Methods. At variance with CB-derived cells, TNF-α and IL-1β alone significantly stimulated the survival of MF-derived CD34$^+$ cells as compared with untreated cells and the CB-derived counterparts. Conversely, ATP and TIMP-1 were ineffective in normal and diseased cells.(**B**) In selected experiments, before Annexin V/PI staining, MF- (n = 10) and CB- (n = 6) derived CD34$^+$ cells were also labeled with a MoAb against the human CD38 antigen and the CD34$^+$ CD38$^-$ cells were gated and cell viability was analyzed. Once again, multiple combinations of cytokines with IL-1β or TNF-α significantly stimulated the survival of MF- and CB-derived CD34$^+$ CD38$^-$ cells. Notably, this was not true for ATP+ TNF-α+ TIMP-1. No differences were observed between MF patients and CB. All data are presented as mean ± SEM. (**p ≤ 0.01; ***p ≤ 0.001; ****p ≤ 0.0001 vs untreated cells (CTR)) ($^{\#}$p ≤ 0.05; $^{\#\#}$p ≤ 0.01 vs CB).*

When we analyzed the CD34$^+$ CD38$^-$ cells (**Figure 3 B**), we found that multiple factors combinations (particularly those including IL-1β) significantly stimulated the cell survival of MF and CB-derived cells as compared with untreated cells. However, no significant differences were observed between patients/controls (**Figure 3 B**) or the two mutated groups (data not shown)

Taken together these data demonstrate that, regardless of mutation status, the survival of MF-derived CD34$^+$ cells is highly stimulated by the *in vitro* treatment with IL-1β or TNF-α. Combinations of pro-inflammatory factors do not have synergistic effects.

Clonogenic output of circulating MF-derived CD34$^+$ cells is positively enhanced by IL-1β + TNF-α ± TIMP-1 combinations

To analyse the functional role of the selected pro-inflammatory cytokines on HSPCs, we investigated their effects on the clonogenic output of circulating MF and CB-derived CD34$^+$ cells.

Factors alone did not induce a significant CFU-C growth from MF CD34$^+$ cells (data not shown). However, when MF-derived CD34$^+$ cells were tested in the presence of combinations of factors two-by-two, the IL-1β + TIMP-1 combination was the only one effective in stimulating the CFU-C growth as compared with untreated cells ($p \leq 0.05$) or CB-derived CD34$^+$ cells ($p \leq 0.05$) (**Figure 4 A**). IL-1β + TNF-α and IL-1β + TIMP-1 significantly promoted the BFU-E growth of the MF-derived CD34$^+$ cells as compared with the untreated samples and the CB counterparts. The CFU-GM growth was positively enhanced by IL-1β + TIMP-1 (**Supplementary Figure 3 A, B**). Of note, when combinations of multiple factors were tested, only IL-1β +TNF-α + TIMP-1 significantly promoted the CFU-C growth ($p \leq 0.05$) of CD34$^+$ cells from CB (**data not shown**).

As shown in **Figure 4 B**, when the growth of MK progenitors was investigated in the presence of inflammatory factors alone, we found that, at variance with CB, the MF-derived CFU-MK growth was significantly inhibited by TNF-α. By contrast, IL-1β has stimulatory activity on MK colony formation. Factors in combination did not significantly modify the growth of patients/CB pure CFU-MK as compared with factors alone.

We also examined the cell-cycle profile of MF-derived and CB-derived CD34$^+$ cells after *in vitro* exposure to the cytokines. We found that most of the untreated CD34$^+$ cells from MF patients were in a dormant state. Factors alone did not significantly increased the percentage of CD34$^+$ cells in S phase as compared with untreated cells, both in MF patients and CB (**data not shown**). Conversely, in MF patients, irrespective of mutation status, cell-cycle progression was observed in presence of various cytokines combinations, with the notable exception of ATP + TNF-α + TIMP-1 (**Figure 4 C, D**).

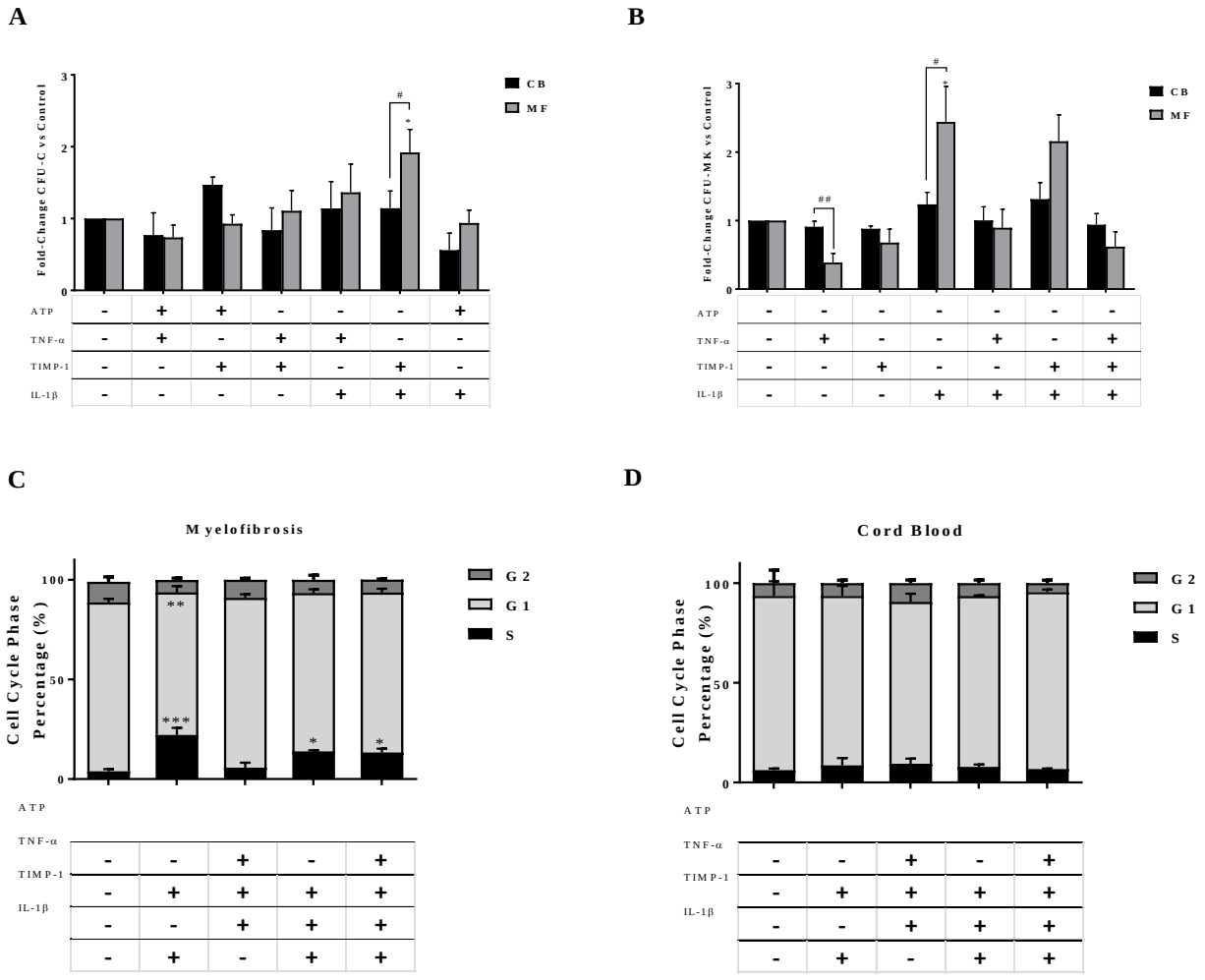

Figure 4

Proliferation of circulating MF-derived CD34+ cells is positively enhanced by IL-1β + TNF-α ± TIMP-1 combinations

Circulating CD34+ cells were isolated from MF patients (n = 20) and CB units (n = 8) and cultured in the presence of the selected two-by-two pro-inflammatory factors. After 14 days, the total CFU-C output was assessed as described in Methods (A). Circulating CD34+ cells were isolated from MF patients (n = 10) and CB units (n = 8) and cultured in the presence or absence of inflammatory factors alone or combined. After 12 days, the CFU-MK growth was assessed as described in Methods (B). The results are expressed as growth fold change versus untreated CTR samples. (A) The clonogenic output of the MF-derived CD34+ cells was significantly stimulated by the IL-1β + TIMP-1 combination as compared with untreated cells or the CB-derived counterparts. No other combinations of factors two-by-two were effective. The mean number of colonies in MF-derived and CB-derived untreated samples was 59 ± 8 and 63 ± 6, respectively. (B) The MF-derived CFU-MK growth was significantly inhibited by TNF-α. By contrast, IL-1β has stimulatory activity on MK colony formation. Factors in combination did not significantly modify the growth of patients/CB CFU-MK as compared with factors alone. Factors alone or in combination did not significantly modify the CFU-MK growth of the CB counterparts. The mean number of CFU-MK in MF- and CB-derived untreated samples was

*26 ± 11 and 46 ± 10, respectively. In (C and D) are shown the results of cell-cycle analysis of MF-derived (n = 10) and CB-derived (n = 8) CD34+ cells after in vitro incubation for 24 hours in the presence or absence of various combinations of pro-inflammatory factors. Results are expressed as the percentage of cells in different phases of the cell cycle. IL-1β plus TNF-α highly promote cell cycling of CD34+ cells from MF patients. IL-1β + TNF-α + TIMP-1 and IL-1β + TNF-α + TIMP-1 + ATP were also effective (C). Conversely, no significant differences were observed when CB-derived cells were analysed (D). All data are presented as mean ± SEM. (*p ≤ 0.05; **p ≤ 0.01; ***p ≤ 0.001 vs untreated cells) (#p ≤ 0.05; ##p ≤ 0.01 vs CB).*

Opposite effects of pro-inflammatory cytokines on clonogenic potential of CD34^{+} cells from JAK2^{V617F} or CALR mutated patients

When clonogenic potential was analysed according to mutation status and in the presence of pro-inflammatory factors alone, no differences were observed between the two mutated groups. Colony composition analysis demonstrated that only IL-1β enhanced the erythroid compartment of the *JAK2^{V617F}*mutated group (**Supplementary Figure 4 A and B**).

By contrast, (**Figure 5 A**), the combination of IL-1β + TIMP-1 and IL-1β + TNF-α significantly promoted the CFU-C growth of *JAK2^{V617F}* mutated patients compared with the *CALR* mutated counterparts. Similar results were obtained when CFU-GM and BFU-E growth were distinctly analysed (data not shown).

A

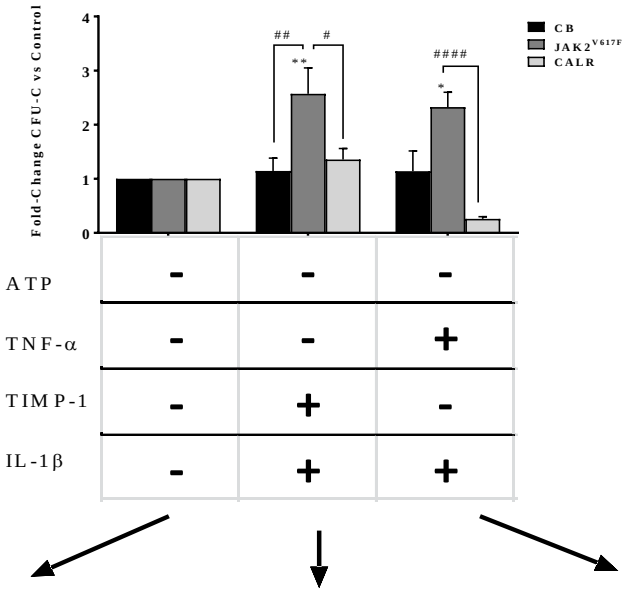

B

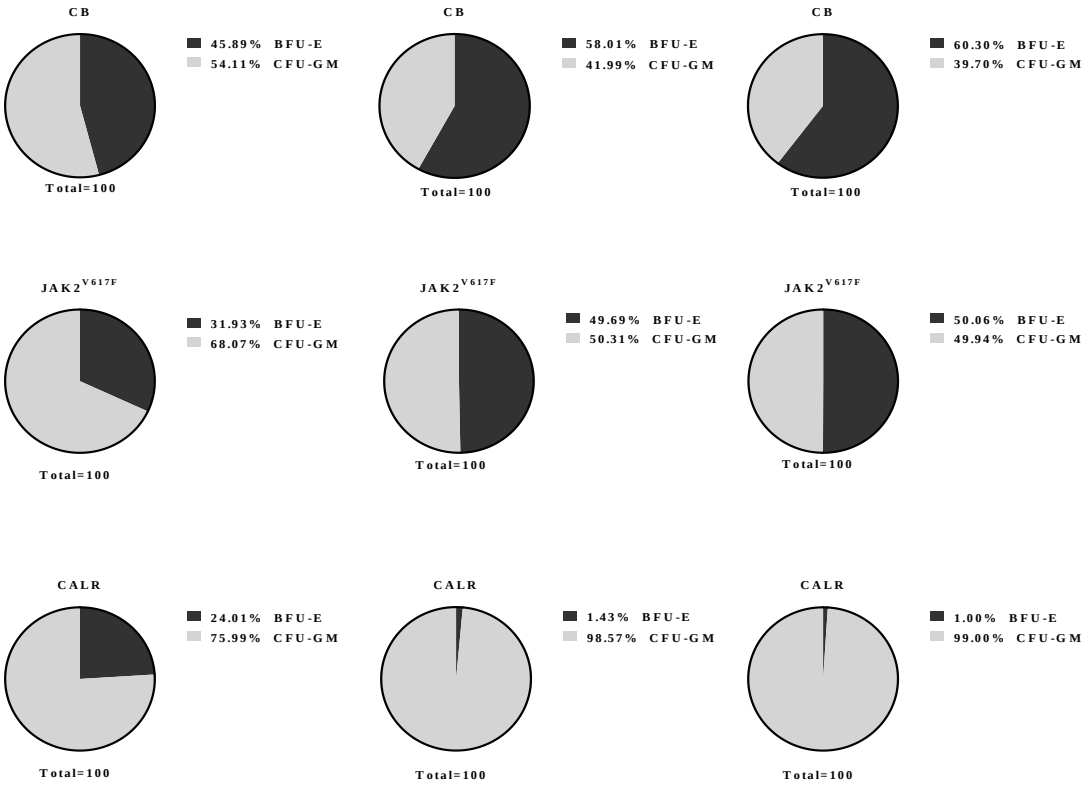

Figure 5

Opposite effects of pro-inflammatory cytokines on cells from JAK2^{V617F} or CALR mutated patients

*(**A**) When clonogenic activity was analyzed according to mutation status, the CFU-C growth of JAK2^{V617F} mutated patients was significantly up-regulated by IL-1β + TIMP-1 and IL-1β + TNF-α as compared with untreated control samples, the CALR mutated counterparts and the CB-derived cells (only IL-1β + TIMP-1). The results are expressed as growth fold change versus untreated CTR samples. All data are presented as mean ± SEM. (*p ≤ 0.05; **p ≤ 0.01 vs untreated cells) ($^{\#}p \leq 0.05$; $^{\#\#}p \leq 0.01$; $^{\#\#\#\#}p \leq 0.0001$ vs CB-derived cells) (**B**) When colony composition was analyzed*

according to mutation status, we found that the erythroid compartment of the untreated samples was reduced in both mutated groups as compared with the CB counterparts. However, no significant differences were observed between the two mutated groups. Interestingly, in the JAK2^{V617F} mutated group, the addition of IL-1β + TIMP-1 and IL-1β + TNF-α enhanced the erythroid compartment as compared with untreated samples. Conversely, some cytokines combinations significantly impaired BFU-E growth in CALR mutated patients. The results are expressed as mean percentage of CFU-GM/BFU-E as compared with the total CFU-C count.

When colony composition was analysed according to mutation status (**Figure 5 B**), both mutated groups showed reduced BFU-E growth of the untreated samples as compared with the CB counterparts. Interestingly, in the *JAK2*^{V617F} mutated group, the addition of different combinations of pro-inflammatory factors enhanced the erythroid compartment as compared with untreated samples. Conversely, some cytokines combinations significantly decreased BFU-E growth in *CALR*-mutated patients.

Multiple combinations did not significantly modify the clonogenic activity and colony composition of the two mutated groups (data not shown).

When we analyzed the percentage of *JAK2*^{V617F} and *CALR* mutant colonies in the absence or presence of IL-1β+ TNFα, we found that the percentage of *JAK2*^{V617F}, but not *CALR*, mutated colonies was increased (data not shown).

MK progenitors of *JAK2*^{V617F} mutated patients were highly stimulated by IL-1β alone. By contrast, TNF-α significantly inhibited the CFU-Mk growth of both *JAK2*^{V617F} and *CALR* mutated patients as compared with CB counterparts (**Supplementary Figure 5**).

Taken together these results demonstrate that the hemopoietic function of MF-derived CD34^{+} cells is highly promoted by the IL-1β or TNF-α ± TIMP-1 combinations, even though TNF-α alone show inhibitory effects on MK progenitors. Interestingly, whereas in the JAK2^{V617F} mutated group, the addition of various combinations of growth factors decreased the erythroid compartment of the CALR mutated patients.

IL-1β and TNF-α significantly promote migration of MF-derived CD34^{+} cells showing enhanced clonogenic ability after migration in JAK2^{V617F} mutated patients

To evaluate whether selected pro-inflammatory factors may differentially regulate the migratory ability of HSPCs from MF patients, we firstly analyzed the plasma concentration of CXCL12. CXCL12 plasma level was markedly higher in patients than in controls, either total (***p ≤ 0.05***) or

subdivided according to mutation status (*JAK2*^{V617F} $p \leq 0.05$; *CALR* $p \leq 0.05$). Conversely, no significant differences were observed between the two mutated groups (**Figure 6 A**).

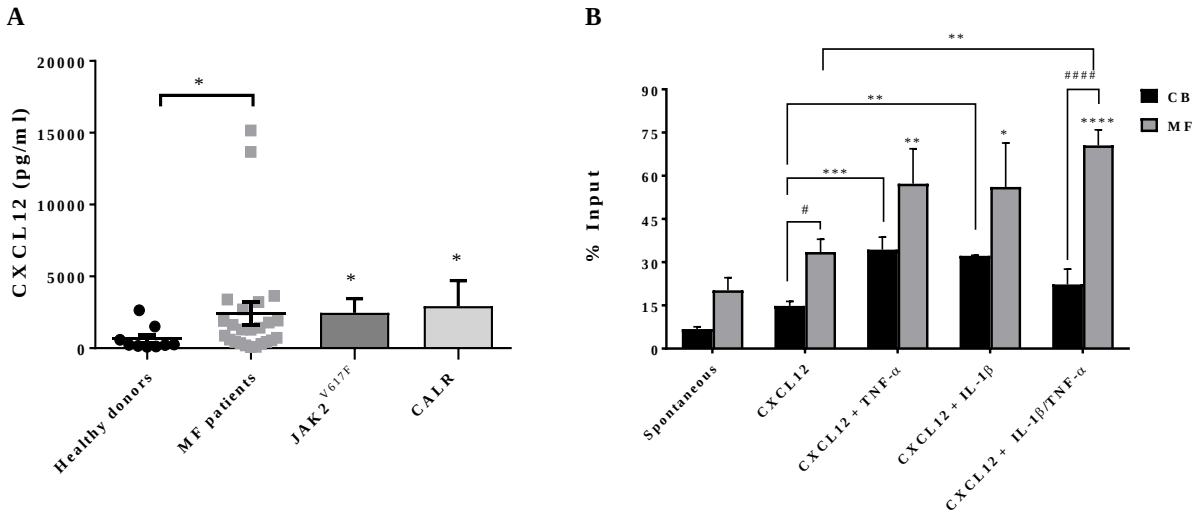

Figure 6

IL-1β and TNF-α significantly increases migration of MF-derived CD34$^+$ cells

*(**A**) CXCL12 plasma levels of MF patients (total n =24; JAK2^{V617F} mutated patients n = 16; CALR mutated patients n = 8) and controls (n = 10). Regardless mutation status, CXCL12 concentration was significantly higher in MF patients (*p ≤ 0.05 vs controls). (**B**) When cells were migrated toward CXCL12 alone, an increased migration ability was observed in MF-derived (n = 15) CD34$^+$ cells as compared with the CB-derived (n = 8) counterparts. The addition of inflammatory factors alone (IL-1β/TNF-α) plus CXCL12 significantly increased the migratory behaviour of MF-derived CD34$^+$ cells as compared with CXCL12 alone. IL-1β + TNF-α synergistically enhanced the migratory behaviour of CD34$^+$ cells as compared with spontaneous migration (****p < 0.0001), CXCL12 alone (**p <0.001) and the CB-counterpart ($^{\#\#\#\#}$p <0.0001). Results are expressed as mean percentages ± SEM of input. (**p ≤ 0.01; ***p ≤ 0.001 vs CXCL12 alone for CB-derived CD34$^+$cells) (*p ≤ 0.05; **p ≤ 0.01; ****p < 0.0001 vs spontaneous migration for MF-derived CD34$^+$ cells) ($^{\#}$p ≤ 0.05; $^{\#\#\#\#}$p <0.0001 vs CB).*

To mirror the *in vivo* pattern of MF, we set up *in vitro* migration experiments in the presence of the identified inflammatory factors and CXCL12. The migration rate of MF- or CB-derived CD34$^+$cells toward inflammatory factors alone (without CXCL12) was not significantly different from that of untreated cells (data not shown).

As shown in **Figure 6 B,** CXCL12 significantly increased the migratory behaviour of MF-derived CD34$^+$ cells as compared with CB counterparts ($p \leq 0.05$). The addition ofIL-1β or TNF-α + CXCL12 shows a trend toward increased migration of CD34$^+$ cells from MF patients, but doesn't

reach statistical significance. At variance with CB derived cells, the addition of both cytokines significantly increased the migratory potential of $CD34^+$ cells from MF patients (***p ≤ 0.01***). No differences were observed between the two mutated groups (data not shown).

The addition of TIMP-1 and ATP alone or inflammatory factors two by two in the presence of CXCL12 did not significantly increase the migration ability of MF-derived $CD34^+$ cells as compared with CXCL12 alone (data not shown). The migratory behavior of the MF-derived $CD34^+$ cells toward multiple combinations of factors was significantly enhanced as compared with the CB-derived counterparts in all tested combinations. Conversely, CB-derived $CD34^+$ cells were almost insensitive (**Supplementary Figure 6**).

To evaluate whether migrated cells toward various pro-inflammatory gradients show different hemopoietic function, we also tested the clonogenic potential of $CD34^+$ cells from MF patients or CB after migration toward CXCL12 alone or CXCL12 plus various combinations of factors (**Figure 7 A, B**). Interestingly, at variance with the CFU-C growth of unmigrated HSPCs from MF patients, IL-1β + TNF-α + CXCL12 and IL-1β + TNF-α + TIMP-1 + CXCL12 selected a subset of MF-derived $CD34^+$ cells with higher clonogenic potential as compared with CXCL12 alone ($p \leq 0.05$, respectively) (**Figure 7 B)**. Conversely, the clonogenic output of CB-derived $CD34^+$ cells after migration toward various combinations of pro-inflammatory factors was unaffected (**Figure 7 A**). Notably, according to mutation status, the CFU-C post migration assay demonstrated once again that various combinations of pro-inflammatory factors significantly stimulate the clonogenic ability of migrated $CD34^+$ cells from $JAK2^{V617F}$, but not *CALR*, mutated patients (**Supplementary Figure 7**).

When the number of granulocyte and erythroid colonies were analysed individually, only BFU-E growth was significantly increased with respect to controls (***p ≤ 0.05***) after cells were migrated toward IL-1β+ TNF-α + CXCL12 ± TIMP-1. Of note, IL-1β + TNF-α + TIMP-1 + CXCL12 significantly stimulated also CFU-GM growth as compared with CXCL12 alone ($p \leq 0.05$, respectively) (data not shown).

Taken together these results demonstrate that, irrespective of mutation status, IL-1β+ TNF-α + CXCL12 ± TIMP-1 selectively enhance the migratory ability of MF-derived $CD34^+$ cells. Interestingly, IL-1β + TNF-α + CXCL12 ± TIMP-1 promotes and selects the circulating HSPCs of $JAK2^{V617F}$mutated patients with higher clonogenic potential.

A

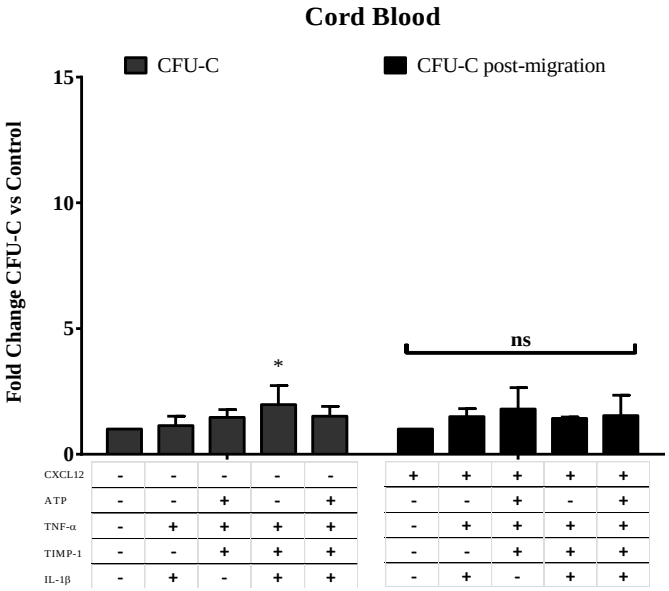

B

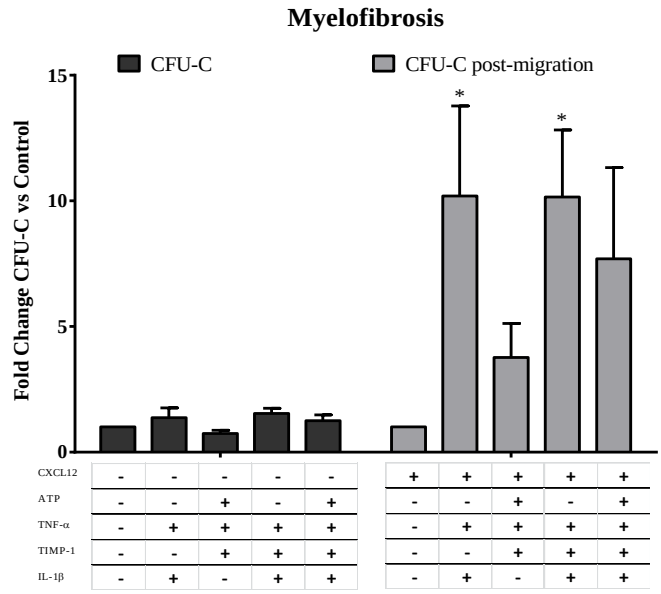

Figure 7

The clonogenic output of MF-derived CD34$^+$ cells after migration toward IL-1β + TNF-α + CXCL12 ± TIMP-1 is potently enhanced

Panels (A and B) show the clonogenic potential of CB-derived (A; n = 6) and MF-derived CD34$^+$ cells (B; n = 14) at baseline with or without various combinations of pro-inflammatory factors (CFU-C) and after migration toward CXCL12 alone or various combinations of pro-inflammatory factors + CXCL12 (CFU-C post-migration). After migration toward IL-1β + TNF-α + CXCL12 ± TIMP-1, the MF-derived, but not CB-derived, CD34$^+$ cells show significantly increased clonogenic potential. Results are expressed as mean fold change of CFU-C ± SEM. ($p \leq 0.05$ vs untreated cells (A) and CXCL12 alone (B)).*

DISCUSSION

Here, we evaluated the *in vitro* effects of four main crucial factors of the inflammatory microenvironment (IL-1β, TNF-α, TIMP-1 and ATP) on survival, clonogenic output and migration ability of MF HSPCs.

First, this study demonstrates that, regardless of mutation status, IL-1β, TNF-α and TIMP-1 are increased in the plasma of MF patients and the presence of IL-1β, TNF-α ± TIMP-1 confers a survival advantage of MF-derived HSPCs. Second, HSPCs from *JAK2*^{V617F} show *in vitro* enhanced proliferation over untreated cells and the CB counterparts in response to IL-1β, TNF-α ± TIMP-1 exposure (alone or, mostly, in combination). Accordingly, IL-1β + TNF-α stimulates cell cycle progression of MF-derived CD34^{+} cells to the S-phase. Third, IL-1β + TNF-α combination promotes the *in vitro* migration of MF-derived HSPCs. Interestingly, after migration toward IL-1β + TNF-α + CXCL12 ± TIMP-1, MF-derived CD34^{+} cells show increased clonogenic ability as compared with CXCL12 alone or the CB counterparts. This finding was mainly due to stimulation of the clonogenic growth of HSPCs from *JAK2*^{V617F} mutated patients.

TNF-α has already been shown to facilitate clonal expansion of *JAK2*^{V617F}-positive cells in MF.[95] The results of this study provide new evidences that, in addition to TNF-α, IL-1β and TIMP-1 promote the *in vitro* maintenance of the HSPCs.

Mutation status is associated with dysregulated hemopoietic function (clonogenic output and colony composition) of MF-derived CD34^{+} cells in presence of IL-1β + TNF-α ± TIMP-1. Specifically, when pro-inflammatory factors were added in culture, CD34^{+} cells from *JAK2*^{V617F}mutated patients showed increased clonogenic potential and increased size of the erythroid progenitors compartment as compared with the CALR-mutated counterparts. Along with the CFU-C growth, IL-1β stimulates the *in vitro* growth of Mk progenitors of *JAK2*^{V617F} mutated patients only. Consistent data on single cell assays suggested that HSC self-renewal capacity is negatively affected by *JAK2*^{V617F}, but progenitor cells have increased proliferation capacity.[110] In addition, these findings can be related to the fact that *JAK2*^{V617F} mutant, in contrast with the *CALR* counterpart, activates not only the Mk cell line but also the erythroid and granulocytic lineages.[111]

Despite increased frequency of MK progenitors (CD34^{+} CD41^{+} cells) in the PB of *CALR* mutated patients, we clearly demonstrate that the hemopoietic function of CD34^{+} cells from *CALR* mutated patients is unmodified (megakaryocytic compartment) or significantly inhibited (erythroid compartment) by IL-1β or various combinations of inflammatory factors including IL-1β. It is therefore likely that these functional abnormalities may contribute to explain the lower haemoglobin

concentration that is displayed by *CALR*-positive patients compared to JAK2^{V617F}-mutated patients.[78] Interestingly, at variance with *JAK2*^{V617F}, *CALR* mutants moderately activate the PI3K/AKT pathway, a critical determinant of erythropoiesis and megakaryocytopoiesis.[111-114]

Of note, we also found increased number of circulating CD34^{+}CD63^{+} cells in MF. However, despite TIMP-1 alone was ineffective, various combinations including TIMP-1 increased the proliferation/migration of MF-derived CD34^{+} cells. This finding was not due to upregulated expression of CD63 receptor on MF-derived CD34^{+} cells after exposure to IL-1β and/or TNF-α (data not shown). It is therefore likely that downstream intracellular signaling pathways are hyperactivated and stimulate clonogenic activity.

Overall, our data indicate that the *in vitro* behavior of the MF-derived HSPCs can be upregulated by regulatory signals provided by the microenvironment and, specifically, through the cooperation between various pro-inflammatory factors. Therefore, the increased number of HSPCs in the peripheral blood of MF may be due not only to the displacement of HSPCs from bone marrow into peripheral blood, but also to the proliferative/survival signals coming from the pro-inflammatory factors within the peripheral blood niche. As a consequence, the pro-inflammatory microenvironment emerges as central site for cell division and proliferation.

In conclusion, the *in vitro* interplay between identified pro-inflammatory cytokines, which are abnormally increased, promotes and selects the circulating MF-derived HSPCs with higher proliferative activity, clonogenic potential and migration ability. Thus, it is likely that the *in vivo* inflammatory niche plays a key role in the maintenance of the malignant hemopoietic clone. Targeting these inflammatory micro-environmental interactions may be a clinically relevant approach for MF.

MATERIALS AND METHODS

Patients and samples

Peripheral blood (PB) was obtained from 10 normal age-matched volunteers and 36 patients with MF in chronic phase. Patients' characteristics according to mutational status are shown in Table I. At the time of the study, patients were at diagnosis (19 cases) or untreated for at least two months. Previous therapies were: hydroxyurea (12 cases) and Ruxolitinib (3 cases). The diagnosis of MF was made according to WHO 2008 criteria.[115] Patients and controls provided written informed consent for the study. This study was approved by the medical Ethical Committee of the University Hospital of Bologna and was conducted in accordance with the Declaration of Helsinki. During the last trimester of pregnancy, an increased number of $CD34^+$ HSPC are mobilized from the fetal liver and can be found in the circulating blood, including umbilical cord blood (CB). Therefore, since HSPC trafficking characterizes both the PB of MF patients and CB, we choose this physiological source for comparison. CB collections (14 cases) from normal full-term deliveries were provided by the Cord Blood Bank of the University Hospital of Bologna after written informed consent.

Characteristics	*JAK2*^{V617F}-mutated patients (no. 23)	*CALR* mutated patients (no.13)	*P* value
Median age, years (range)	65 (40–82)	73 (70–84)	**0.01**
Male sex, n° (%)	12 (52%)	7 (54%)	1
Median allele burden, % (range)	89 (0,4–99)	56,5 (47–98)	0.07
Median WBC,$\times 10^9$/L (range)	8,6 (2,5–157,6)	6,6 (2,3–16)	0.48
Median hemoglobin, g/dL (range)	11,9 (8,6–15,1)	9,3 (7,7–12,7)	**0.04**
Median platelet count, $\times 10^9$/l (range)	270 (41–707)	198 (86–419)	0.44
High/intermediate 2 IPSS category, n° (%)	12 (52)	7 (54)	1
Unfavorable karyotype, n° (%)	9 (39)	3 (23)	0.46
PMF diagnosis, n° (%)	14 (61)	9 (69)	0.7
BM fibrosis grade ≥ 2, n° (%)	14 (61)	13 (100)	**0.03**
Patients with splenomegaly, n° (%)	19 (83)	10 (77)	0.7
Median follow-up, months (range)	45 (1,9–114,9)	48 (10–136,3)	0.24

Cell isolation

PB, anticoagulated with ethylenediamine tetraacetic acid (EDTA), was obtained from patients/controls. Mononuclear cells (MNCs) were separated from MF and CB samples by stratification on Lympholyte-H 1.077 g/cm^3 gradient (Gibco-Invitrogen, Milan, Italy), followed by red blood cell lysis for 15 min at 4°C. MNCs were then processed on magnetic columns for

$CD34^+$cell isolation (mean purity 94% ± 5%) (MACS CD34 Isolation kit; Miltenyi Biotech, Bologna, Italy), as previously described.[64]

Plasma levels measurement of selected circulating cytokines

We measured the cytokines plasma levels of patients/controls by ELISA, according to the manufacturer's instructions. EDTA-anticoagulated PB was centrifuged for 15 minutes at 1000g within 30 minutes of collection. The plasma was then collected and stored at -80°C until quantification. In particular, the TIMP-1 ELISA kit was provided from Boster Immunoleader (Boster Biological Technology Co., Pleasanton, CA, USA) and CXCL12 ELISA kit from Krishgen ByoSistems (Ashley CT, Whittier, CA, USA). The Ciraplex^{TM} immunoassay kit / Human 9-Plex Array (Aushon BioSystems, Billerica, MA, USA) was used for the measurement of various cytokines including IL-1β and TNF-α.

Phenotype of circulating $CD34^+$ cells

The phenotype of circulating $CD34^+$ cells was evaluated in PB from MF patients and in CB samples by conventional immunofluorescence, as previously described.[116] Antibodies used to characterize the $CD34^+$ cells are listed in Supplementary Table S1. A minimum of $1x10^4$ $CD34^+$ cells were acquired by flow cytometer BD Accuri C6 (Becton Dickinson). Analysis was performed excluding cellular debris in a SSC/FSC dot plot. The percentage of positive cells was calculated subtracting the value of the appropriate isotype controls. The absolute number of positive cells/μl was calculated as follows: percentage of positive cells x White Blood Cells count/100.

Apoptosis assay

Freshly isolated $CD34^+$ HSPCs (2-5 x 10^5) from MF patients or CB units were maintained in RPMI 1640 with 10% FBS, with or without IL-1β (1,10 ng/mL), TNF-α (10,100 ng/mL), TIMP-1 (100,300 ng/mL), and ATP (100,1000 μM), alone or in different combinations. After 4 days, cells were stained for 15 min at RT with Annexin-V-FLUOS Staining Kit (Roche, Penzberg, Germany). Samples were then immediately analyzed by BD Accuri C6 (BD Bioscience). Results are expressed as percentage of live cells compared to the whole cells.

Erythroid and granulocytic progenitors assays

MF/CB-derived $CD34^+$ cells were cultured *in vitro* to achieve hematopoietic cell differentiation and the formation of multi-lineage colony-forming units (CFU-Cs), including colony forming unit-

granulocyte macrophage (CFU-GM) and BFU-E. Specifically, $CD34^+$ cells were seeded in methylcellulose-based medium (human StemMACS HSC-CFU lite w/Epo, Miltenyi Biotech) at 5 x 10^2 cells/mL in 35-mm Petri dishes in the presence or absence of the selected pro-inflammatory factors: TIMP-1 (100 ng/mL; Thermo Scientific, Pierce Biotechnology, Rockford, IL, USA), ATP (1000 μM; Sigma Aldrich, Milan, Italy), TNF-α (10 ng/mL; Thermo Scientific) and IL-1β (1 ng/mL; Thermo Scientific), alone or in combination. After 2 weeks of incubation at 37°Cin 5% humidified CO_2 atmosphere, CFU-C growth was evaluated by standard morphologic criteria using an inverted microscope (Axiovert 40, Zeiss).

Megakaryocytic progenitors assay

Megakaryocytic colonies (Colony Forming Unit-Megakaryocyte (CFU-MK)) were obtained using MegaCult™-C assay (Stem Cell Technologies; Vancouver, BC, Canada), according to the manufacturer's protocols. Briefly, 5×10^3 MF/CB-derived $CD34^+$ cells were seeded in a collagen-based medium in double chamber slides in the presence or absence of the inflammatory factors, alone or in combination. Cultures were incubated for 12 days and then dehydrated, fixed and stained with a primary antibody to the Mk-specific antigen GPllb/llla (CD41) linked to a secondary biotinylated antibody-alkaline phosphatase avidin conjugated detection system. CFU-Mk were counted using a light microscope.

Cell cycle analysis

A total of 10^6 $CD34^+$ cells was maintained in Roswell Park Memorial Institute (RPMI)-1640 (Lonza) supplemented with 10% fetal bovine serum (FBS Thermo Fisher Scientific, Waltham, MA USA). Cells were resuspended in complete medium at a concentration of 1 x 10^6/mL, and primed for 24 hours with the pro-inflammatory cytokines (1 ng/mL IL-1β, 10 ng/mL TNF-α, 100 ng/mL TIMP-1, 1000 μM ATP), alone or in combination. Treated cells were first permeabilized with NP-40 (15 min at RT) and then labeled with propidium iodide (PI)/RNAse staining kit (BD Bioscience) for 15 min at RT, in the dark. The DNA content was assessed by BD Accuri C6 (BD Bioscience) and results were analyzed by FCS express 4 software.

Changes in the cell-cycle distribution were evaluated using PI. The percentage of cells in the G0/G1, S, and G2/M phases was determined by measuring simultaneously the DNA and RNA total cellular content.

Migration assay

Migration of MF/CB purified $CD34^+$ cells was assayed towards a CXCL12 gradient (150 ng/mL) in transwell chambers (diameter 6.5 mm, pore size 8 µm; Costar; Corning), as previously described [38]. Briefly, 50 µl of RPMI 1640 plus 10% FBS containing 0,5 x 10^5 cells were added to the upper chamber and 150 µl of medium with or without CXCL12 ± IL-1β (1 ng/mL), TNF-α (10 ng/mL), TIMP-1 (100 ng/mL), and ATP (1000 µM) (alone or in combination) were added to the bottom chamber. After overnight incubation at 37°C in 5% humidified CO2 atmosphere, inserts (upper chambers) were removed and cells transmigrated into lower chamber were recovered and counted by Trypan Blue exclusion test in a Neubauer chamber using an inverted microscope (Nikon) with a 10x magnification. The amount of migrated cells was expressed as a percentage of the input, applying the following formula: (number of migrated cells recovered from the lower compartment/total number of cells loaded in the upper compartment) x 100. In addition, migrated cells were assayed in methylcellulose-based medium for their ability to form hematopoietic colonies (as above described).

Mutation analysis

JAK2^{V617F} allele-burden was assessed in granulocyte DNA by quantitative polymerase chain reaction–based allelic discrimination assay (ipsogen *JAK2* MutaQuant Kit) on 7900 HT Fast Real Time PCR System (Applied Biosystem).[117] *CALR* exon 9 sequencing was performed by Next Generation Sequencing (NGS) approach with GS Junior (Roche-454 platform); analysis was carried out with AVA Software (GRCh38 as reference).[118] Rare *CALR* mutations identified by NGS were confirmed by Sanger sequencing.

Individual colonies were harvested at day 12-14 from 3*JAK2*^{V617F} and 3 *CALR* mutated patients (20 individual colonies each condition).Molecular characterization of single colonies was performed on DNA extracted using REPLI-g Single Cell Kit (QIAGEN, Marseille, France), which provides accurate genome amplification from single cells or limited samples with high efficiency. Briefly, 4 µL of cell material (supplied with PBS) were firstly lysed. After denaturation, isothermal amplification reaction was performed and amplified DNA was used for *JAK2*^{V617F} and *CALR* mutations assessment, as above described.

Cytogenetic analysis

Chromosome banding analysis was performed on bone marrow cells by standard banding techniques according to the International System for Human Cytogenetic Nomenclature. At least

20 metaphases were required. Unfavourable karyotype included complex karyotype or single or two abnormalities including +8, -7/7q-, i(17q), -5%5q-, 12p-, inv(3) or 11q23 rearrangement.[119,120]

Statistical analysis

Numerical variables have been summarized by their median and range, and categorical variables by count and relative frequency (%) of each category. Comparisons of quantitative variables between groups of patients were carried out by the nonparametric Wilcoxon rank-sum test. All *p* values were considered statistically significant when ≤ 0.05 (2-tailed). Statistical analyses were performed using Graphpad (Graphpad Software Inc., La Jolla, CA) and SPSS software (PASW Statistics for Windows, Version 18.0. Chicago, IL).

Supplemetary Materials

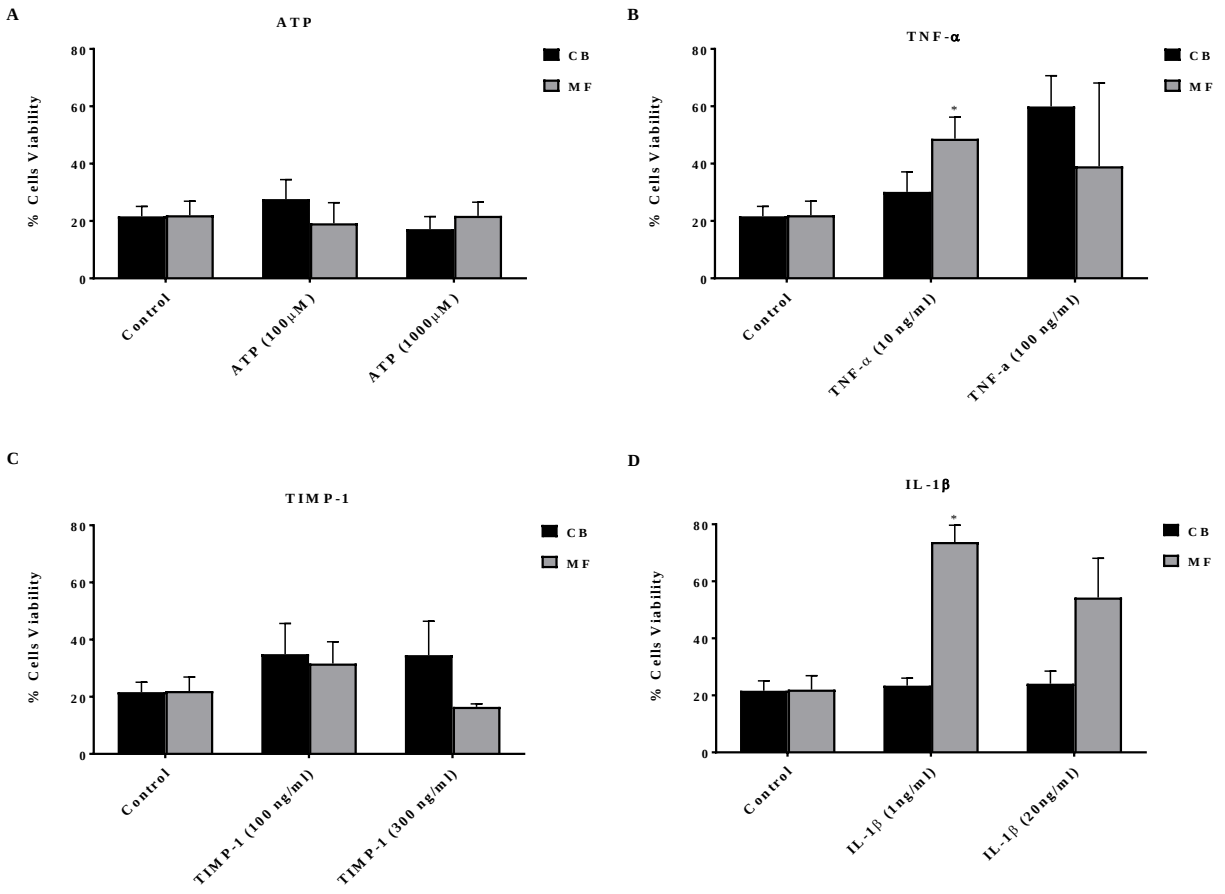

***Supplementary Figure S1**:*

*Survival of MF- and CB-derived CD34+ cells after in vitro treatment with increasing doses of inflammatory factors. CD34+ cells from MF patients (n = 4) or CB (n = 3) were in vitro treated for 4 days with factors alone (ATP (100, 1000 μM), TNF-α (10,100 ng/mL), TIMP-1 (100,300 ng/mL) and IL-1β (1,20 ng/mL)) and the percentage of cell viability was assessed after AnnexinV/PI staining, as described in methods. (*p ≤ 0.05 vs untreated cells).*

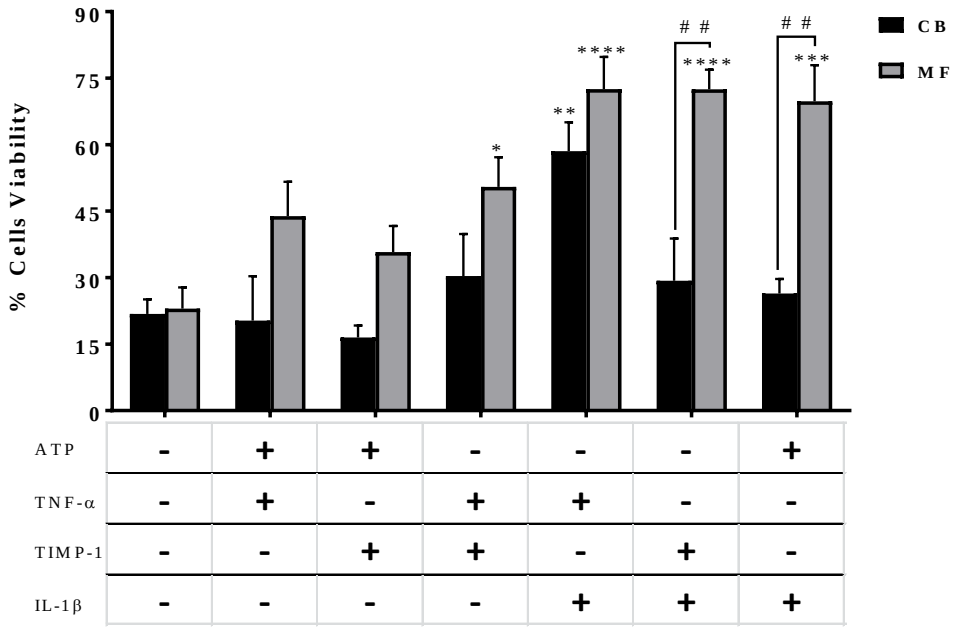

Supplementary Figure S2:

Survival of CD34$^+$ cells from MF patients is increased by various combinations of pro-inflammatory factors.

*CD34$^+$ cells from MF patients (n = 20) or CB (n = 8) were in vitro treated for 4 days with factors two by two and the percentage of cell viability was assessed after AnnexinV/PI staining, as described in Methods. Cells viability of MF-derived CD34$^+$ cells was significantly increased by IL-1β + TNF-α, IL-1β + TIMP-1, TNF-α + TIMP-1 and IL-1β + ATP as compared with untreated cells. Conversely, only the IL-1β + TNF-α combination was effective in stimulating the in vitro survival of the CB-derived CD34$^+$ cells. Comparing MF vs CB, IL-1β + TIMP-1 and IL-1β + ATP significantly promoted the survival of the MF-derived cells. All data are presented as mean ± SEM. (*p ≤ 0.05; **p ≤ 0.01; ***p ≤ 0.001; ****p ≤ 0.0001 vs untreated cells (CTR)) (##p ≤ 0.01 vs CB).*

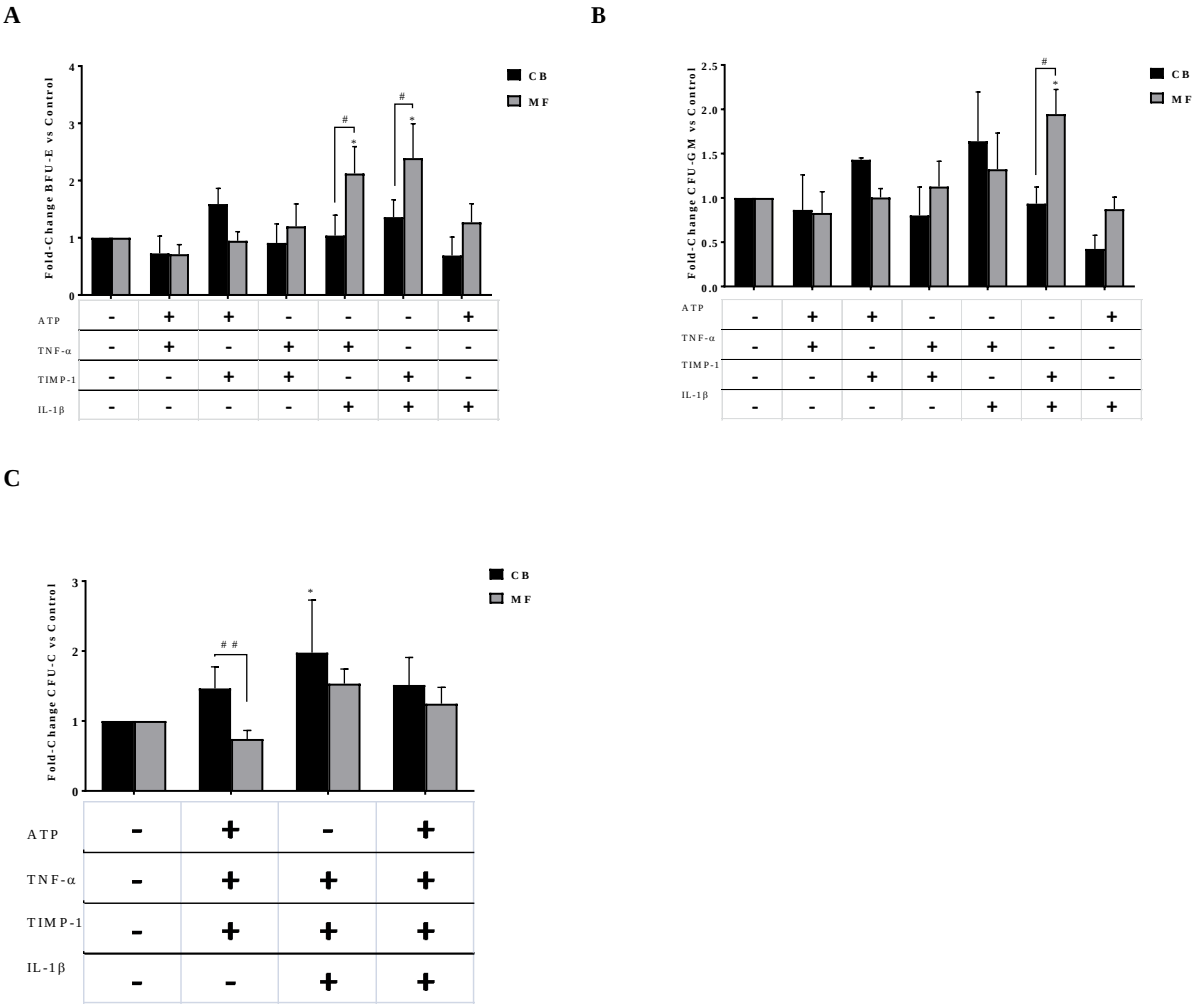

Supplementary Figure S3:

Effects of inflammatory factors on BFU-E/CFU-GM growth from MF- and CB-derived CD34$^+$ cells. *Circulating CD34$^+$ cells were isolated from MF patients (n = 20) and CB units (n = 8) and cultured in semisolid medium in the presence of the selected two-by-two or multiple pro-inflammatory factors. After 14 days, the BFU-E/CFU-GM (A and B) and the total CFU-C (C) output was assessed. (A) When IL-1β + TIMP-1 and IL-1β + TNF-α were added in culture, the BFU-E growth of MF-derived, but not CB-derived, CD34$^+$ cells was significantly increased as compared with the untreated samples and the CB counterparts. None of the others combinations were effective. (B) The growth of CFU-GM from MF-derived CD34$^+$ cells showed the same pattern displayed by BFU-E. (C) When various combinations of inflammatory factors were tested, MF-derived CD34$^+$ cells showed a decreased number of CFU-C compared to CB in response to ATP, TNFα, and TIMP. All data are presented as mean ± SEM. (*p ≤ 0.05 vs untreated cells) (# p ≤ 0.05; ##p ≤ 0.01 vs CB).*

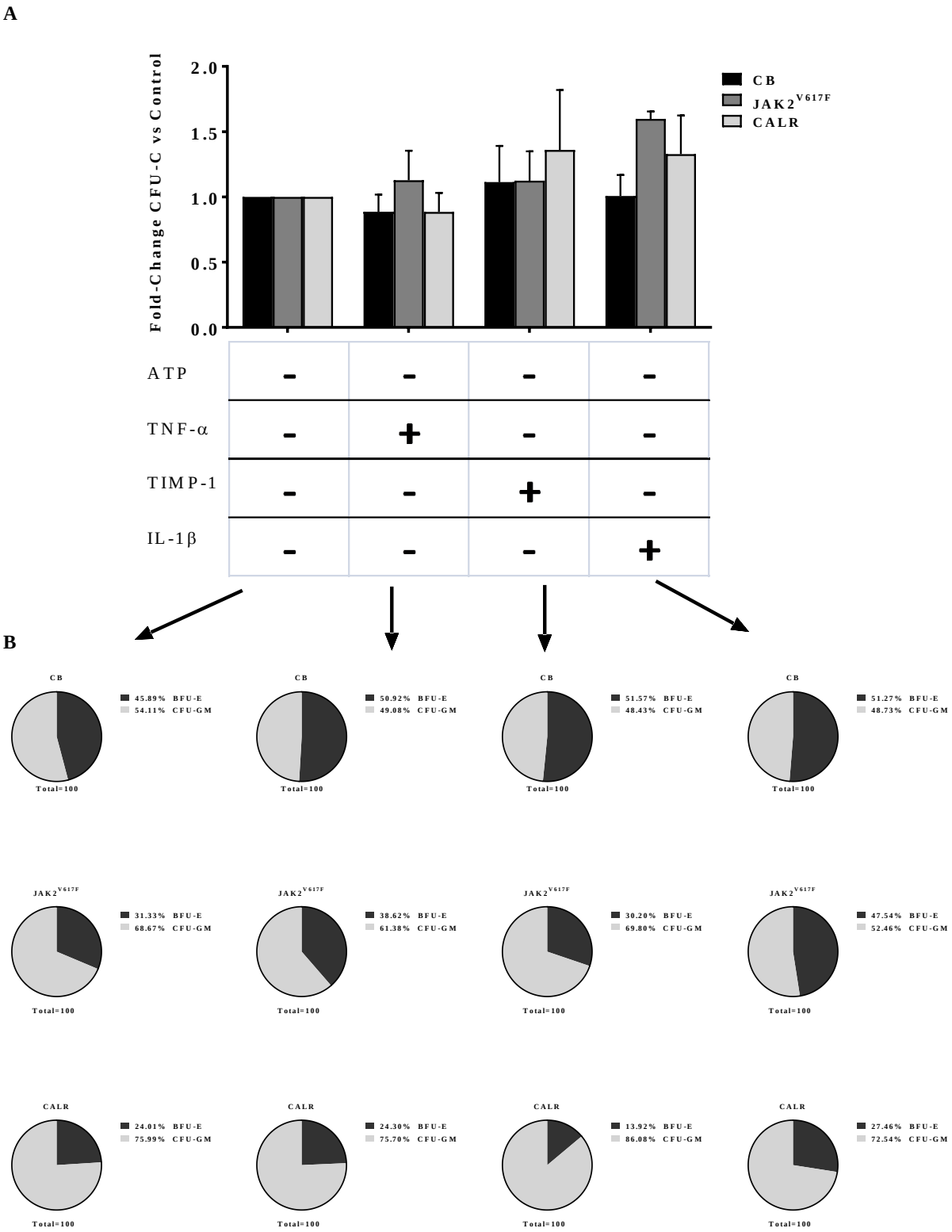

Supplementary Figure S4:

Effects of pro-inflammatory factors alone on CFU-C growth of CD34+ cells from JAK2V617F and CALR mutated patients. *(A) When CFU-C growth of CD34+ cells from JAK2V617F (n = 10) and CALR (n = 6) mutated patients was assessed in the presence of factors alone, no differences were observed between CB samples and between the two mutated groups. (B) Colony composition analysis demonstrated that only IL-1β enhanced the erythroid compartment of the JAK2V617F mutated group.*

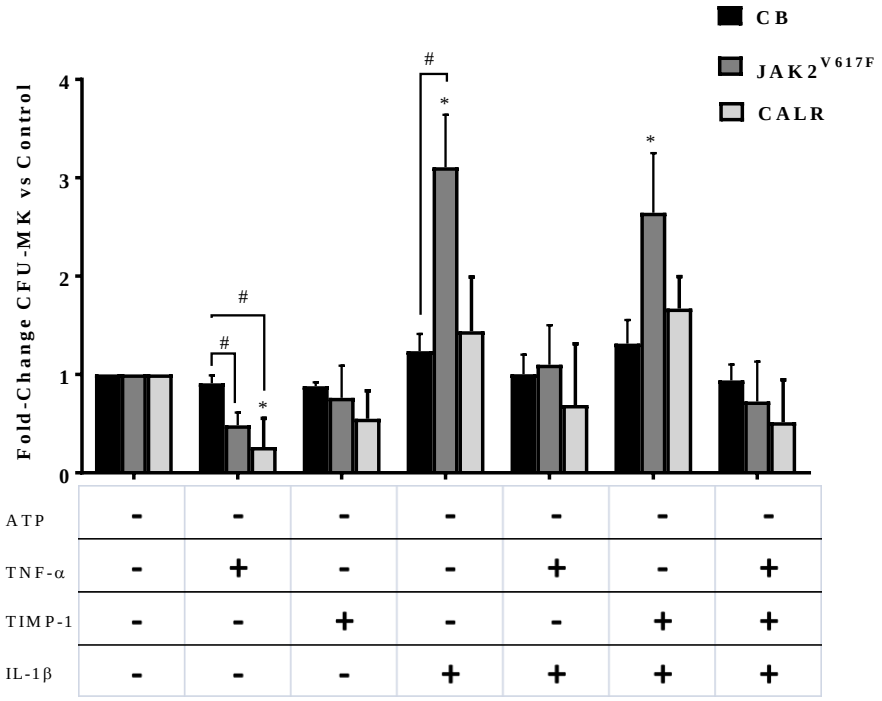

Supplementary Figure S5:

CFU-MK growth according to mutation status. *CFU-MK growth from JAK2V617F (n = 6) and CALR (n = 4) mutated patients was significantly inhibited by TNF-α as compared with CB counterparts. By contrast, IL-1β and IL1β + TNF-α stimulated the CFU-MK growth of JAK2V617F mutated patients (*p ≤ 0.05 vs untreated cells) (# p ≤ 0.05; ##p ≤ 0.01 JAK2V617F/CALR mutated patients vs CB).*

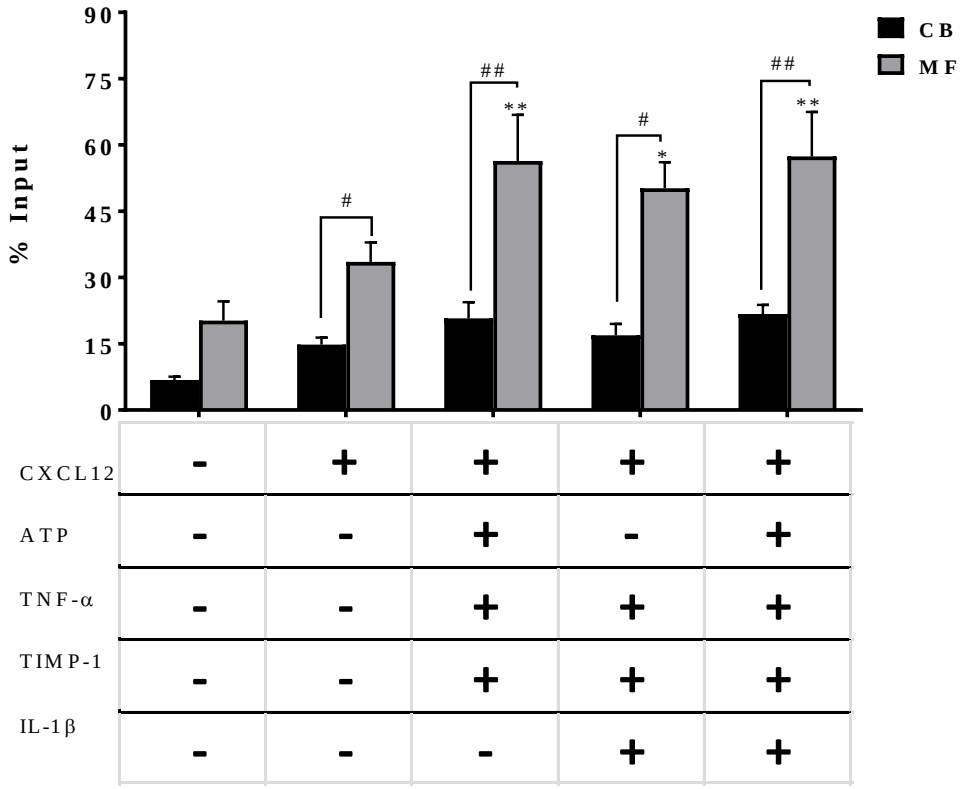

Supplementary Figure S6:

Various combinations of pro-inflammatory factors significantly promote migration of MFderived CD34$^+$ cells.

*When migration toward multiple combinations of factors + CXCL12 was analysed, the migration ability of MFderived (n = 15), but not CB-derived (n = 8), CD34$^+$ cells was significantly increased. (*p ≤ 0.05; **p ≤ 0.01 vs spontaneous migration) (# p ≤ 0.05;##p ≤ 0.01 vs CB). Results are expressed as mean percentages ± SEM of input.*

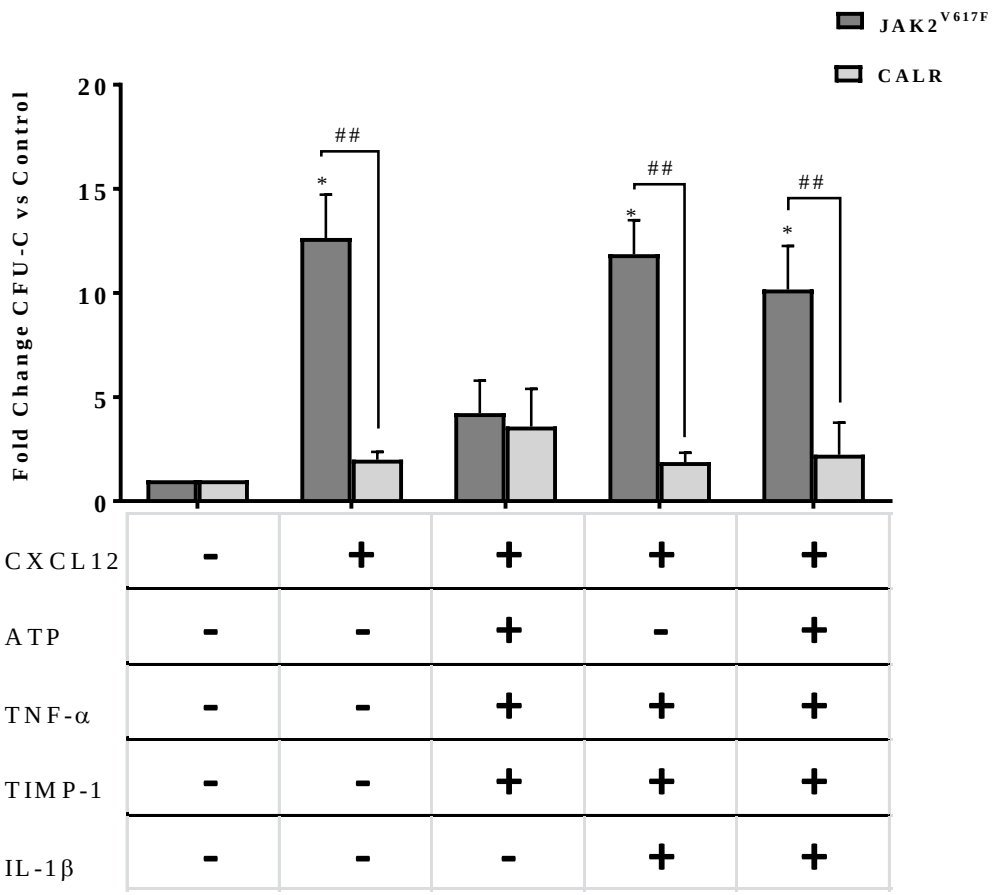

Supplementary Figure S7:

CFU-C post-migration assay according to mutation status. *The clonogenic potential of CD34^{+} cells from JAK2V617F (n = 8)/CALR (n = 6) mutated patients after migration toward CXCL12 alone or various combinations of proinflammatory factors + CXCL12 (CFU-C post-migration) is shown. After migration toward various combinations of pro-inflammatory factors, only the JAK2V617F-derived CD34^{+} cells show significantly increased clonogenic potential. Results are expressed as mean fold change of CFU-C ± SEM. (*p ≤ 0.05 vs spontaneous migration) (##p ≤ 0.01 JAK2V617F vs CALR mutated patients)*

– Results Ib

Published in

Mediators of Inflammation

2016;2016:5860657. Epub 2016 Sep 8.

http://dx.doi.org/10.1155/2016/5860657

CIRCULATING CALRETICULIN IS INCREASED IN MYELOFIBROSIS IRRESPECTIVE OF MUTATION STATUS: CORRELATION WITH INTERLEUKIN-6 PLASMA LEVELS, BONE MARROW FIBROSIS AND SPLENOMEGALY

D. Sollazzo*, D. Forte*, N. Polverelli, M. Perricone, M. Romano, S. Luatti, N. Vianelli, M. Cavo, F. Palandri§, L. Catani§

(*and § equally contributed)

Department of Experimental, Diagnostic and Specialty Medicine, Institute of Hematology 'L. and A. Seràgnoli', University of Bologna, Bologna, Italy

Key-words: Circulating Calreticulin, Myelofibrosis, Inflammation, Disease activity

ABSTRACT

MF is a clonal neoplasia of the hemopoietic stem/progenitor cells associated with genetic mutations in the Janus kinase 2 (*JAK2*), myeloproliferative leukemia virus oncogene (*MPL*) and *CALR* genes. MF is also characterized by a state of chronic inflammation. Calreticulin (CRT), as a multifunctional protein, is involved in a spectrum of cellular processes including inflammation and cancer initiation/progression. Based on this background, we hypothesised that in MF circulating CRT might reflect the inflammatory process and potentially serve as a previously undescribed marker of the disease. In the present study we show that, irrespective of mutational status, circulating CRT is increased in MF compared to healthy controls. Also, in MF CRT levels highly correlate with bone marrow (BM) fibrosis, splenomegaly and Interleukin-(IL)-6 plasma levels.In turn, higher IL-6 levels also correlated with disease severity in terms of increased spleen size, marrow fibrosis, number of circulating $CD34^{+}$ cells and lower hemoglobin values. These results suggest that the abnormally elevated circulating CRT takes part in the inflammatory network of MF, correlates with disease severity and may therefore be considered as a novel biomarker of disease activity.

INTRODUCTION

MF is a Philadelphia-negative myeloproliferative neoplasm (Ph-neg MPN) that may arise *de novo* (Primary Myelofibrosis, PMF) or after Essential Thrombocythemia (ET; PET-MF) and Polycythemia Vera (PV; PPV-MF). It is a clonal disorder of the hemopoietic stem/progenitor cells that is clinically characterized by worsening constitutional symptoms, progressive splenomegaly, bone marrow (BM) fibrosis and cytopenias as well as by an increased risk to develop thrombotic complications, second neoplasia and acute leukemia. MF is characterized by unfavourable prognosis with greatly shortened surviva.[71-73,121]

Approximately 50 to 60% of MF patients carry a mutation in the *JAK2* gene, while 20-25% of patients show recurrent mutations in the *CALR* gene and an additional 5 to 10% have activating mutations in the thrombopoietin receptor gene (myeloproliferative leukemia virus oncogene, *MPL*). Finally, less than 10% of patients have non-mutated *JAK2*, *MPL* and *CALR* genes ("triple negative").[76,79,121] Regardless of molecular status, all patients have a dysregulation in the JAK/STAT signalling.[76,122]

Together with molecular abnormalities, MF is characterized by abnormal expression of several pro-inflammatory and immunoregulating cytokines secreted by activated leukocytes and platelets/megakaryocytes. This inflammatory microenvironment has emerged as a key-player in MF pathogenesis, since it has been suggested that in MF stromal cells are primed by the malignant hematopoietic clone, which, in turn, conditions the stroma to create a favourable microenvironment that nurtures and protects the malignant cells. The up-regulated production of several pro-inflammatory cytokines, including TNF-α and IL-6, by both hemopoietic stem/progenitor cells and the surrounding stromal cells generates a microenvironment that selects for the malignant clone, leading to genomic instability and cancer progression.[80,81,91,123,124] Interestingly, cytokines levels were found to correlate with survival in PMF.[84]

Physiologically, CRT was first described as an endoplasmic reticulum protein responsible for Ca^{2+} homeostasis and glycoprotein folding; currently, CRT is recognized as a multifunctional chaperone detected in other cellular compartments, such as cytosol, nucleus and at the cell surface, as well as extracellularly, where it is involved in cell proliferation, apoptosis, adhesion, innate and adaptive immune processes including cancer cell elimination by immunogenic cell death and fibrosis.[125]CRT, both in vitro and in vivo, can inhibit the process of tumor-related angiogenesis.[126,127] In addition to its physiological roles, CRT over-expression is linked to various pathological conditions including chronic inflammatory diseases, autoimmunity, fibrosis-related

disorders and malignant evolution.[128-130] CRT may interact with different ligand/receptors to affect their signalling and therefore impact on apoptosis induction and/or phagocytic removal of apoptotic cells.[126] In MF, the mutated CRT protein was found to constitutively activate the MPL receptor signalling.[112,131]

Given the CRT involvement in inflammation, fibrosis and cancer, we hypothesised that in MF circulating CRT might reflect the inflammatory process and potentially serve as a previously undescribed marker of the disease. Here, for the first time, we characterized the circulating CRT levels of MF patients. Moreover, we investigated the correlation between CRT levels and various clinical and laboratory parameters.

RESULTS

Here we investigated 30 patients with MF: they were *JAK2*^{V617F} (16 cases), *CALR* (10 cases) and *MPL* (3 cases) mutated. One patient was triple-negative. Patients characteristics according to mutational status are shown in Table I. At the time of the study, patients were at diagnosis (17 cases) or untreated for at least two months. Previous therapies were: hydroxyurea (10 cases) and ruxolitinib (3 cases).

As shown in **Figure 1A**, we found significantly higher CRT plasma levels in MF patients as compared with healthy subjects (median: 5.2 ng/mL, range 1.4-25, vs 1.8 ng/mL, range 1.2-3.7; $p<0.0003$). Among MF patients, CRT plasma levels were not affected by mutational status, with no significant differences among patients carrying the *JAK2*, *CALR* or the *MPL* mutation (Figure 1B). No differences were observed between the CRT plasma levels of type 1 (8 cases) and type 2 (2 cases) *CALR* mutated patients. Also CRT plasma levels did not correlate with *JAK2*^{V617F} and *CALR* mutation load. No correlation was also observed between circulating CRT levels and hemoglobin levels, white blood cells/ platelets count, and circulating $CD34^{+}$ cells number.

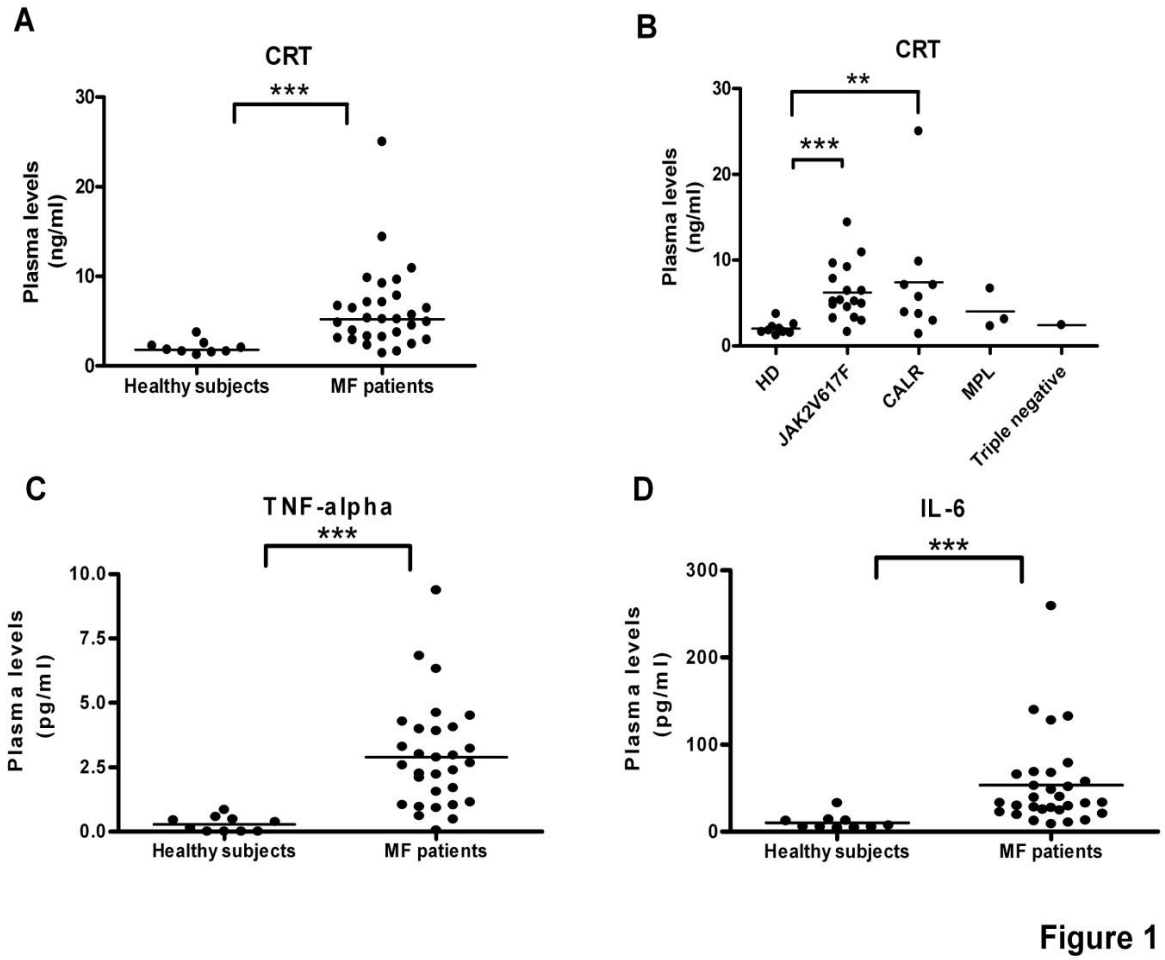

Figure 1

Figure 1

Analysis of the circulating levels of CRT, IL-6, and TNF-α proteins. The CRT plasma levels of total MF (a) or MF subdivided into JAK2^{V617F}-mutated (n = 16), CALR-mutated (n = 10), MPL-mutated (n = 3), and triple-negative-mutated (n = 1) groups (b) were measured by ELISA. *Compared with age-matched controls (HD; n = 10), CRT plasma levels were significantly increased in MF patients (p = 0.0028). Of note, there was no significant difference between the mutated groups. Irrespective of mutational status, TNF-α (c) and IL-6 (d) blood plasma levels were also increased in MF (p = 0.008). For all graphs, one symbol represents one individual, and the height of the bar represents the median value. $^{**}p \leq 0.01$; $^{***}p \leq 0.001$.*

Along with CRT plasma levels, circulating TNF-α (median: 2.62 pg/mL, range 0.05-9.37) and IL-6 (median: 33.3 pg/mL, range 8.7-258.9) were also increased in MF patients as compared to healthy subjects (median: 0.26 pg/mL, range 0-0.84 and median: 6.37 pg/mL, range 4.5-32.8, respectively; p<0.0001) (**Figure 1C** and **1D**). TNF-α and IL-6 plasma levels were not affected by mutational status and allele burden (data not shown). Interestingly, in MF patients there was a positive correlation between the plasma levels of CRT and BM fibrosis (p<0.04; r=0.39), splenomegaly (p<0.009; r=0.47) and circulating IL-6 (p<0.03; r=0.42) (**Figure 2A, 2B, 2C**). This

correlation was also irrespective of mutational status. In turn, IL-6 plasma levels correlated with BM fibrosis ($p<0.006$; $r=0.49$), splenomegaly ($p<0.02$; $r=0.46$), the number of circulating $CD34^+$ cells ($p<0.03$; $r=0.48$) and negatively with hemoglobin values ($p<0.05$; $r=-0.39$; **Figure 3A**, 3B, 3C, 3D).

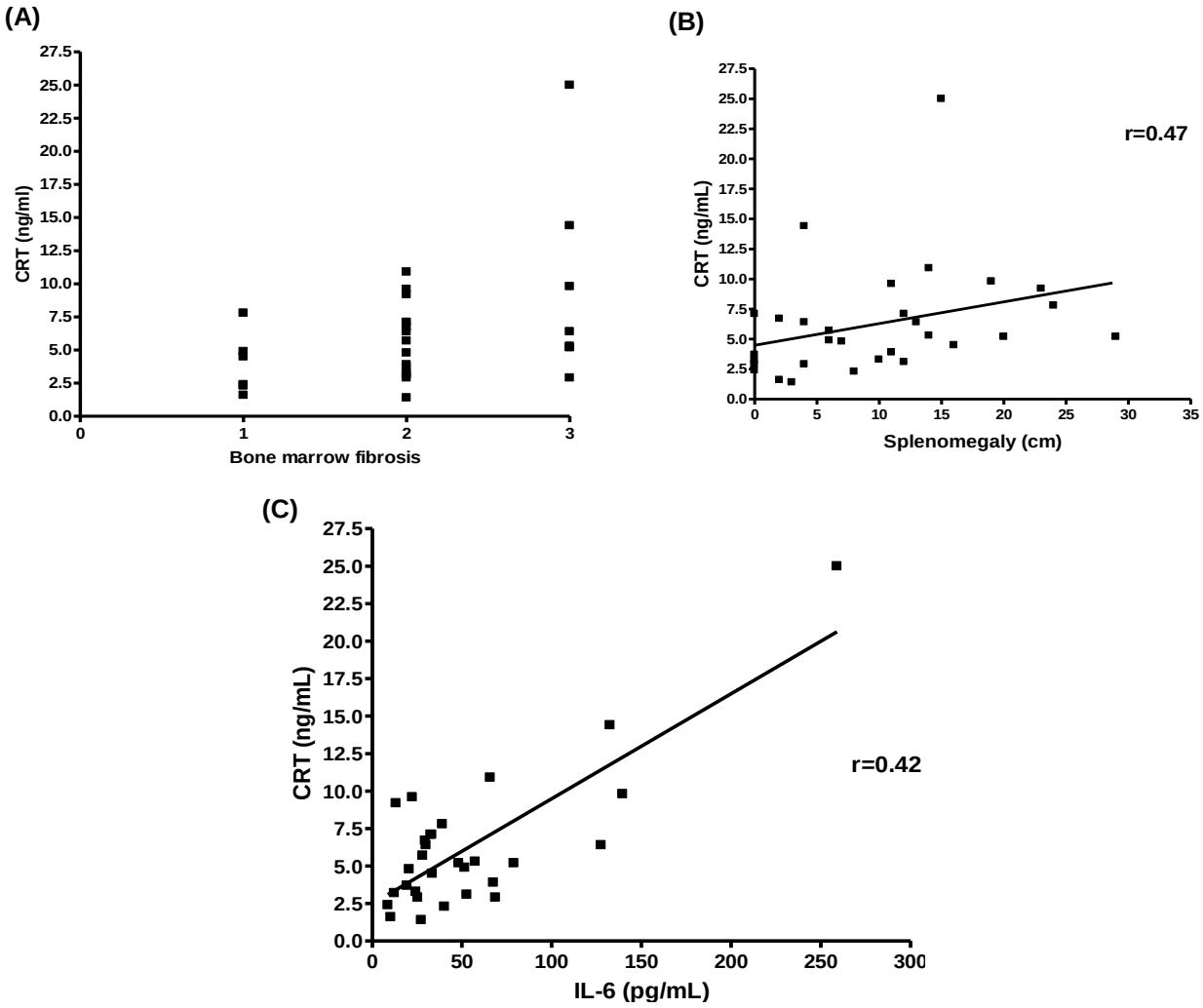

Figure 2

Correlation between CRT plasma levels and BM fibrosis, splenomegaly, and circulating IL-6. *Circulating CRT positively correlates with fibrosis, splenomegaly, and soluble IL-6 in MF. Scatter plots demonstrating correlation between the plasma levels of CRT and BM fibrosis ($p = 0.038$; $r = 0.39$), splenomegaly ($p = 0.0089$; $r = 0.47$), and circulating IL-6 ($p = 0.028$; $r = 0.42$) in MF patients (a, b, and c, resp.) are shown. x-axis of (a) shows BM fibrosis scale.*

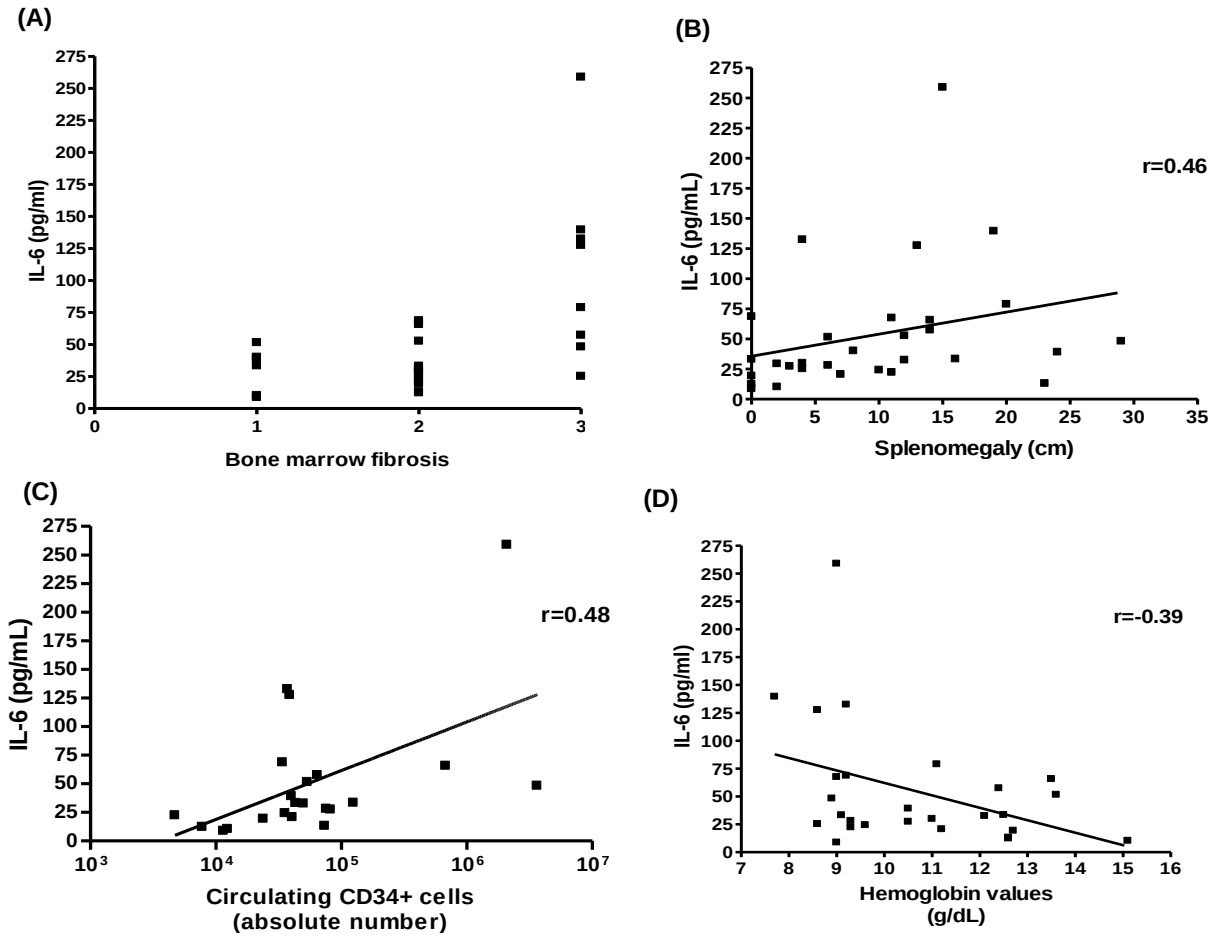

Figure 3

Correlation between IL-6 plasma levels and BM fibrosis, splenomegaly, number of circulating CD34 $^{+}$ cells, and hemoglobin values. *Irrespective of mutational status, IL-6 plasma levels correlated with BM fibrosis ($p = 0.0056$; $r = 0.49$), splenomegaly ($p = 0.018$; $r = 0.46$), and the absolute number of circulating CD34^{+} cells ($p = 0.029$; $r = 0.48$) and negatively correlated with hemoglobin values ($p = 0.047$; $r = -0.39$); (a, b, c, and d, resp.). x-axis of (a) shows BM fibrosis scale*

DISCUSSION

There has been a lack of understanding regarding the role of soluble CRT in MF. The first result of this study is that in MF CRT plasma levels are increased compared to healthy controls. CRT has been found to have a preferential expression in megakaryocyte/platelets, either from normal subjects or patients with Ph-neg MPN (and regardless of mutational status).[132] Therefore, these cells, which show abnormal number/function in MF, are likely to be the major contributors to the augmented amount of circulating CRT. Previous studies support the hypothesis that extracellular and soluble CRT is mainly released from dead, dying or inflamed/stressed cells.[125,128] Consequently, the high CRT levels detected in MF may primarily be due to the chronic inflammatory state that characterizes both the marrow and peripheral niche, and reflect an impairment in tissue homeostasis.

The second result is that CRT plasma levels are equally increased in *JAK2*^{V617F} and *CALR* mutated MF patients. In this study, we used an antibody that is directed against the N terminus of CRT and is expected to label both mutated and unmutated proteins. Therefore, the circulating protein that was detected in *CALR* positive patients is likely to be the sum of mutated (hemopoietic restricted) and unmutated molecules. This datum may suggest that the acquisition of mutations in the *CALR* gene, although causing the hyper-activation of the MPL receptor,[112,131] does not induce an increased circulating CRT amount.

Herein, we demonstrated also that CRT protein levels were found to directly correlate with the clinical aggressiveness of the disease in terms of larger spleen size and more severe marrow fibrosis. In addition, we found a direct correlation between circulating plasma levels of CRT and IL-6, one of the most potent pro-inflammatory cytokines that is up-regulated in MF.[133] In turn, higher IL-6 levels also correlated with disease severity in terms of increased spleen size, marrow fibrosis, number of circulating $CD34^+$ cells and lower hemoglobin values. The correspondence between CRT and IL-6 plasma levels may be at least partially justified by the recent discovery that soluble CRT induces active mRNA transcription through MAPK and NF-kB activation in macrophages, thereby augmenting their IL-6 and TNF-α production.[134] In addition, recently, conditioned media from cells expressing type I mutant *CALR* have been shown to exaggerate cytokines production from normal monocytes.[135] It is therefore likely that in MF the increased circulating CRT may contribute to the disease-related inflammation/fibrosis through positively enhancing IL-6 production. By contrast, despite TNF-α is a negative regulator of CRT

expression,[136] no correlation was observed between circulating CRT and TNF-α plasma levels in our MF patients, suggesting the presence of a TNF-α-independent mechanism of regulation.

Finally, considering the role of CRT in cancer, high abundance of the protein may have a positive or negative prognostic value. This may relate to the differential role of the endoplasmic reticulum-associated protein that promote cancer cells survival in harsh condition through its chaperone/Ca^{2+} homeostasis function versus the role of cell surface CRT on cancer cells that may induce anticancer immune response [as reviewed in [130]]. Moreover, since CRT overexpression increases the growth of various types of cancer cells,[129] including solid tumors and acute myeloid leukemia, we can hypothesize that the increased circulating CRT might promote the survival/growth of myeloid cells in the PB niche of MF.

Taken together, our data highlight the role of this protein in the inflammatory network of MF. A mutual interaction among CRT and other inflammatory cytokines including IL-6 may indeed contribute to the generation/maintenance of inflammation/fibrosis of MF. Further studies may elucidate whether other cytokines may also contribute to the generation/maintenance of BM fibrosis. Particularly, TGF-β, which is up-regulated in MF, has been recently recognized as a potent upstream regulator of CRT expression[137] and might therefore be involved in a pro-fibrotic bi-directional cross-talk with circulating CRT.

Potential limitation of the present study is the small sample size of patients. Nonetheless, our data create the rational basis for future studies investigating the role of circulating CRT in the inflammatory network of MF and other Ph-negative MPNs in larger cohorts of patients. Indeed, high CRT plasma levels in MF are signs of chronic systemic inflammation. Notably, due to correlation with fibrosis and splenomegaly, circulating CRT may be considered as a novel biomarker of disease activity/burden in MF patients and its measurement may be useful in clinical practice.

Although further research is needed to determine the spectrum of functions of CRT outside the cells, here we conclude that in MF the abnormally elevated plasma CRT levels are independent on mutation status but parallel the degree of disease activity and inflammation. Therefore, since soluble CRT links with disease activity and inflammatory status, our findings may contribute to identify patients with more severe disease, who might benefit from tailored therapy.

MATERIALS AND METHODS

Study population

Peripheral blood (PB) was obtained from 30 patients with MF in chronic phase and in 10 healthy age-matched volunteers. The diagnosis of MF was made according to WHO 2008 criteria.[138] Patients and controls provided written informed consent for the study. This study was approved by the medical Ethical Committee of the University Hospital of Bologna and was conducted in accordance with the Declaration of Helsinki.

Table 1

Patients characteristics according to mutational status. Compared to CALR-mutated patients, patients with $JAK2^{V617F}$ mutation were older (p = 0.01) and had higher hemoglobin levels (p = 0.04).

Characteristics	$JAK2^{V617F}$-mutated patients (number = 16)	CALR-mutated patients (number = 10)	MPL-mutated patients (number = 3)	"Triple-negative" patients (number = 1)
Median age, years (range)	73 (67–84)	65.5 (44–82)	76 (72–76)	67
Male sex, number (%)	9 (56)	6 (60)	1 (33.3)	0 (0)
Median allele burden, % (range)	89 (0.4–99)	56.5 (52–98)	NA	NA
Median WBC, $\times 10^9$/L (range)	10.6 (2.5–157.6)	7.15 (2.3–48.3)	6.2 (4.9–25)	6.7
Median hemoglobin, g/dL (range)	11.1 (8.6–15.1)	9.3 (7.7–14)	9.7 (7.2–9.9)	8.5
Median platelet count, $\times 10^9$/L (range)	280 (41–507)	195.5 (86–419)	196 (46–303)	632
High/intermediate 2 IPSS category, number (%)	9 (56)	6 (60)	3 (100)	1 (100)
Unfavorable karyotype, number (%)	8 (50)	2 (20)	2 (66.6)	1 (100)
Diagnosis, number (%)				
PMF	8 (50)	6 (60)	3 (100)	1 (100)
PET	3 (19)	2 (20)	—	—
PPV	5 (31)	2 (20)	—	—
BM fibrosis grade ≥ 2, number (%)	12 (75)	10 (100)	2 (66.6)	0 (0)
Patients with splenomegaly, number (%)	14 (87.5)	8 (80)	3 (100)	0 (0)

WBC: white blood cells; IPSS: International Prognostic Scoring System; PMF: primary myelofibrosis; NA: not available. Splenomegaly was evaluated by palpation as cm below costal margin. Only patients with a spleen palpable ≥ 5 cm below costal margin by palpation were considered as carrying splenomegaly.

Assay of circulating proteins

Here we analysed the plasma levels of CRT in patients/controls. EDTA-anticoagulated PB was centrifuged for 15 minutes at 1000g within 30 minutes of collection. The plasma was then collected and stored at -80°C until quantification. CRT was evaluated by a commercially available ELISA assay (Cusabio Biotech Co., Wuhan, P.R.China), according to the manufacturer's instructions.

Briefly, a standard curve of 100-µl aliquots of known concentrations of recombinant CRT was run and triplicate 100 µL samples were added to the wells. CRT binding was detected using a biotin/avidin system. The plates were then assessed by ELISA on a plate reader at 450 nm. The Ciraplex^{TM} immunoassay kit / Human 9-Plex Array (Aushon BioSystems, Billerica, MA, USA) was used for the measurement of circulating IL-6 and TNF-α.

Molecular pattern

Molecular analyses were assessed at diagnosis or before treatment start on DNA obtained from granulocytes. Driver mutations were analysed as previously described.[115] Specifically, *JAK2*^{V617F} mutation was evaluated with ipsogen *JAK2* MutaQuant Kit (Qiagen, Marseille, France) on 7900 HT Fast Real Time PCR System (Applied Biosystem, Monza, Italy). The percentage of mutant *JAK2*^{V617F} allele was expressed as the ratio of *JAK2*^{V617F} copies to total copy number (CN) of *JAK2* (CN of *JAK2*^{V617F} + CN of *JAK2* wild type). *CALR* exon 9 *s*equencing was performed by Next Generation Sequencing (NGS) approach with GS Junior (Roche-454 platform; Roche Diagnostics, Monza, Italy); analysis was carried out with AVA Software (GRCh38 as referenced). Type 1 and type 2 *CALR* mutations were identified as previously described.[76] Rare *CALR* mutations identified by NGS were confirmed by Sanger sequencing. *MPL* mutations were investigated by ipsogen *MPLW515K/L* MutaScreen Kit (Qiagen) and by Sanger sequencing (for *MPLS505N* and other secondary exon 10 mutations).

Cytogenetic analysis

Chromosome banding analysis was performed on BM cells by standard banding techniques according to the International System for Human Cytogenetic Nomenclature. At least 20 metaphases were required. Unfavorable karyotype was defined according the Dynamic International Prognostic Score System - plus (DIPSS, [139]) and included complex karyotype or single or two abnormalities including +8, -7/7q-, i(17q), -5%5q-, 12p-, inv(3) or 11q23 rearrangement.

Statistical analysis

Statistical analyses (Student's T Test and Spearman correlation analysis) were performed using Graphpad (Graphpad Software Inc., La Jolla, CA). All *p* values were considered statistically significant when ≤0.05 (2-tailed).

– Results II

Published in

Oncotarget.

2017 Jan 10;8(2):2261-2274. doi: 10.18632/oncotarget.13664.

THE TISSUE INHIBITOR OF METALLOPROTEINASES-1 (TIMP-1) PROMOTES SURVIVAL AND MIGRATION OF ACUTE MYELOID LEUKEMIA CELLS THROUGH CD63/PI3K/AKT/P21 SIGNALING

D. Forte[1], V. Salvestrini[1], G. Corradi[1], L. Rossi[1], L. Catani[1], R. M. Lemoli[2], M. Cavo[1] and A. Curti[1]

[1] Dept. of Experimental, Diagnostic and Specialty Medicine (DIMES), Inst. of Hematology "L. and A. Seràgnoli", University of Bologna, Italy

[2] Clinic of Hematology, Department of Internal Medicine (DiMI), University of Genoa, Genoa, Italy

Key words. Acute Myeloid Leukemia, inflammation, microenvironment, migration, TIMP-1

ABSTRACT

We and others have shown that the TIMP-1, a member of the inflammatory network exerting pleiotropic effects in the BM microenvironment, regulates the survival and proliferation of different cell types, including normal hematopoietic progenitor cells. Moreover, TIMP-1 has been shown to be involved in cancer progression. However, its role in leukemic microenvironment has not been addressed. Here, we investigated the activity of TIMP-1 on Acute Myelogenous Leukemia (AML) cell functions. First, we found that TIMP-1 levels were increased in the BM plasma of AML patients at diagnosis. *In vitro,* recombinant human (rh)TIMP-1 promoted the survival and cell cycle S-phase entry of AML cells. These kinetic effects were related to the downregulation of cyclin-dependent kinase inhibitor p21. rhTIMP-1 increases CXCL12-driven migration of leukemic cells through PI3K signaling. Interestingly, activation of CD63 receptor was required for TIMP-1's cytokine/chemokine activity. Of note, rhTIMP-1 stimulation modulated mRNA expression of HIF-1α, downstream of PI3K/Akt activation. We then co-cultured AML cells with normal or leukemic MSCs to investigate the interaction of TIMP-1 with cellular component(s) of BM microenvironment. Our results showed that the proliferation and migration of leukemic cells were greatly enhanced by rhTIMP-1 in presence of AML-MSCs as compared to normal MSCs. Thus, we demonstrated that TIMP-1 modulates leukemic blasts survival, migration and function via CD63/PI3K/Akt/p21 signaling. As a "bad actor" in a "bad soil", we propose TIMP-1 as a potential novel therapeutic target in leukemic BM microenvironment.

INTRODUCTION

AML is a clonal disorder which originates from a rare population of leukemia stem cells (LSCs).[140] Over the last years major efforts have been made to improve the clinical outcome of AML patients; however, their overall prognosis is still poor especially for patients harboring unfavorable biologic factors at diagnosis.[141,142]

Recent reports have unveiled a pathogenetic link between inflammation and oncogenesis.[143-146] Whereas this finding is well-accepted for solid tumors, the relationship between inflammatory networks and leukemogenesis has not been fully elucidated. Nonetheless, recent data highlight how HSPCs fate is dictated by intrinsic and extrinsic factors and how HSPCs may actively sense danger signals and pro-inflammatory cytokines.[2,147,148] Moreover, the cross-talk between leukemic cells and BM stromal cells may create a suitable environment that promotes malignant transformation and disease progression. Several factors and pathways have been implicated and described.[149,150] Among them, the tuned regulation of the balance between synthesis and degradation of extra-cellular matrix (ECM) macromolecules by matrix metalloproteinases (MMPs) and their inhibitors is critical.[151] Indeed, an altered MMPs/Tissue Inhibitor of MetalloProteinases-1 (TIMP-1) expression or activity affects steady state hematopoiesis and results in increased cell proliferation, thus favoring oncogenesis, including leukemogenesis.[152] Indeed, TIMP-1 levels increase in response to inflammation.[101] Initially described as an endogenous inhibitor of MMPs and the membrane-bound metalloproteinase ADAM-10, TIMP-1 also displays cytokine-like functions, mediated by the engagement of a specific membrane receptor, namely CD63.[153] CD63 is known as a member of the tetraspanins, that are a superfamily of cell surface-associated membrane proteins involved in cell activation, adhesion, differentiation and tumor invasion.[154] In breast cancer and melanoma cells, CD63 is abundantly expressed and interacts with TIMP-1 at cell surface, resulting in activation of cell survival signalling.[155,156] At the functional level, TIMP-1 exerts pleiotropic effects in the BM microenvironment, such as the regulation of cellular proliferation, apoptosis and differentiation.[156-158] In particular, we previously found that TIMP-1 regulates the function of HSPCs promoting clonogenic efficiency and survival of normal $CD34^+$ cells via the activation of the CD63/PI3K/pAkt signaling pathway, suggesting that TIMP-1 may be a key player in the network of pro-inflammatory factors modulating HSPC functions. Similarly, in solid tumors, TIMP-1 improves the metastatic potential of cancer cells.[159] Interestingly, upregulated TIMP-1 levels are associated with unfavourable prognosis in several tumors including breast or colorectal cancer and lung

carcinoma.[160-162] In hematological malignancies, TIMP-1 promotes differentiation of lymphoma cells whereas increased TIMP-1 serum levels are associated with advanced myeloma.[163-166]

In the present study we investigated, *in vitro*, the function and molecular pathways mediated by TIMP-1 in the microenvironment of AML, providing further evidence to support the relationship between inflammation and leukemia. A better definition of the mechanisms regulating the interplay of leukemic cells within BM microenvironment, may have important clinical implications for the development of novel and effective therapeutical strategies.

RESULTS

TIMP-1 is detectable in BM and PB of AML patients

In normal hematopoiesis, TIMP-1 regulates the survival and proliferation of different cell types.[101,104] However, its role in AML BM microenvironment is not yet clear. Therefore, we first evaluated the BM plasma and PB serum level of TIMP-1 in leukemic patients at diagnosis. We found detectable amounts of TIMP-1 both in BM and PB with a median concentration of 112.6 ng/ml (range 72.25-157.3 ng/ml) and 139.4 ng/ml (range 84.47-273.9 ng/ml), respectively (**Figure 1A-B**). In particular, compared with control BM samples, the plasma levels were increased in AML patients ($p \leq 0.05$). These results extend previous data in other hematological malignancies, such as pediatric ALL[167] and suggest the potential functional role of TIMP-1 within AML microenvironment. Moreover, they indicate the optimal concentration of TIMP-1 for functional studies.

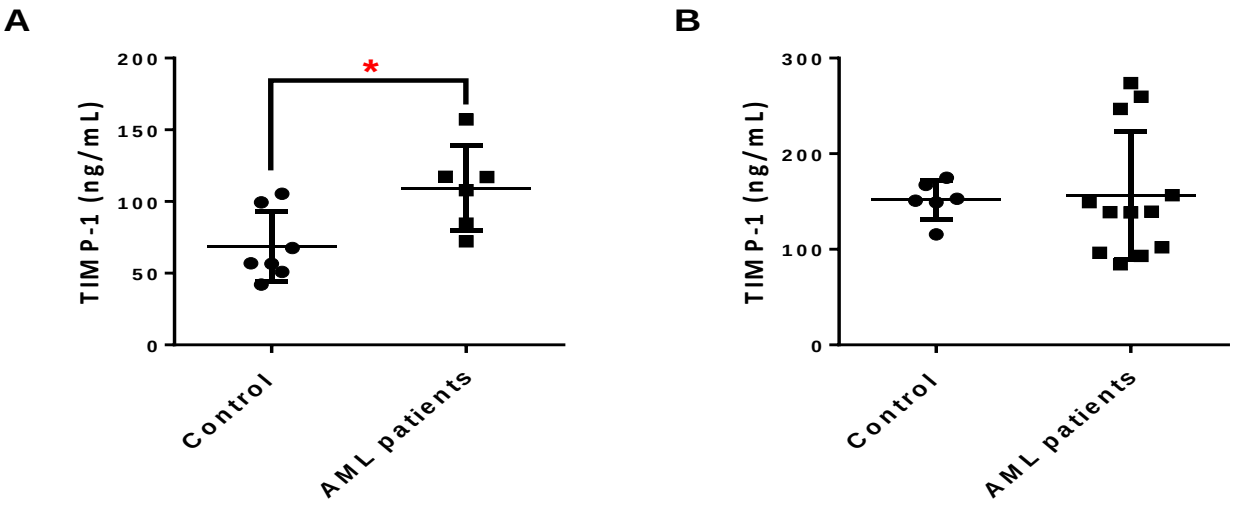

Figure 1

TIMP-1 levels were measured by ELISA in in plasma and serum of AML patients and control samples. *A) BM plasma concentrations of TIMP-1 were compared between AML patients at diagnosis (n=6) and control samples (*p < 0.05). B) In addition, PB serum concentrations of TIMP-1 were quantified in patients (n=12) and compared to control samples.*

TIMP-1 increases the clonogenic efficiency of AML blasts maintaining an apoptosis-resistant phenotype

In our previous work,[104] we found that TIMP-1 increases the clonogenic efficiency of normal HSPCs isolated from umbilical CB units. Thus, we studied the effects of increasing concentration of TIMP-1 (ranging between 10-300 ng/ml) on the clonogenic output of 14 primary AML at diagnosis. As shown in **Figure 2A**, TIMP-1 (at 100 ng/mL) significantly increased colony formation (CFU-L) from AML patients ($p \leq 0.01$). In addition, the CFU-GM growth was positively enhanced by TIMP-1 (**Supplementary Figure 1**, $p \leq 0.01$).

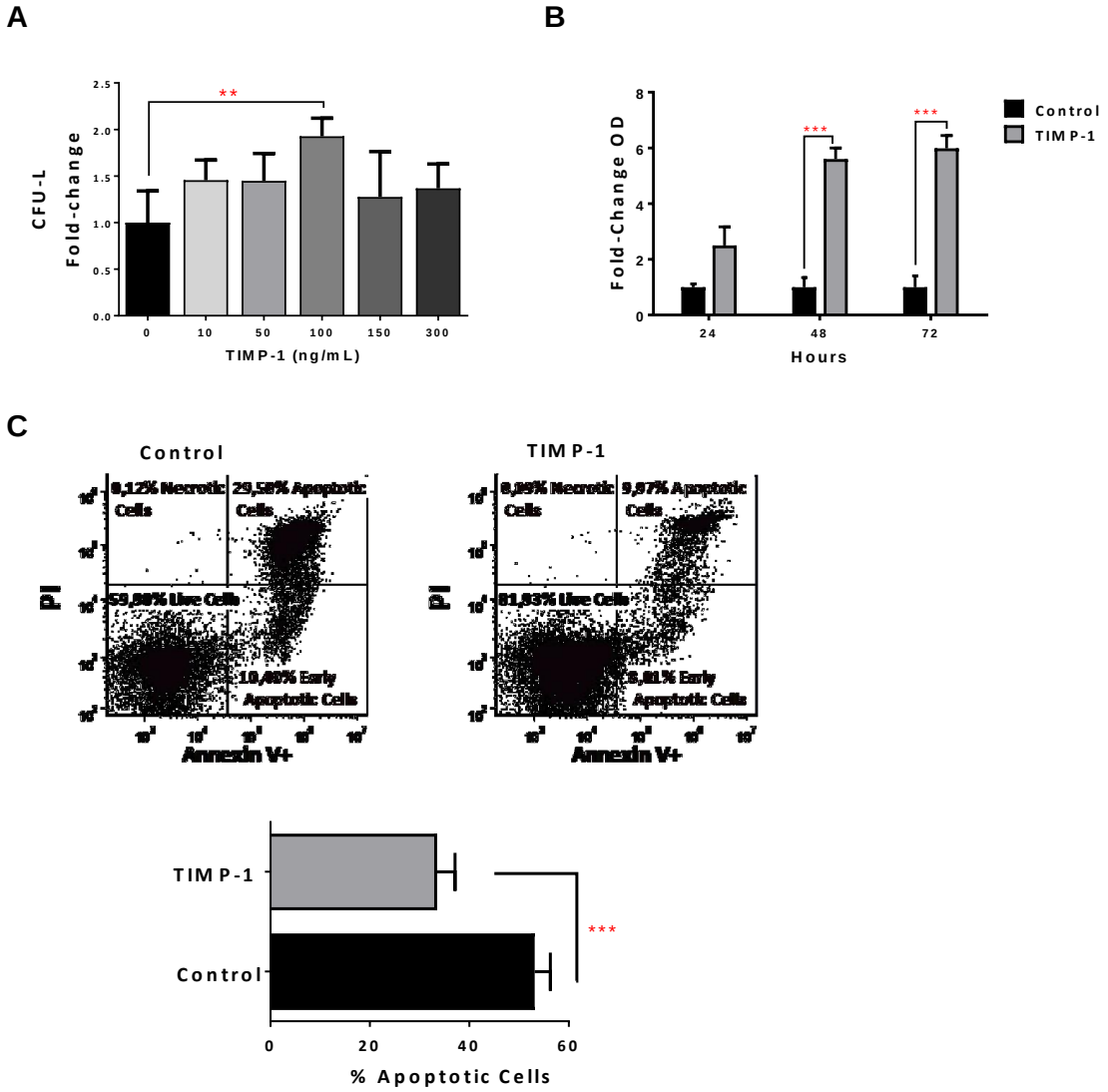

Figure 2

Clonogenic output and survival of leukemic blasts is positively enhanced by exposition to TIMP-1

*Circulating leukemic blasts were isolated from AML patients (n=12) and cultured in semisolid medium in the presence of TIMP-1. After 14 days, the total CFU-L output was assessed as above described. A) The clonogenic output of the AML-derived leukemic cells was significantly stimulated by TIMP-1 (100 ng/ml, **p ≤ 0.01). No other concentration of*

TIMP-1 were effective. The results are expressed as growth fold change versus untreated control samples. The mean number of colonies in untreated (0 ng/ml) and treated (100 ng/ml) AML samples was 18.8 ± 5.8 vs 30.2 ± 9.2, respectively. Specifically, only 2 patients (PT #6 and #13 in the Table patients) were not responsive to TIMP-1 treatment in CFU-L assay. Data are presented as mean ± SEM of 12 patients, the error bars are the mean of each duplicate.

*Survival of leukemic blasts from AML patients is positively enhanced by TIMP-1. B) AML blasts were cultured for 24-48-72 hrs in the presence of TIMP-1 (48-72 hrs, *** $p \leq 0.001$; n=3). Survival rate is evaluated by cell titer assay and expressed as fold-change taking the value of untreated cells at each time point as 1. C) AML cells from 14 patients were in vitro treated for 2 days with TIMP-1 and the percentage of cell viability was assessed after AnnexinV/PI staining, as described in methods. Representative dot-plots showing the percentage of live, apoptotic and necrotic cells in leukemic blasts as determined by flow cytometry. Mean of percentage in apoptotic cell (Annexin V positive and both Annexin V/ PI positive cells) in the presence or absence of TIMP-1 (***$p \leq 0.001$). The mean percentage of apoptotic cells (Annexin V positive and both Annexin V/ PI positive cells) was 53.0 ± 3.1% (range: 34.5-74.6) for control and 33.0 ± 3.5% (range: 15.4-53.0) for TIMP-1 treated cells. Data are presented as mean ± SEM*

When we tested myeloid differentiation markers (CD38 and CD11b) or hemopoietic stem/progenitor cells marker (CD34) in the blasts of AML patients, we did not find any differences between untreated or TIMP-1 treated AML samples (data not shown). We then investigated whether TIMP-1 promotes the survival of AML blasts. To this end, we treated leukemic cells with the optimal concentration of TIMP-1 (i.e. 100 ng/mL) and we evaluated cell viability at different time points by colorimetric assay (MTS assay). As summarized in **Figure 2B**, after 48 and 72 hours, the addition of TIMP-1 significantly increased the number of viable leukemic blasts, as evaluated as fold-change over control sample (5.6- and 5.9-fold increase, respectively; $p \leq 0.001$). Moreover, when we evaluated the apoptotic rate of leukemic blasts, we found that AML cells incubated for up to 72 hours in presence of TIMP-1 showed a significant decrease in their programmed cell death (**Figure 2C**). In particular, the mean percentage of apoptotic cells was reduced in presence of TIMP-1 as compared to control samples (33 ± 3.5% and 53 ± 3.14%, respectively; $p \leq 0.001$). Overall results and data from a representative example (panel C) are shown in **Figure 2** and from individual patients (**Supplementary Figure 2**). Taken together, these data demonstrate that TIMP-1 promotes the survival and the clonogenic activity of leukemic blasts by significantly reducing apoptosis.

TIMP-1 stimulates cell cycling of leukemic blasts in association with p21$^{WAF1/CIP1}$ downregulation

We then studied the effect of TIMP-1 on cycling of AML cells. As shown in **Figure 3A**, after 24 hours of TIMP-1 incubation, we observed a reduced percentage of cells in G0/G1 phase (percentage of untreated G0/G1-phase cells 86.66 ± 1.34 % vs 77 ± 3.03 % of TIMP-1-treated cells; $p \leq 0.05$). Simultaneously, we detected a slight, but significant, increase in the percentage of leukemic cells in S-phase (percentage of untreated S-phase cells 7.4 ± 0.77 % vs 15.5 ± 3.1% of TIMP-1-treated cells; $p \leq 0.01$). These data suggested a role of TIMP-1 in promoting AML cell cycle progression. In order to confirm this observation, we analyzed the effect of TIMP-1 on expression of p21$^{WAF1/CIP1}$, a cell cycle inhibitor (**Figure 3B**).[168] Interestingly, the normalized mean fluorescence intensity (nMFI) of p21 expression was significantly reduced in leukemic cells after exposure to TIMP-1 for 24 hours as compared with untreated cells (nMFI: 3.1±1.1 vs 4.5±1.5, respectively; $p \leq 0.05$; data not shown). To further confirm our results, we analysed p21 protein reduction by western blot (**Figure 3C**). This assay confirmed the reduction of p21 protein after treatment with TIMP-1, whereas transcript levels were not affected (data not shown). These results suggest that TIMP-1 stimulates cell-cycle progression of leukemic blasts from AML patients.

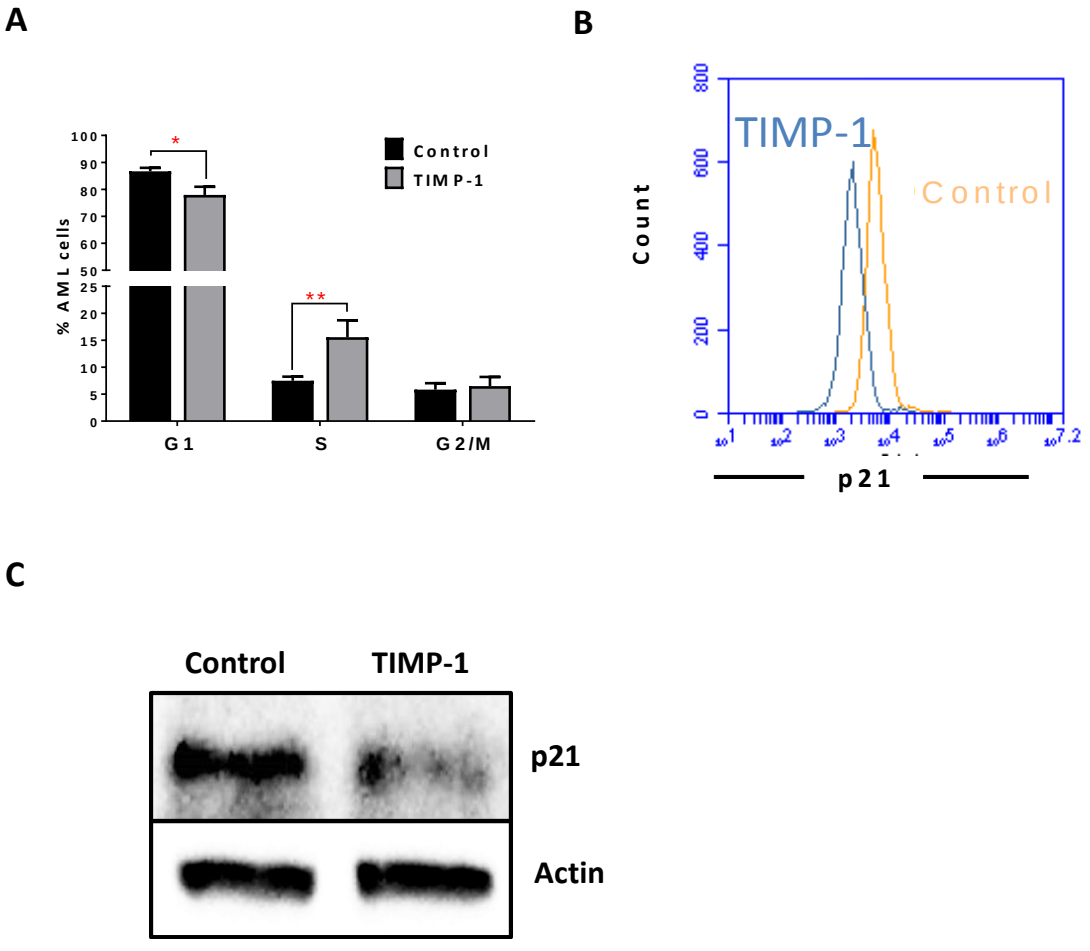

Figure 3

TIMP-1 promotes cell cycle of leukemic blasts.

*A) Results are expressed as the percentage of cells in different phases of the cell cycle. TIMP-1 promote cell cycling of leukemic blasts cells from AML patients (phase G1 *p ≤ 0.05 and phase S **p ≤ 0,01; n=9). Their distribution in the different phases of cell cycle was assessed by PI staining after 24 hrs. Data are presented as mean ± SEM. B) Representative histogram of $p21^{WAF1/CIP1}$ of leukemic blasts after exposure to TIMP-1 for 24 hrs. The downregulation of cyclin-dependent kinase inhibitor p21WAF1/CIP1, which promotes cell cycle progression, were measured by flow cytometry as MFI, and is shown only in the presence of TIMP-1 (MFI: 2275 ± 524 TIMP-1 treated cells vs 3110 ± 223,1 untreated cells; n=12). Specifically, only 2 patients (PT #11 and #15 in the Table patients) were not responsive to TIMP-1 treatment in p21 downregulation. C) AML cells were incubated with TIMP-1 for 24 hrs and the relative level of p21 protein was determined by western blotting (n=2). Representative western blot of one AML patient. β-actin was used as a loading control.*

TIMP-1 enhances CXCL12-driven migration of AML blasts

To test the effect of TIMP-1 on the migratory capacity of AML cells, we assessed, *in vitro,* the response of AML cells toward a CXCL12 gradient in presence or absence of TIMP-1. As reported in **Figure 4A**, the migration rate of AML cells, when TIMP-1 was added in absence of CXCL12, was not significantly higher than control samples. Although these results could rely, at least in part, on TIMP-1's survival effects, the addition of TIMP-1, in presence of CXCL12, increased the migration rate of leukemic cells over that observed with medium (spontaneous migration) and CXCL12 alone ($p \leq 0.0001$ and $p \leq 0.01$, respectively). Conversely, when TIMP-1 was added to CXCL12 as chemo-attractant, the migration of AML cells was not significantly increased. No differences in spontaneous or CXCL12-induced migration were observed when PB or BM cells were compared (data not shown). However, migration of TIMP-1 treated PB cells toward CXCL12 gradient was slightly higher than the migration of the BM cells (PB vs BM, 57.14% ± 5.5% vs 46.09% ± 7.7%, respectively; p=ns). To further support this finding, we investigated the migratory response of AML cells after pre-incubation with AMD3465, a potent and selective CXCR4 antagonist and anti-TIMP-1 neutralizing Ab. After incubation with AMD3465, the migration of leukemic blasts was inhibited and the effect of CXCL12 was comparable to medium alone (**Figure 4B**). Importantly, pre-incubation with the CXCR4 inhibitor completely abrogated the effect of TIMP-1 treatment toward CXCL12-gradient ($p \leq 0.001$). Also, anti-TIMP -1 neutralizing Ab reversed the effects of TIMP-1 on migratory response of AML cells.

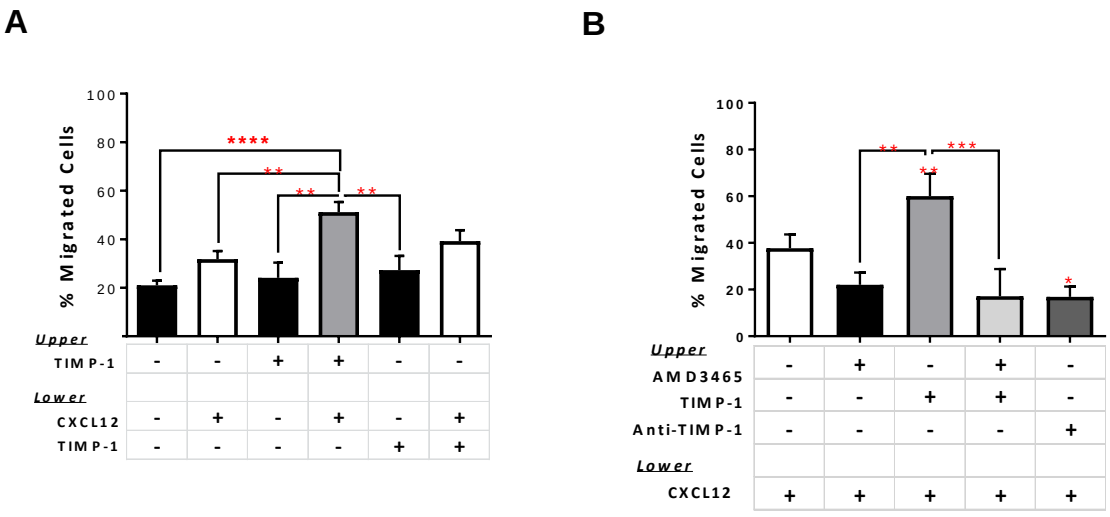

Figure4

Pre-treatment with TIMP-1 significantly promotes migration of AML cells.

*A) AML cells were seeded in the upper compartment of a chamber Transwell migration assay ±TIMP-1 (100 ng/ml) (n=18). TIMP-1 was added to the bottom compartment with or without CXCL12 (100 ng/ml), whereas was used alone in the top compartment. After over-night at 37°C, cells in the bottom compartments were counted and percentage of migrated cells calculated. (**p ≤ 0.01; ****p ≤ 0.0001; n=18). The mean number of migrated cells was 13031 ± 2161 for spontaneous migration, 15410 ± 2367 for migration toward CXCL12 gradient, 23581 ± 3204 in the presence of TIMP-1 toward CXCL12 gradient and 22070 ± 4050 in the presence of TIMP-1 and CXCL12 as chemo-attractants.*

*B) Migrated AML-derived leukemic blasts toward CXCL12 gradient after pre-treatment with AMD3465 (CXCR4 antagonist) for 30 min ± TIMP-1 (n=9) or anti-TIMP-1 neutralizing Ab (5µg/ml; n=3) to evaluate the effects on migratory rate (*p ≤ 0.05; **p ≤ 0.01; ***p ≤ 0.001). Data are presented as mean ± SEM*

CD63 is required for TIMP-1-mediated effects on AML blasts

To elucidate the molecular pathway ignited by TIMP-1 and its cytokine-like activity in leukemic blasts, we first investigated the expression and the functionality of CD63, which is known to mediate TIMP-1 effect.[153] The mean percentage of CD63-positive blasts from the total of AML patients was 60.83% ± 5.485% (range, 26.40-93.40). In particular, the mean percentage was 64.05% ± 8.024% (range, 32.1-93.4) in PB samples and 56.53% ± 7.476% (range, 26.4-79.6) in BM samples. Of note, we did not find any significant correlation between patient characteristics and CD63 expression or different functions mediated by TIMP-1 (data not shown). Interestingly, migrated leukemic blasts toward CXCL12 plus TIMP-1 had a significantly increased expression of CD63 as compared to the cells migrated toward CXCL12 alone ($p \leq 0.05$) (**Figure 5A**). We then,

sorted CD63 positive and negative leukemic blasts and tested their ability to respond to TIMP-1 in migration assay. Noteworthy, only the migratory capacity of $CD63^+$ fraction appeared significantly promoted ($p \leq 0.05$; **Figure 5B**), while the proportion of migrating $CD63^-$ AML cells in presence of TIMP-1 cells was comparable to that migrated with CXCL12-gradient alone. Overall, these findings support the hypothesis that TIMP-1 modulates the CXCL12-mediated migration through the interaction with the CD63 receptor, exerting cytokine-like function in leukemic blasts.

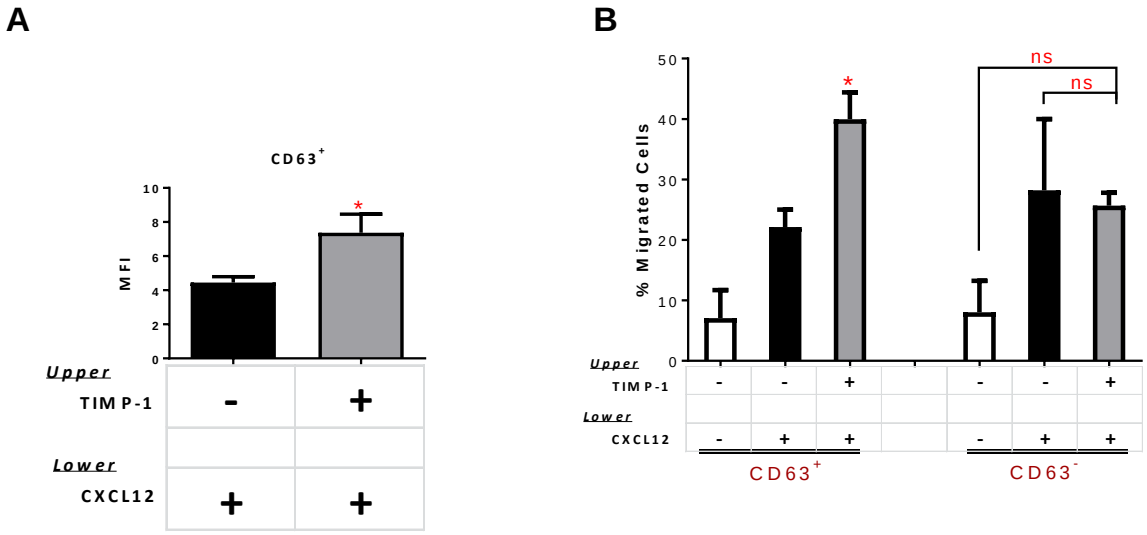

Figure 5

TIMP-1's effects on migration are mediated by the CD63 tetraspanin receptor.

A)AML cells were seeded in the upper compartment of a chamber transwell migration assay ±TIMP-1 (100 ng/ml). After 24 hrs migrated AML-derived leukemic blasts toward CXCL12 gradient after pre-treatment with TIMP-1 show increased expression of TIMP-1 receptor (CD63) as compared with untreated cells. Results are expressed as normalized Mean Fluorescence Intensity (nMFI). ($p \leq 0.05$; n=10).*

B) Based on CD63 expression, leukemic blasts were sorted in two separate fractions, $CD63^-$ and $CD63^+$, and their capability to respond to TIMP-1 stimulation was assessed by migration assay. AML cell fractioning were seeded in the upper compartment of a chamber Transwell migration assay ± TIMP-1 (100 ng/ml) toward CXCL12 ($p \leq 0.05$; n=3). The mean number of migrated $CD63^+$ cells was 705 ± 46 for spontaneous migration, 2213 ± 287 for migration toward CXCL12 gradient, 3720 ± 600 in the presence of TIMP-1 toward CXCL12 gradient. The mean number of migrated $CD63^-$ cells was 805 ± 52 for spontaneous migration, 2695 ± 555 for migration toward CXCL12 gradient, 2575 ± 370 in the presence of TIMP-1 toward CXCL12 gradient. Data are presented as mean ± SEM.*

TIMP-1 induced PI3K/Akt and HIF-1α signaling pathway in leukemic blasts

We then investigated the signaling pathway activated by TIMP-1 exposure. We previously demonstrated that in normal $CD34^+$ cells PI3K/AKT is the main signaling pathway induced by TIMP-1.[103] Based on these results, we tested TIMP-1 effects on AML cell function in presence of the PI3K-inhibitor LY294002. Pre-incubation of AML cells with LY294002 plus TIMP-1 significantly decreased their clonogenic output as compared to TIMP-1 alone ($p \leq 0.05$) (**Figure 6A**), reverted TIMP-1-mediated anti-apoptotic activity ($p \leq 0.0001$) (**Figure 6B**) and its migratory capacity on AML cells (**Figure 6C)** ($p \leq 0.0001$).These results suggest that, similarly to normal HSC, in leukemic blasts the pathway of PI3K/AKT may be involved in the signaling induced by TIMP-1. To further support this hypothesis, we examined the activation/phosphorylation of Akt in TIMP-1-treated AML cells. We firstly observed that the addition of TIMP-1 resulted in pAkt-Thr308 phosphorylation of $CD63^+$, but not $CD63^-$, AML cells **(Figure 6D)**, confirming that CD63 binding may be important to pAkt activation by TIMP-1. Next, we assessed by flow cytometry the levels of Akt phosphorylation in leukemic blasts after exposure to TIMP-1. As indicated in **Figure 6E**, the mean value of nMFI of phospho-Akt was 3.5 ± 0.32 in untreated cells vs 4.8 ± 0.7 after TIMP-1 treatment ($p \leq 0.05$). Moreover, we determined the levels of pAkt upon TIMP-1 treatment in AML cells by Western blotting (**Supplementary Figure 3**). As expected, after PI3K inhibition the treatment with TIMP-1 had no effect on Akt phosphorylation. Finally, we examined the effect of TIMP-1 on the expression of HIF-1α, described as a downstream pathway following PI3K/Akt activation. Of note, the expression of HIF-1α mRNA in leukemic blasts was found to be modulated by TIMP-1 stimulation. Specifically, after 24 hours in presence of TIMP-1, a significant increase in the expression of HIF-1α was observed ($p \leq 0.05$; **Supplementary Figure 4**). Together, these data support the hypothesis that TIMP-1 modulates the function of leukemic blasts via PI3K/Akt and HIF-1α axis.

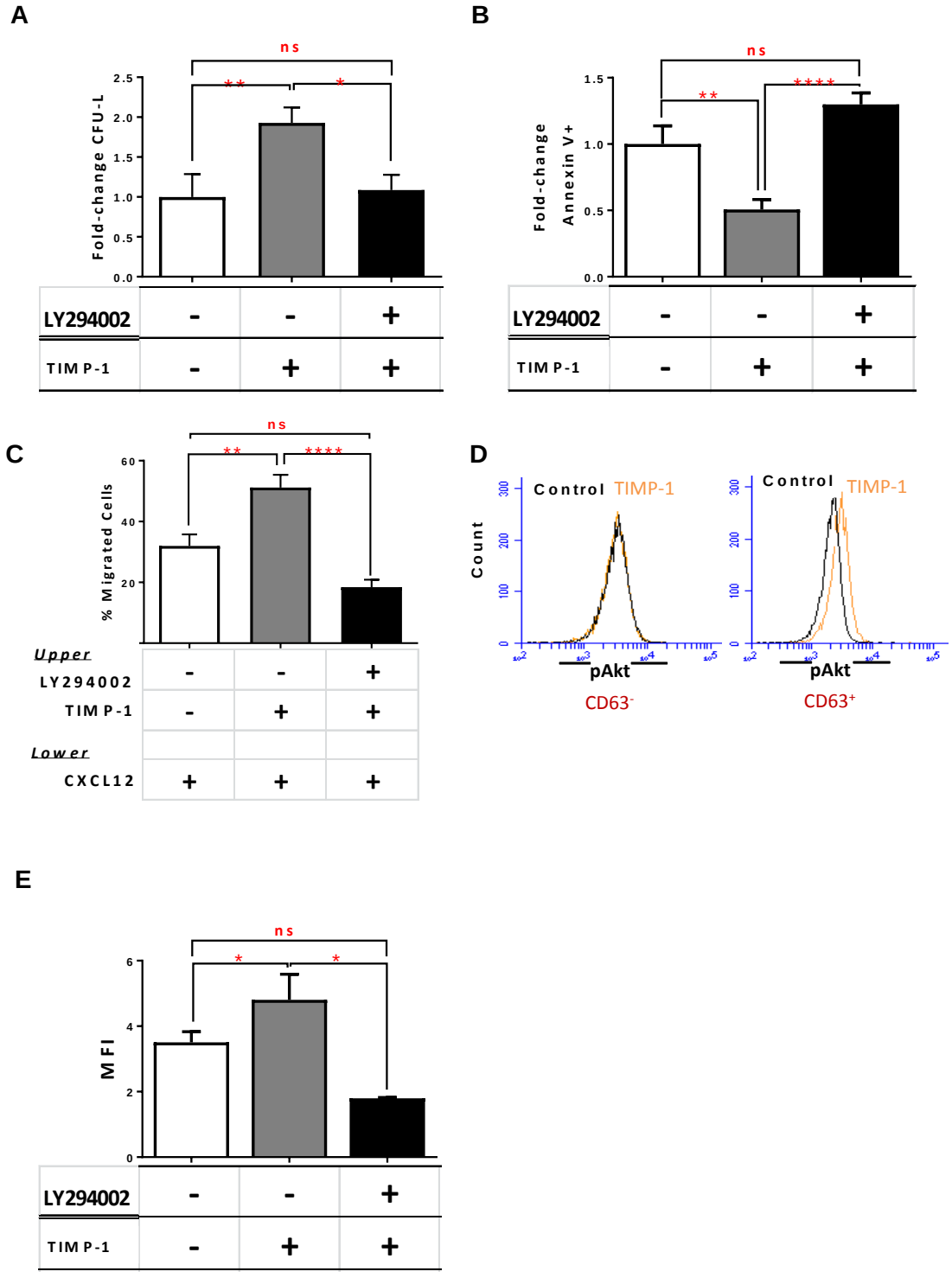

Figure 6

TIMP-1 effects in AML cells are mediated by PI3K/Akt and HIF-1α signaling axis

*A) AML cells were cultured in the presence or absence of TIMP-1 (100 ng/mL) after pre-treatment with LY294002 (20 μM) and the correspondent clonogenic output was assessed after 14 days of culture (*p ≤ 0.05; **p ≤ 0.01; n=3). The*

*mean number of CFU-L was 19.7 ± 5.6, 30.3 ± 9.6 and 14.0 ± 6.2 for control, TIMP-1-treated and LY294002-pre-treated AML cells, respectively. The results are expressed as growth fold-change versus untreated control samples. B-C) In the same culture condition we tested apoptosis after 24 hrs (n=8) and migratory behaviour toward CXCL12 gradient (**p ≤ 0.01; ****p ≤ 0.0001; n=8). The mean numbers of migrated cells were 9032 ± 2970, 16432 ± 3881 and 8450 ± 1638 for control, TIMP-1-treated and LY294002-pre-treated AML cells, respectively. The results are expressed as fold-change versus untreated control samples and as mean of migrated cells, respectively. D) Representative panel of pAkt levels in TIMP-1-treated versus untreated cells of $CD63^-$ leukemic blasts (left panel) or $CD63^+$ leukemic blasts (right) (n=3). E) Level of Akt phosphorylation (Thr308) in total AML cells exposed for 15 minutes to TIMP-1 (100 ng/mL) or after pre-treated with LY294002, as assessed by flow cytometry. Results are expressed as normalized MFI: 3.5 ± 0.32 (MFI 1387 ± 264) untreated cells vs 4.8 ± 0.7 (MFI 1524 ± 274) TIMP-1 treated cells (*p ≤ 0.05; n=13). Specifically, only 3 patients (PT #4-#7-#8 in the Table patients) were not responsive to TIMP-1 treatment in pAkt activation (*p ≤ 0.05; n=13).*

The leukemic BM microenvironment enhances the effects of TIMP-1 on migration of leukemic blasts

It is known that migration of AML cells is regulated by stromal cells, such as MSCs, producing CXCL12.[169,170] To further investigate the role of TIMP-1 within BM microenvironment of AML patients, we tested the migratory ability of leukemic blasts after co-cultures with normal or leukemic MSCs in presence or absence of TIMP-1. No significant biological difference was found between normal and AML-MSCs in terms of phenotype and differentiation capacity (data not shown). As shown in **Figure 7A**, the CXCL12-driven migration of leukemic blasts was not affected by TIMP-1 pre-incubation in co-cultures with normal MSCs. Conversely, when leukemic blasts were co-cultured with AML-MSCs, the addition of TIMP-1 resulted in increased migration rate as compared to that observed in presence of normal MSCs ($p \leq 0.01$). Interestingly, when we analyzed the levels of TIMP-1 in the supernatants of co-cultures of AML cells with leukemic or normal MSCs, we found that TIMP-1 level was higher in presence of HD-MSCs over AML-MSCs (263 ± 19.68 ng/ml and 162 ± 24.43 ng/ml, respectively; $p \leq 0.05$; **Figure 7B)**.

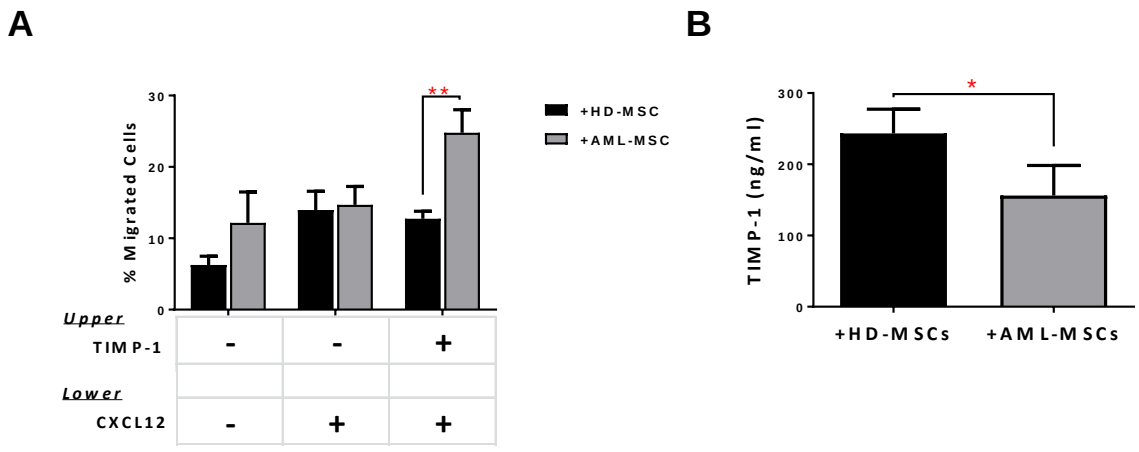

Figure 7

TIMP-1's effects on BM microenvironment: TIMP-1 significantly promotes migration of AML-derived leukemic cells after co-culture with AML MSCs

*AML cells were co-cultured with normal (n=2) or leukemic MSCs (n=3) for 3 days ± TIMP-1 (100 ng/ml). After co-culture, AML cells were collected, counted and seeded in the upper compartment of a chamber Transwell migration assay toward CXCL12-gradient (100 ng/ml). A) The addition of TIMP-1 for 3 days in the presence of leukemic MSCs affects the migratory behaviour of AML-derived blasts cells toward CXCL12 alone (**p ≤ 0.01) (n=6). The mean numbers of migrated cells were 7784 ± 2794 for spontaneous migration, 7315 ± 1776 for migration CXCL12-driven and 17732 ± 6735 for migration CXCL12-driven after TIMP-1 treatment after co-cultures with AML-MSCs. On the contrary the mean numbers of migrated cells were 2730 ± 770 for spontaneous migration, 6223 ± 1811 for migration CXCL12-driven and 5613 ± 1167 for migration CXCL12-driven after TIMP-1 treatment after co-cultures with HD-MSCs. B) Leukemic cells were co-cultured in presence of a normal or leukemic stroma layer. After 3 days of co-culture, supernatants were collected and analysed for TIMP-1 level using ELISA (*p<0.05; n=3). Data are mean ± SEM. "HD" means healthy donor.*

TIMP-1 enhances leukemic cell survival and proliferation in presence of leukemic MSCs

Recently, several studies have demonstrated the essential role of BM stromal-derived factors in regulation AML cell proliferation, thus conferring chemo-resistance to leukemic cells.[141,149] To test the differential effect of TIMP-1 on AML cell survival in presence of normal versus leukemic MSCs, co-cultures were set up in the presence or absence of TIMP-1. As shown in **Figure 8A**, the survival of leukemic blasts was not affected by TIMP-1 in co-cultures with normal MSCs. However, TIMP-1 showed a slight reduction in apoptotic rate in co-culture with AML-MSC ($p \leq 0.05$). Moreover, AML cell proliferation was evaluated with normal MSCs or AML-MSCs in the presence or absence of TIMP-1 plus growth factors, thus mimicking the BM microenvironment.

When AML cells were co-cultured with normal MSCs cell proliferation was not significantly modified after exposure to TIMP-1. By contrast, in co-cultures with AML-MSCs, the combination of TIMP-1 plus growth factors resulted in highly significant increase of the proliferation index as compared with blasts co-cultured with growth factors alone ($p \leq 0.01$; **Figure 8B-C**). In addition, a non-significant trend to increased cell proliferation was found from CD63-positive fractions in AML cells (data not shown).

Taken together, the results reported in **Figures 7** and **8** support the notion that leukemic microenvironment is deeply dysregulated in AML and TIMP-1 may preferentially exert its effects on leukemic cells in presence of leukemia-derived MSCs.

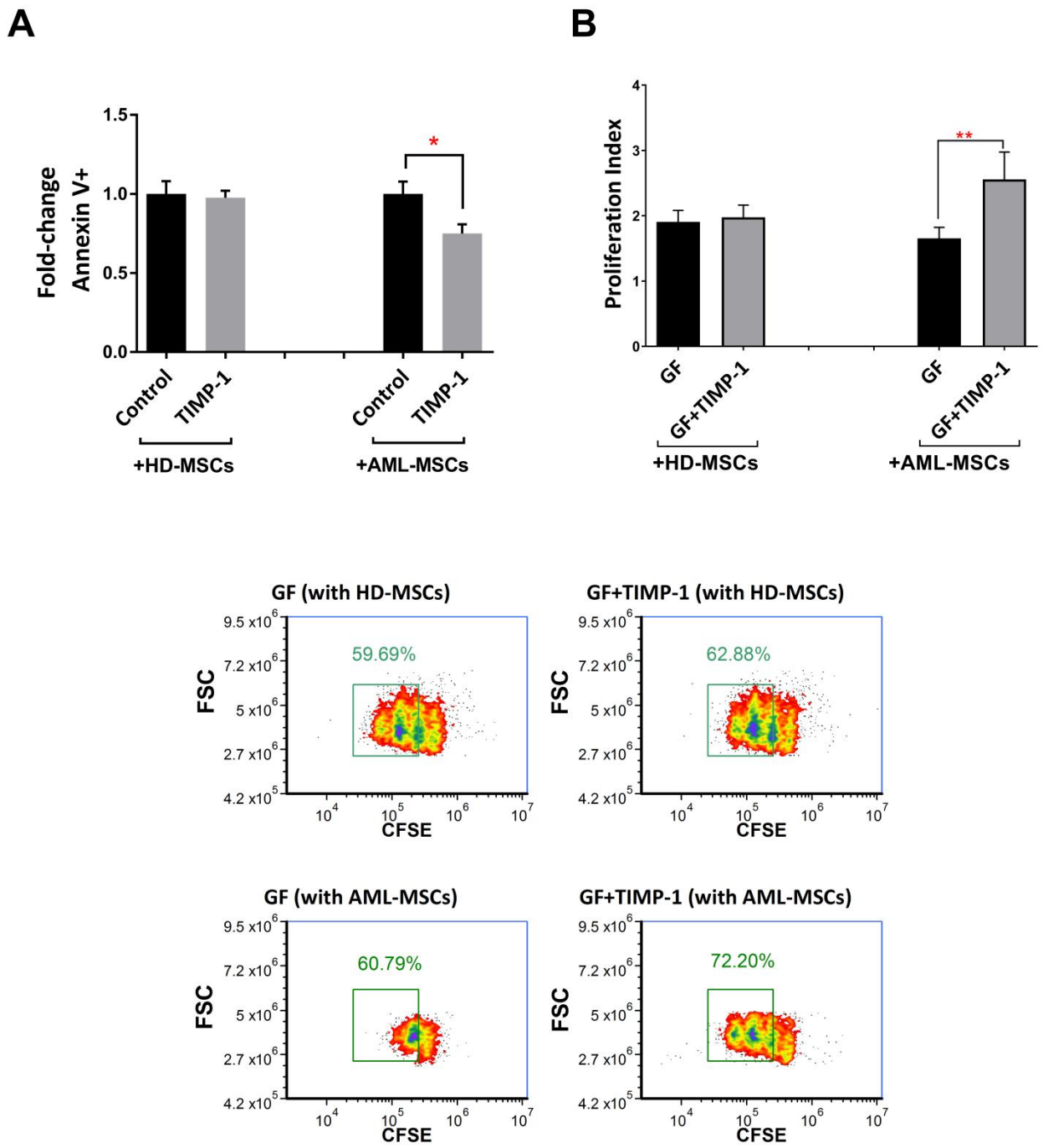

Figure 8

TIMP-1's effects on BM microenvironment: TIMP-1 promotes cell survival and proliferation in AML-derived blasts in the presence of AML-MSCs.

*A) AML cells were co-cultured with normal (n=2) or leukemic MSCs (n=3) for 3 days ± TIMP-1 (100 ng/ml) to test survival of leukemic cells (*p < 0.05; n=4). B) AML cells were co-cultured with normal or leukemic MSCs for 5 days with growth factors ± TIMP-1 (100 ng/ml). Proliferation index of CFSE-labeled leukemic blasts was calculated. Cells*

*maintained in culture in the presence of medium alone was evaluated as 1 of proliferation index. AML MSCs displayed, at culture day 5, a significantly increased proliferation index, as compared to leukemic cells co-coltured with normal MSCs (**p ≤ 0.01; n=12). C) Representative dot-plots showing the percentage of proliferative cells gated with reduced CFSE content by flow cytometry. Left panels, AML cells were co-cultured with normal (on the top) or leukemic MSCs (on the bottom) for 5 days with growth factors only. Right panels, AML cells were co-cultured with normal (on the top) or leukemic MSCs (on the bottom) for 5 days with growth factors ± TIMP-1. Data are mean ± SEM. GF, growth factors.*

DISCUSSION

Here we demonstrate that TIMP-1 increases the clonogenic efficiency, the survival and the migratory capacity of AML blasts by binding to CD63 receptor which, in turn, results in the activation of PI3K, Akt phosphorylation and regulation of downstream targets, such as p21 and HIF-1α. Moreover, we showed the potential role of TIMP-1 in the interplay between leukemic blasts and AML MSCs. Together, these findings suggest that TIMP-1 displays cytokine-like features in the BM microenvironment of AML patients, suggesting a link between the inflammatory microenvironment and leukemogenesis.

Several papers report that the activation of PI3K/Akt signaling is associated with poor outcome in hematological malignancies and this pathway is crucial to cancer cell survival and growth.[171] Here we demonstrate that, similarly to CB-derived $CD34^+$,[104] binding of TIMP-1 to CD63 receptor is instrumental for modulation of AML cell functions. Whereas the role of CD63 in regulating cancer cell functions, such as cell activation, adhesion, differentiation and migration, is well-established in solid tumors,[153,156] its role remain unclear as for hematological disease. *Schubert et al.*[172] showed higher CD63 expression in AML-long-term surviving capacity (LTSC) growth in NOD/SCID mice, hinting the potential role in cell adhesion and motility. In the present paper we demonstrate that about half of leukemic blasts are CD63 positive. At the functional level, binding to CD63 is required for TIMP-1-mediated main effects on AML blasts along the PI3K/Akt pathway, as previously observed in CB $CD34^+$ cells. In addition, we found that TIMP-1 stimulates the cell-cycle progression of leukemic blasts with a subsequent down-regulation of the cell-cycle inhibitor p21. Similarly to other pro-inflammatory cytokines (e.g. IFN-γ and IL-4), TIMP-1 was shown to be an inducer of HIF-1α expression in a liver metastasis model.[173] Moreover, HIF-1α mRNA and protein are overexpressed in human cancer and leukemic stem cells.[174,175] Our data suggest, for the first time, that upregulation of HIF-1α mRNA may be mediated by TIMP-1 in AML.

Leukemic blasts have been shown to have higher levels of TIMP-1 transcripts and increased TIMP-1 expression was also observed in Non-Hodgkin lymphomas and Burkitt B-cell lymphoma cell lines.[164-166] Accordingly,[167] in the present work we found that the BM plasma levels of TIMP-1 are detectable in AML patients. At variance from normal CB-derived $CD34^+$ cells, where TIMP-1 was shown to affect only the clonogenic potential, in AML TIMP-1 exerts additional effects, such as improving cell survival and CXCL12-mediated migration. In the leukemic microenvironment, CXCL12 is secreted both by BM stromal and AML cells and critically modulates cell survival and retention of LSCs within BM.[176,177] Our demonstration that TIMP-1 pre-treatment of leukemic

blasts promotes their migration towards CXCL12 support the finding of high levels of TIMP-1 in the BM of AML patients, suggesting a role for this molecule in promoting the migration of leukemic blasts and their dissemination in extramedullary site.

The dynamic interplay between leukemic cells and stromal cells is a crucial aspect of AML.[178] It is clear that leukemic cells alter their BM microenvironment to support leukemic hematopoiesis while disrupting normal HSC homeostasis.[65] This interaction via cytokines, chemokines and adhesion molecules is responsible for reduced chemo-sensitivity of leukemic sub-clones.[179] By contrast, the potential role of TIMP-1 in the interaction of leukemic cells with BM stromal cells is mostly unknown. Of note, previous investigations demonstrated that among 23 cytokines differentially expressed, at the molecular level, between normal and leukemic BM, only TIMP-1 was confirmed at the protein level suggesting a role in leukemia initiation and progression.[167] Moreover, the crosstalk between the matrix metalloproteinases system and chemokines network may modulate different regulators of cytokine release by primary human AML cells (e.g. NF-kB).[152] In this view, our functional data support a role of TIMP-1 as an adverse factor within leukemic microenvironment. Interestingly, TIMP-1 has been shown to preferentially increase AML blasts survival, proliferation and migration in presence of AML-MSCs. Such discrepancy in comparison to normal MSCs is far to be completely elucidated. A possible explanation is that secreted TIMP-1 from normal MSCs saturate potential TIMP-1 receptors, reverting and masking the pro-survival and pro-migratory effects of exogenous TIMP-1. Indeed, previous studies demonstrated the different production of TIMP-1 by normal human MSCs (hMSCs), AML long-term marrow cultures (LTMC) and leukemic BM.[180,181] Although limitation of the present study is the small sample size of patients, our findings point to an abnormal interplay between leukemic cells and their microenvironment and suggest that AML stroma may be a novel target to prevent the development of leukemia.

In conclusion, according to the "bad seeds in bad soil" concept,[92] our data provide new evidence for TIMP-1 as a ‘bad’ linker between inflammation and leukemogenesis. Our preclinical results may provide the biological background for further investigating TIMP-1 as a potential therapeutic target in the context of leukemic microenvironment.

MATERIALS AND METHODS

Primary samples

Peripheral blood (PB, n=9) and bone marrow (BM, n=9) samples were obtained from AML patients (n=18) at diagnosis after informed consent was signed. The percentage of AML blasts was always > 90%. Patient characteristics are summarized in Supplementary Table 1. As control samples, buffy-coats from blood transfusion processing and BM samples from patients with lymphomas, undergoing staging, with no sign of BM involvement were used. Control samples were rendered anonymous and not referred to individuals. Mononuclear cells (MNCs) were separated by stratification on Lympholyte-H 1.077 g/cm^3 gradient (Gibco-Invitrogen, Milan, Italy), followed by red blood cell lysis for 15 min at 4°C. Briefly, AML blasts were cultured in RPMI 1640 (Thermo Fisher Scientific,Waltham, MA), supplemented with 10% fetal calf serum (Thermo Fisher Scientific,Waltham, MA). Mesenchymal stromal cells (MSCs) were obtained from BM of healthy donors (n=2) or AML patients (n=3) as previously described.[182] MSCs were cultered at a density of 5,000 to 10,000 cell/cm^2 in DMEM (Lonza, Veriers, Belgium) supplemented with 10% FBS. The isolated MSCs at passage 3 was evaluated by flow cytometric analysis for immunophenotype and were used for co-culture experiments (passage 3 to 5) after irradiation (10,000 Gy).

Measurement of TIMP-1 levels

Serum was obtained from PB and plasma from BM samples of AML patients at diagnosis and stored at -80°C. The concentration of TIMP-1 in the supernatants from primary AML cells co-cultured with MSCs and the serum/plasma samples have been analysed by an ELISA assay (Boster Biological Technology Co., Pleasanton, CA) according to manufacturing instruction.

Colony-forming unit (CFU) assays

AML cells were cultured in methylcellulose medium (human StemMACS HSC-CFU lite w/ Epo, Miltenyi Biotech, Germany) at 1-5x10^{5}cells/mL in 35-mm Petri dishes in the presence or absence of TIMP-1 (10-300 ng/mL, Thermo Scientific, Pierce Biotechnology, Rockford, IL, USA). Cell cultures were maintained at 37°C in a fully humidified atmosphere with 5% CO_2 and after 14 days

CFU-Ls were scored. The experiments were performed in duplicates plates and a colony was considered to be an aggregate of 20 and more cells.

Apoptosis assay

AML cells were cultured in the presence of TIMP-1 (100 ng/mL) and the apoptotic rate was evaluated at different time points by AnnexinV/Propidium Iodide Staining (Annexin-V-FLUOS-kit,Roche, Penzberg, Germany). Sample acquisition and analysis was performed on a BD Accuri C6 flow cytometer (BD Biosciences). Where indicated, cells were cultured in the presence of LY294002 (PI3K inhibitor). Cell viability was also measured by CellTiter 96 Aqueous One Solution (Promega). AML cells were cultured in presence of TIMP-1 (100 ng/mL) for 24-48 hours and cell cycle distribution were evaluated at different time points. Treated cells were first permeabilized with NP-40 (15 min at RT) and then labelled with propidium iodide (PI)/RNAse staining kit (BD Bioscience) (15 min at RT, in the dark). The DNA content was assessed by BD Accuri^{TM}C6 (BD Bioscience) and results were analyzed by FCS express 4 software.

Cell sorting and flow cytometry

Flow cytometry studies were performed as previously described.[104] Leukemic blasts were labelled with an anti-CD63 antibody phycoerythrin (PE)-conjugated (eBioscience, San Diego, CA) and sorted on a FACS Aria (Becton Dickinson, BD Bioscience, San Jose, CA).

Cells were acquired and sorted on a FACS Aria (Becton Dickinson, BD Bioscience). Sorting gates were carefully drawn in order to avoid any cross-contamination among the two populations. Purity checks by flow cytometry was performed on each isolated cell population and the mean purity was 90% ± 5%.

Phospho-Akt intracellular staining was performed as previously described.[104] Leukemic blasts were treated with TIMP-1 (100 ng/ml) for 3.5-15 min at 37°C, 5% CO_2. After fixation in 4% paraformaldehyde (PFA) in PBS/permeabilization, cells were washed with phosphate-buffered saline (PBS), 0.1% bovine serum albumin (BSA) and incubated with pAkt (Thr308) (C31E5E) Rabbit monoclonal antibody (PE-conjugate; Cell Signaling) for 30 min at room temperature (RT) in the dark. Data were analyzed using FCS express 4 Flow Cytometry analysis software (De Novo Software, Glendale, CA, USA).

For intracellular analysis of p21 protein, leukemic blasts were treated with TIMP-1 (100 ng/ml) for 24 hours at 37°C, 5% CO_2. After fixation in 4% PFA, 0.1% Saponin was used to permeabilize the cells. As above cells were incubated with p21 antibody or negative control antibody and analysed by flow cytometry.

Where indicated, cells were cultured in the presence of 20μM PI3K inhibitor (LY294002) (Sigma-Aldrich,Saint Louis, MO, USA) or 5μM CXCR4 antagonist (AMD3465) for 30 minutes (Abcam, Cambridge, UK), followed by exposure to TIMP-1 (100 ng/ml). In selected experiments, cells were cultured in the presence of anti-TIMP1 antibody (5μg/ml) (ab77847, Abcam, Cambridge, UK).

Negative controls were isotype-matched irrelevant MoAbs from BD Pharmingen or eBioscience and were used for setting limits of nonspecific immunoglobulin cell binding. Specifically, the following MoAbs were used: APC or PE Mouse IgG1, κ Isotype Control (Clone MOPC-21) and PE-Cyanine7 or FITC IgG1, k Isotype Control (Clone P3.6.2.8.1).

In order to normalize our data for p21 and pAkt staining, we calculated the normalized MFI (nMFI), as MFI of the stained sample/MFI of the negative control sample.

CFSE labelling and analysis

Leukemic proliferation was monitored by flow cytometry, monitoring Green fluorochrome carboxyl fluorescein diacetate succinimidyl ester (CFSE, Molecular Probes Europe, Leiden). AML cells were labelled with CFSE (5μM) for 4 min at RT in PBS, 0.1% BSA, followed by the addition of ice-cold RPMI with 10% FBS to prevent further dye uptake. Cells were washed 3 times in ice-cold medium and maintained in culture for 5 days in RPMI with 10% FBS, with or without TIMP-1 (100 ng/ml) supplemented with growth factors (GF): stem cell factor (SCF; 50 ng/mL, Amgen, Thousand Oaks, *CA*), interleukin (IL)-3 (50 ng/mL, Miltenyi Biotech, BO, Italy), granulocyte macrophage colony-stimulating factor (GM-CSF; 10 ng/ml, Peprotech, London, UK). Data were analyzed by FCS express 4 Flow Cytometry analysis software.

Migration assay

Migration of leukemic blasts was assayed towards a CXCL12 gradient (100 ng/mL, Meridian Life Science,Memphis, TN) in trans-well chambers (diameter 6.5 mm, pore size 8 μm; Costar; Corning,

New York, USA). Briefly, 50 µl of RPMI 1640 plus 10% FBS containing $0,5x10^5$ cells pre-incubated or not with TIMP-1 were added to the upper chamber and 150 µl of medium ± CXCL12 were added to the bottom chamber. After overnight incubation at 37°C in 5% humidified CO_2 atmosphere, inserts (upper chambers) were removed and transmigrated cells were counted by Trypan Blue exclusion test in a Neubauer chamber. The amount of migrated cells was expressed as a percentage of the input, applying the following formula: (number of cells recovered from the lower compartment/total number of cells loaded in the upper compartment) x 100%.

Co-culture experiments

AML cells were cultured with MSCs at ratio 1:10 in a direct cell-to-cell contact co-cultures. After 3 days in presence or absence of TIMP-1 (100 ng/ml) the migratory behaviour of leukemic blasts was assessed by migration assay toward CXCL12 gradient. After 5 days with SCF (50 ng/mL), IL-3 (50 ng/mL), GM-CSF (10 ng/ml) ± TIMP-1 proliferation was evaluated by flow cytometry, monitoring CFSE labelling. After separation, MSC monolayers were examined by microscopy to confirm that the monolayer was not damaged. To verify lack of significant contamination in collected AML cells, the expression of CD45 was measured.

Western blot analysis

AML cells were collected by centrifugation, washed with PBS 1% Phenylmethanesulfonyl fluoride PMSF (Sigma-Aldrich) and total protein extracts were separated by sodium dodecyl sulfate polyacrylamide gel electrophoresis, transferred onto nitrocellulose membrane (GE Healthcare, Buckinghamshire, UK), and then subjected to Western blotting. Membranes were saturated for 1 hour at room temperature in blocking buffer (1X tris-buffered saline, 5 M NaCl, 20 mM Tris-HCl; pH 8.0, 0.1% Tween-20, 4% BSA) and then incubated overnight at 4°C with the specific primary antibodies: rabbit anti-pAkt Thr308 [1:3000] (18F.H11; Abcam) or p21 [1:1000] (#2947, Cell Signaling) in 4% BSA in TTBS (TBS 0,1% Tween-20) for 15–20 h at 4°C. Membranes were washed three times for 5 min in TTBS and secondary antibodies (donkey anti-rabbit HRP (sc-2313), donkey anti-mouse HRP (sc-2314) [1:40000] (Santa Cruz Biotecnology) were added for 1h at room temperature, and then membrane-bound were washed three times for 5 min in TTBS as described previously. Signal intensities in single blots were measured by means of ChemiDoc-It

instrument equipped with a dedicated software (Launch VIsionWorksLS, Euroclone). Protein expression was quantified by band densitometric analysis using IMAGEJ 1.44p Launcher software (National Institutes of Health, Bethesda, MD, USA).

RNA Extraction and Real-time polymerase chain reaction (Real Time PCR) analysis

Total RNA was isolated from treated cells using RNAeasy Micro Plus Kit (Qiagen, MI, Italy). First-strand synthesis was performed with Improm2 (Promega,Madison, WI) and Real Time PCR was performed with Taqman probe sets (Applied Biosystems,Foster City, CA) on a ABI Prism 7700 Sequence Detector for 40 cycles. Primer sequence used for HIF-1α or p21. A human internal control glyceraldehyde-3-phosphate dehydrogenase (GAPDH) was included in every reaction for normalization and expression was measured for each assay relative to the GAPDH internal standard (ΔCt). The fold change was calculated from the formula $2^{\Delta\Delta Ct}$.

Statistical analysis

The results are expressed as the mean ± SEM. Differences between groups were compared by using either a Student's t-test or ANOVA (GraphPad software, La Jolla, CA). P values ≤ 0.05 were considered statistically significant.

SUPPLEMENTARY FIGURES

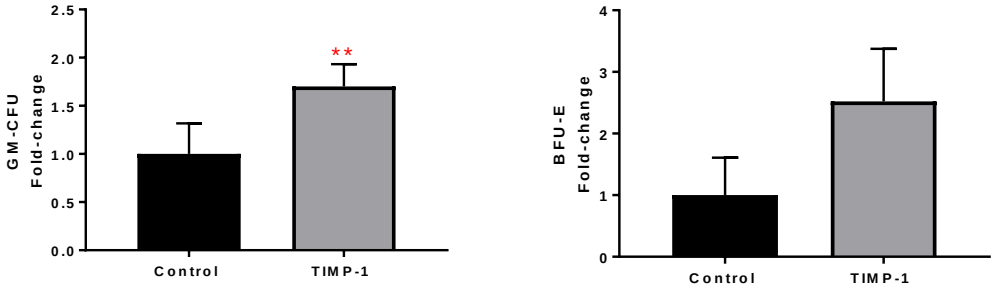

Supplementary Figure S1:

Effects of TIMP-1 on CFU-GM/BFU-E growth from AML-derived cells.

*Circulating leukemic blasts were isolated from AML patients and cultured in semisolid medium in the presence of TIMP-1. After 14 days, the total CFU-L output was assessed as above described. A) The CFU-GM growth of the AML-derived leukemic cells was significantly stimulated by TIMP-1 (100 ng/ml, **p ≤ 0.01) (n=12). The mean number of CFU-GM colonies in untreated (0 ng/ml) and treated (100 ng/ml) AML samples was 17.5 ± 5.5 vs 28 ± 9.6, respectively. B) The growth of BFU-E showed the same pattern displayed by CFU-GM but not significantly (n=5). The mean number of BFU-E colonies in untreated (0 ng/ml) and treated (100 ng/ml) AML samples was 7.4 ± 4.49 vs 11 ± 4.7, respectively. The results are expressed as growth fold change versus untreated control samples.*

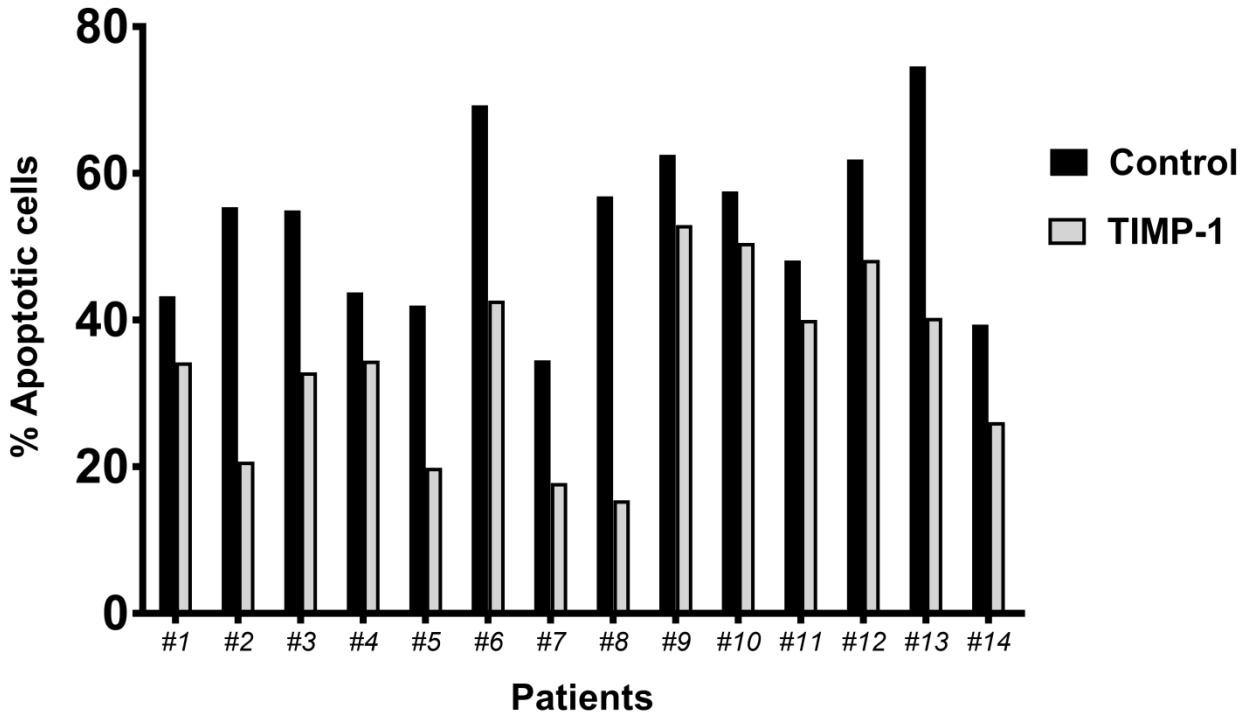

Supplementary Figure S2:

Effects of TIMP-1 on survival in 14 AML patients

AML cells from 14 patients were in vitro treated for 2 days with TIMP-1 and the percentage of cell viability was assessed after AnnexinV/PI staining, as described in methods. For each patient the percentage of apoptotic cells was reported in the absence (black columns) or in presence of TIMP-1 (grey columns).

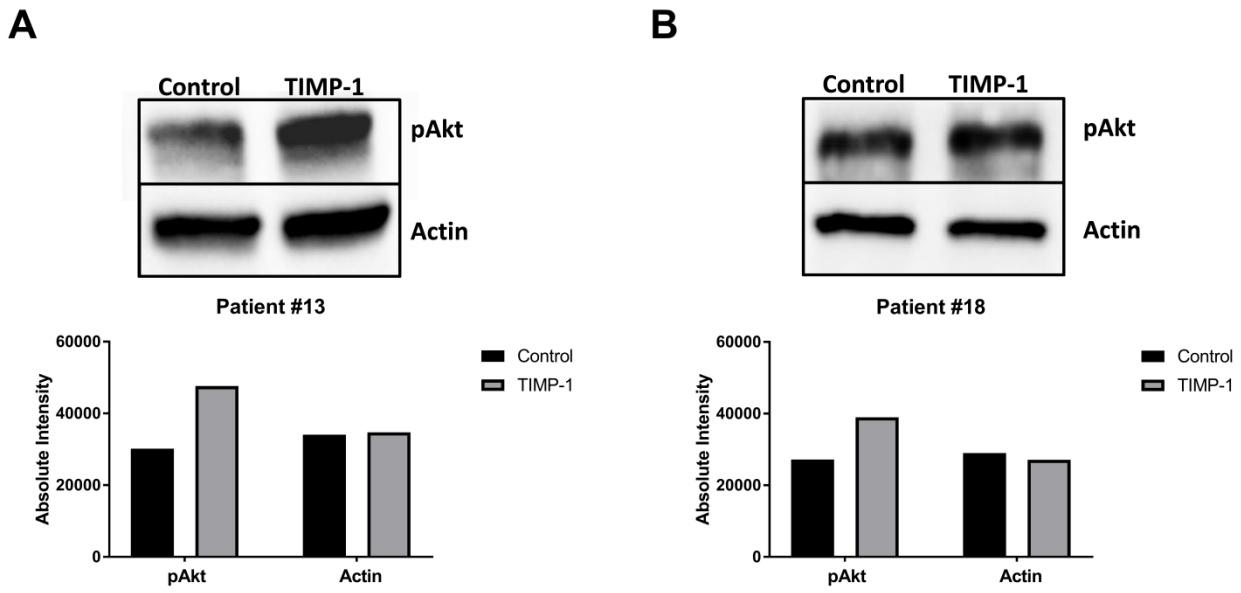

Supplementary Figure S3:

Western blot analysis and absolute quantification of pAkt in AML cells after TIMP-1 treatment.

Representative Western-blot bands of leukemic blasts from two AML patients. Western-blot bands for pAkt (first lane) in AML cells untreated (left band, control) and TIMP-1 treated (right band, TIMP-1) for patient #13 (A) and patient #18 (B). Graphic representation of quantification for pAkt expression and the relative β-actin (data shown below).

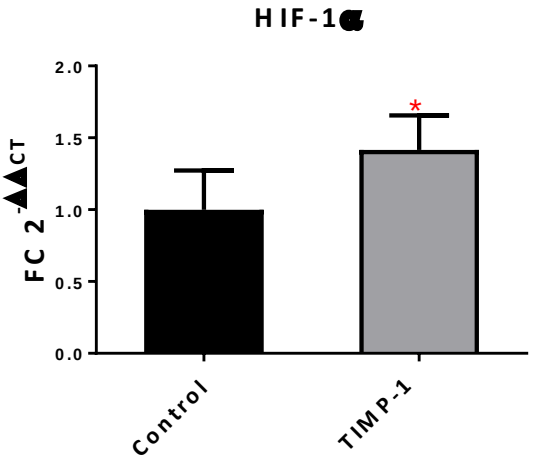

Supplemetnary Figure S4:

TIMP-1 increased the expression of HIF-1αat mRNA level

After 24 hours, total RNA was extracted and the correspondent levels HIF-1α was assessed by Real-Time PCR. Results was expressed as fold-change taking the value of untreated cells as 1 ($p \leq 0.05$; n=5).*

– Results III

LEUKEMIC STEM CELLS CO-OPT NORMAL BONE MARROW NICHES AS A SOURCE OF ENERGY AND ANTIOXIDANT DEFENCE

INTRODUCTION

Acute Myeloid Leukemia (AML) is a heterogeneous disease caused by various genetic lesions. In infants, translocations between the *mixed lineage leukemia 1* gene (*MLL*1) and other genes occur in more than 70% AML cases, which exhibit a particularly aggressive phenotype. One of the most common MLL translocation affects the *MLLT3*/*AF9* gene.[183,184] AML patients often poorly respond to chemotherapy and conventional high-dose chemotherapy ultimately results in drug resistance. Studies have shown that a decrease in apoptosis may be an indicator of progression since certain defects in the normal apoptotic process could favor the accumulation of genetic abnormalities in AML. Particularly, a cell population capable of initiating leukemia, named Leukemia-initiating cells (LICs), are considered to be involved in disease initiation, progression, and relapse.[185-188] Firstly described as a rare and quiescent population, LICs (often called Leukemic Stem cells, LSCs) therefore share some similarities with normal HSCs, but differ from them inmetabolic pathways.[189] LSCs have a high metabolic demand for their activity, since the disruption of either glycolysis or mitochondrial respiration impairs leukemogenesis.[36,190] Notably, LSCs of human AML present low oxidative stress and utilize mitochondrial respiration to support metabolic homeostasis.[36] Cancer cells adapt to metabolically adverse conditions in several tumors and this metabolic reprogramming is fundamental for cancer survival and drug-resistance. Intriguingly, cancer cells take advantage of environmental stress and metabolic changes. This 'metabolic rewiring' of tumor cells favors their survival by promoting energy metabolism and drug resistance.[144] LICs maintain low oxidative stress compared to the bulk of the leukemia. Cummulative evidence suggests remodel and exploit the HSC microenvironment for survival.[17,35,191,192]

Among different niche cells,bone marrow stromal stem/progenitor cells (BMSCs) have been recognized as important HSC supportive cells.[193] BMSCs cultured traditionally as adherent cells can support ex vivo expansion of hematopoietic progenitors but cannot preserve/expand HSCs.[194] A subset of BMSCs identified by the expression of the intermediate filament protein nestin have HSC niche functions. Moreover, Nes^+ BMSCs are highly enriched in fibroblastic colony-forming units in culture (CFU-F) and exhibit increased capacity for self-renewal and multilineage differentiation, compared with traditional plastic-adherent BMSCs. Nes^+ BMSCs localize near HSCs and support HSC maintenance and homing in the BM.[195]

Nes^{+} BMSCs can be propagated in vitro as non-adherent ‘mesenspheres’, which can self-renew and expand in serial transplantations. When propagated under these conditions, human Nes^{+} BMSCs preserve better their primitive properties (compared with standard adherent culture), including their capacity for multilineage differentiation and their ability to support HSCs. Although the underlying mechanisms remain largely unclear, we hypothesize that this system might allow to study the interaction of BMSCs with LSCs ex vivo. The dynamic interplay between leukemic cells and stromal cells is regarded as a crucial aspect in AML progression.[56] However, the contribution of the microenvironment to tumorigenesis has been best studied in solid tumors, whereas elucidating its role in leukaemogenesis is still in its infancy.

ROS are mainly generated by mithocondria. Several works have demonstrated the alteration of antioxidant status as a distinct feature of AML, and oxygen radical levels were significantly higher in malignant cells than in normal leukocytes.[196,197] Altered intracellular and extracellular ROS may participate in AML. The antioxidant molecules eliminate ROS that otherwise damage cellular components such as DNA, proteins, and lipids. Surprisingly, leukemic cells maintain relatively high ROS levels, without displaying a detrimental output that would compromise their survival.[69] Reflecting their activated oxidative energetic metabolism, an increase of ROS level could increase the proliferation, differentiation, and maturation of HSCs.[198] One proposed mechanism that allows normal HSCs to maintain low level of ROS is the preferential mitochondria transfer from HSCs to BMSCs. In leukemia,*Moschoi et al.*[199] proposed a mitochondrial transfer between AML cells and BMScs through endocytic pathways. Strikingly, mitochondrial transfer is associated with increased oxidative phosphorylation andprotection/recovery from chemotherapy-induced DNA damage. As reported in other studies, HSCs containing more mitochondriaexhibit increased levels of oxygen consumption and ROS.However, ROS-mediated (geno)toxicity in HSCs is counterbalanced by higher levels of DNA repair and antioxidant pathway gene expression.[200]

Non-adherent mesensphere cultures represent a useful platform to study the crosstalk between BMSCs and LSCs and highlight mitochondrial exchange under chemotherapeutic drug.

The driving hypothesis of this study is that co-opting mechanisms of the BM microenironment promote AML resistance under microenvironmental stress.

Regarding this, we designed a novel protocol to co-culture mesenspheres with leukemic blasts, in order to assess whether survival advantage through combined effects on ROS and metabolic reprogramming.

RESULTS

Co-cultures with BM mesenspheres from wild-type (WT) mice promotes survival in MLL-AF9 leukemic blasts

BM mesenspheres from WT mice were grown and expanded under specific culture conditions, with chicken embryo extract (CEE, a culture supplement that stimulates stem cell self-renewal) and cytokine-rich medium.. The BM-derived cells were isolated from long bones or spines of WT mice. The spheres could be serially expanded under this culture conditions and generated more spheres over serial passages. In addition, the mesenspheres remained in suspension and morphologically identical over >2 months on Poly-HEMA coated plates. Although only a small number of primary mesenspheres could be obtained from murine long bones compared to spines, they could be propagated during multiple divisions at the same culture conditions with pronounced properties. Expanded mesensphere-forming cells maintained expression of CD105, CD146 and CD63, but did not express CD45, CD31 (data not shown).

We investigated the effects of mesenspheres from WT mice on the survival of leukemic cells of doxycycline-inducible rtTA;MLL-AF9 mouse strain and we set up a novel cultures system. Firstly, to mimic a metabolic stress cellular condition, the mesenspheres (~50 aggregates spheres) were added to leukemic cells (40.000 cells) in medium lacking FBS. In particular, the percentage of apoptotic leukemic cells in mono-cultures was 77.15% ± 3.452 as compared to a significant decrease in co-cultures, 53.34% ± 3.415 ($p<0.0001$) (**Figure 1A**, left columns). Furthermore, the anti-apoptotic effects of the mesenspheres were stimulated with increasing co-culture times (data not shown).

In addition, although it has previously been reported that MSCs support tumor development by increasing drug resistance,[149] we tested the protection from chemotherapy-induced apoptosis by their interactions with mesenspheres in our co-cultures system (**Figure 1A**, right columns). Cell cultures were treated for 24 h with cytarabine (AraC), a chemotherapeutic agent used in AML therapy.[201] As shown in **Figure 1**, the co-cultures with mesenspheres reduced the cytotoxicity of AraC in the leukemic cells (~20% less apoptosis than that observed in the AraC-treated leukemic cells cultured alone, $p< 0.0002$).

These results suggest amesenspheres-driven microenvironmental protective effects by modulating metabolic stress and drug-response.

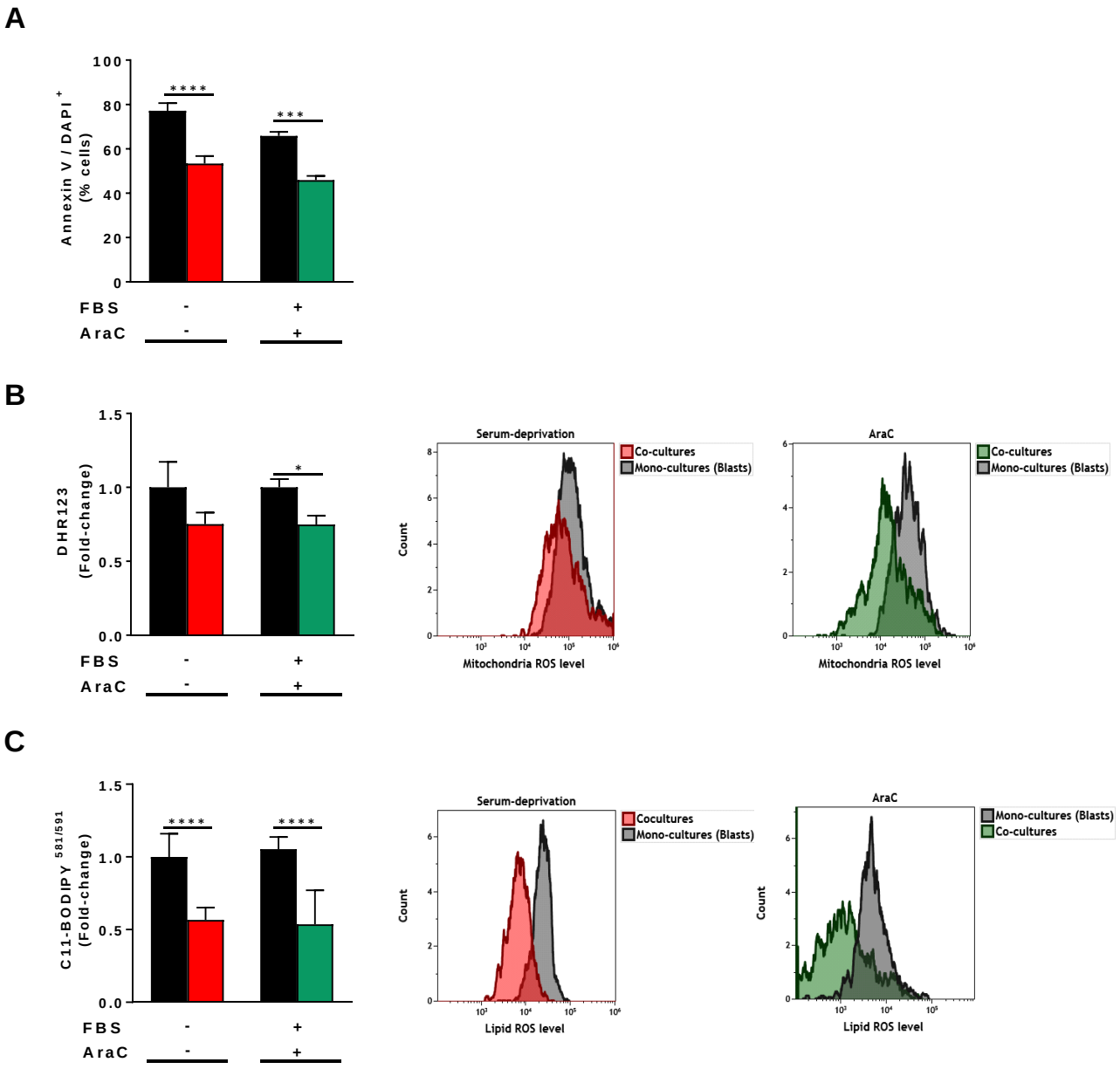

Figure 1

WT mouse BM-mesenspheres effects on survival, ROS levels and lipid peroxidation of co-cultured MLL-AF9 mouse leukemic blasts.

A*, Leukemic blasts (200 x 10*^{3} *cells/ml) were cultured with WT mice BM-derived mesenspheres (~250/ml) and the apoptotic rate was determined after 24 h by flow-cytometry following staining with Annexin V and DAPI, as described in Materials and Methods section. Significant differences of leukemic blasts in co-cultures (stained with CD45, red and green columns) from the corresponding mono-cultures of leukemic blasts (black columns) with FBS deprivation (left panel, n=22; ****P < 0.0001) and AraC-treated groups (right panel, n=19; *** P < 0.001). Unpaired two-tailed t test.*

B*, the above cultures described were also assessed by intracellular ROS production with DHR123 by flow-cytometry. Geometrical mean (G Mean) values of the fluorescence intensities normalized to the FBS deprivation- or Ara-induced ROS production from mono-cultures (leukemic blasts, black columns). Significant differences of leukemic blasts in co-*

*cultures (stained with CD45, red and green columns) from the corresponding mono-cultures of leukemic blasts with FBS deprivation (left columns, n=11; *P < 0.05) or AraC-treated groups (right columns, n=15; *P < 0.05) with co-cultures. Representative histograms showing the fluorescent intensities of mono-cultures (leukemic blasts, grey) and co-cultures (red or green) with FBS deprivation (left panel) or Ara-induced condition (right panel). Unpaired two-tailed t test.*

***C**, the above cultures described were also subjected to detection of lipid peroxidation using C(11)-BODIPY(581/591) by flow-cytometry. Geometrical mean (G mean) values of the fluorescence intensities normalized to the FBS deprivation- or Ara-induced lipid peroxidation. Significant differences of leukemic blasts in co-cultures (stained with CD45, red and green columns) from the corresponding mono-cultures of leukemic blasts with FBS deprivation (left columns, n=6; ****P < 0.0001) and AraC-treated groups (right columns, n=23; ****P < 0.0001) with co-cultures. Representative histograms showing the fluorescent intensities of lipid peroxidation of mono-cultures (leukemic blasts, grey) and co-cultures (red or green), on the left panel with FBS deprivation and on the right with AraC-treated condition. Unpaired two-tailed t test.*

Error bars represent mean values ± SEM.

BM WT mice mesenspheres inhibit ROS production in MLL-AF9 leukemic blasts

Because leukemic phenotype was found to correlate with ROS-dependent signaling and elevated ROS levels,[196] we further estimated how mesenspheres influenced the levels of ROS and mitochondrial oxidants on leukemic cells. DHR123, uncharged and nonfluorescent probe used as ROS indicator, is known to accumulate in mitochondria. Moreover, DHR123 is generated by oxidation of rhodamine123 (RH123), which displays an intense green fluorescence. We found a down-regulation of ROS levels in leukemic blasts after 24 hours co-cultures in FBS-deprivated medium. Indeed, decreasing amounts of DHR123 fluorescence were detected in co-cultured leukemic cells after FBS-deprivation ($p<0.0335$) (**Figure 1B**, left columns and related overlay of DHR123-FITC histograms).

Because AraC enhanced the ROS production,[202] we treated leukemic blasts with AraC to examine AraC-induced ROS effects. Our data indicated that in the presence of mesenspheres leukemic blasts showed a reduced amount of RH123 fluorescence expression in comparison with mono-cultured leukemic blasts ($p<0.0228$) (**Figure 1B**, right columns).

Overall, these findings demonstrate that mesenspheres reduce oxidative stress of leukemic blasts in the presence of AraC, supporting the idea that stromal cells-mediated chemoprotection of leukemic blasts may depend on the mitochondrial ROS levels modulation.

BM Mesenpsheres from WT mice down-regulated ROS-mediated lipid peroxidation tested by BODIPY C-11 $^{591/581}$

Excessive ROS levels can cause detrimental oxidative stress that results in cell death and lipid peroxidation.[203] Mitochondrial ROS production in living cells can be tested by assessing the extent of lipid peroxidation as an indirect means. To figure out these effects in our novel co-cultures experiments, we measured the oxidative sensitivity of C11-BODIPY$^{581/591}$ of leukemic blasts. Specifically, when cells were labeled with C11-BODIPY$^{581/591}$ reagent and upon oxidation, the fluorescence of this fluorophore shifts from red to green, indicating the increasing lipid peroxidation.As reflected by the increase in green fluorescence of the C11-BODIPY dye, lipid peroxidation of mono-cultured leukemic blasts significantly ($p<0.0001$) increased as compared to co-cultures in FBS-deprivated medium (**Figure 1C** and related overlay of C11-BODIPY$^{581/591}$-FITC histograms). Co-cultures of leukemic blasts with mesenspheres in the absence of FBS was associated with significant decreased lipid peroxidation (fold-change with 0.56 ± 0.03 in co-cultures, ns).

Concomitantly, AraC-treated leukemic cells showed a significant reduction of lipid peroxidation after co-cultures with mesenspheres (fold-change 0.53 ± 0.2; $p<0.0001$) (**Figure 1 C**, right columns and related overlay histograms).

Taken together, mesenspheres reduce lipid peroxidation both in FSB-deprivated and AraC-added medium, providing further evidences on the protective role of mesenspheres against induction of oxidative stress.

Effects of conditioned medium (CM) from mono-cultures and co-cultures on MLL-AF9 leukemic blasts

Because direct contact has a positive effect on *leukemic* cell survival and reduce ROS/lipid peroxidation levels, it could be interesting to investigate also the role of CM. We used CM from mono-cultured (leukemic blasts or mesenspheres) and co-cultured cells in the presence or the absence of FBS and AraC. Apoptosis, ROS levels and lipid peroxidation were tested in CM-treated leukemic blasts.

Only when we used CM from FBS-deprived co-culture experiments, we found an improvement in survival of leukemic blasts ($p<0.05$) (**Figure 2A**). Interestingly, the CM from mesenspheres alone was sufficient to support the survival of leukemic blasts, in the absence of FBS. On the contrary, the CM from mono/cocultures with AraC-treatment was not able to support leukemic blasts survival. Regarding ROS levels (**Figure 2B**) and lipid peroxidation analysis (**Figure 2C**), CM from co-

cultures were able to sustain a decrease in ROS levels. Similar resultswere observed when we tested the lipid peroxidation in the same conditions with CM.

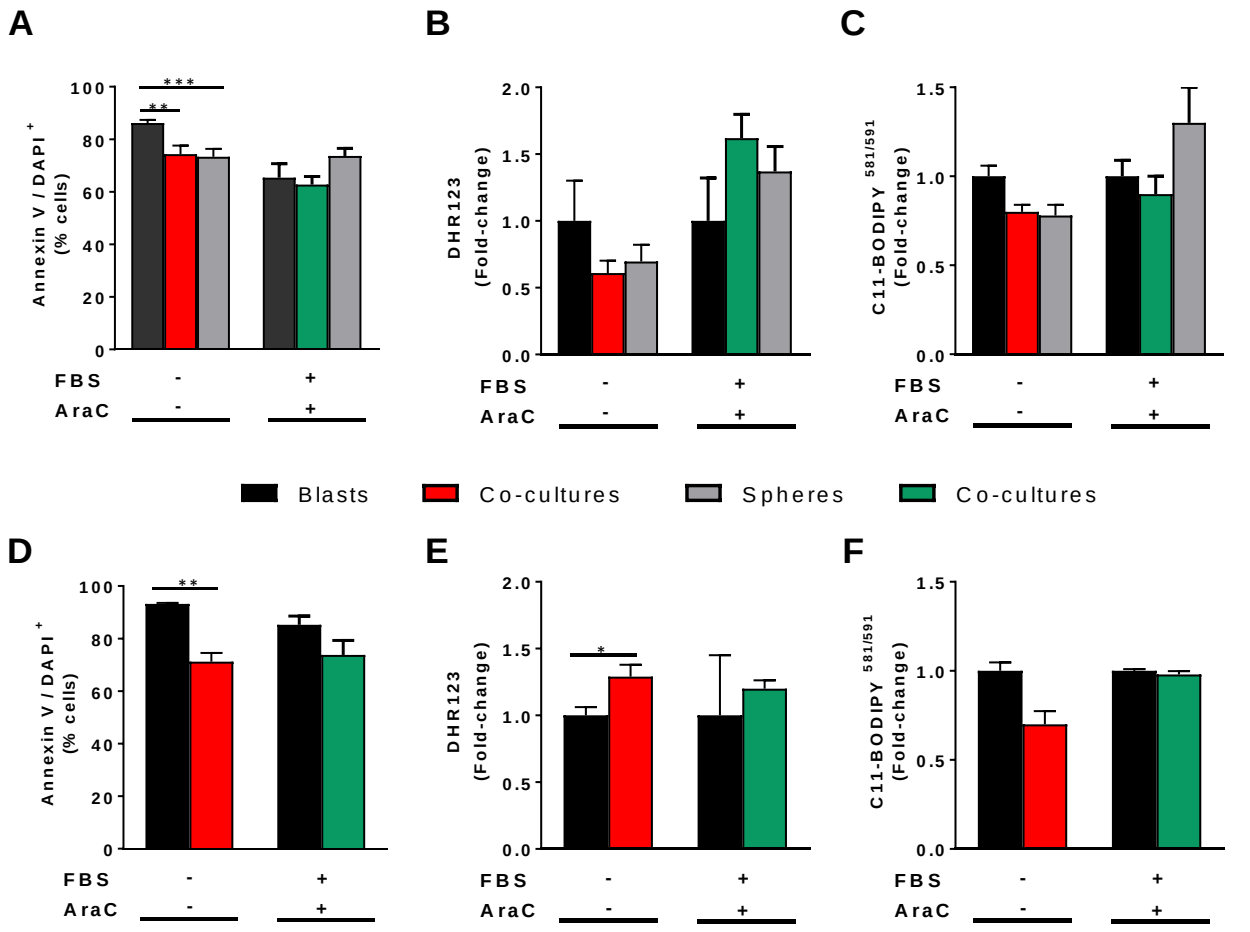

Figure 2

Influences of CM or transwell systems on survival, lipid peroxidation and ROS levels of MLL-AF9 mouse leukemic blasts co-cultured with WT mouse BM-mesesnpheres.

Leukemic blasts (200 x 10^3 cells/ml) and mesenspheres (~250/ml) were grown in serum-free or AraC-induced medium either in isolation or in co-cultures. After 24 h the CM collected from each conditions (from leukemic blasts alone, from spheres alone and co-cultures) was used to seed new leukemic blasts (200 x 10^3 cells/ml) as described in Materials and Methods section.

A**, the percentage of apoptotic leukemic blasts exposed to CM were determined after 24 h by flow-cytometry following staining with Annexin V and DAPI in CD45 positive cells. Significant differences between the corresponding leukemic blasts grown in CM from mono-cultures of leukemic blasts and leukemic blasts grown in CM from spheres alone (P < 0.001, grey columns) or in CM from co-cultures (**P < 0.01, red columns), in the conditions without FBS (left columns, n=13). No significant difference in the AraC-induced CM conditions (right columns, n=15 for each group). One-way ANOVA followed by post-hoc multiple comparison.*

***B**, the level of ROS production using DHR123 by flow-cytometry. Geometrical mean values of the fluorescence intensities normalized to the FBS deprivation- or Ara-induced ROS production from mono-cultures (leukemic blasts) with CM from mono-cultures of leukemic blasts. Any significant differences from the corresponding mono-cultures of leukemic blasts with FBS-deprivated CM (left panel, n=6) and AraC-treated CM (right panel, n=12). One-way ANOVA followed by post-hoc multiple comparison.*

***C**, the level of lipid peroxidation using C(11)-BODIPY(581/591) in the above cultures described with CM. Geometrical mean values of the fluorescence intensities normalized to the FBS deprivation- or Ara-induced lipid peroxidation from mono-cultures (leukemic blasts) CM. Any significant differences from the corresponding mono-cultures of leukemic blasts with FBS deprivated CM (left panel, n=5) and AraC-treated CM (right panel, n=6). One-way ANOVA followed by post-hoc multiple comparison.*

WT mice mesenspheres (in the upper chamber) and leukemic blasts (in the lower chamber) were cultured for 24 h in 96-well Transwell.

***D**, Detection of apoptosis with Annexin V/DAPI by flow cytometry of mono-cultures (black columns) and co-cultures (red and green) using 96-well Transwell. Significant differences between the corresponding mono-cultures of leukemic blasts and co-cultures with FBS deprivation (left panel, n=6;**P < 0.01) . Any significant differences between mono-cultures and co-cultures in Transwell experiments with Arac-induced conditions (right panel, n=10). Unpaired two-tailed t test. **E**, level of ROS production using DHR123 by flow cytometry of mono-cultures and co-cultures in 96-well Transwell. Significant differences from the corresponding mono-cultures of leukemic blasts with FBS deprivation compared to co-cultures (left panel, n=4; *P < 0.05). Any significant difference in AraC-treated groups with Transwell experiments (right panel, n=6). Unpaired two-tailed t test.*

***F**, lipid peroxidation production using C(11)-BODIPY(581/591)by flow cytometry of mono-cultures (black column) and co-cultures (red and green columns) in 96-well Transwell. Any significant difference in FBS deprivation (left panel, n=4) and AraC-treated groups with Transwell experiments (right panel, n=4). Unpaired two-tailed t test.*

Cell-cell contact is required for AraC-mediated protective effects of mesenspheres on leukemic blasts

To confirm the effects of co-cultures, we repeated the same experiments in transwell conditions, allowing exchange of soluble factors without any physical contact between two cell populations. Under this condition in the absence of FBS, we found a significant reduction of apoptotic leukemic cells in the presence of mesenspheres ($p<0.01$).

As shown in **Figure 2D** in the presence of AraC, separation of leukemic blasts and mesenspheres did not allow protection of leukemic blasts from mesenpsheres, which points out the requirement of direct cell-to-cell interactions.

Moreover, we did not find any protective role from mesenspheres on lipid peroxidation and ROS levels of leukemic blasts, in both conditions, FBS-deprivated and AraC-treated (**Figure 2D, E, F**).

Altogether we demonstrated that the effects of mesenspheres could be contact-dependent, excluding the involvement of paracrine signaling.

Mesenpheres promote the increase of intracellular GSH in leukemic blasts tested with Mitotracker and mBCI

The GSH/GSSG pool is considered a major indicator of the cellular redox status and oxidative stress.[204] Accordingly, we checked how GSH levels were altered in the presence of mesenspheres or after drug treatment. We therefore measured reduced GSH in leukemic blasts with the membrane indicator monochlorobimane (mBCI) to support the hypothesis that mesenspheres counterbalance the oxidative stress. As shown in the **Figure 3**, we reported a profile of reduced GSH (expressed as histograms) of leukemic blasts under different conditions. In particular, we found a significant ($p<0.001$) increase of GSH level in leukemic blasts co-cultured with mesenspheres (mean of mono-cultures 49.95 ± 4.3 vs mean of co-cultured leukemic blasts of 75.33 ± 3.34).

This effect was maintained after treatment with AraC. After 24 hrs of co-cultures with AraC, we observed a significant increase of GSH in leukemic blasts (81.5 ± 8.6),compared with mono-cultures (mean of 47.08 ± 1.289; $p<0.001$)

Mitochondria are not able to synthesize GSH but they transport and accumulate GSH.[204]

We co-stained the leukemic cells with Mitotracker Red CMXRos and mBCI to observe possible differences in the proportion of mitochondria with GSH. In our representative dot plot, we showed a reduction of mitochondria stained also with mBCI in co-cultures, suggesting a presence of anti-oxidant GSH after co-cultures. After AraC treatment, the mean percentage of mitochondria unstained for mBCI was significantly reduced in leukemic blasts co-cultured (4.3% ± 0.62) as compared to an incerease of unstained mitochondria for mBCI in mono-cultures (16.14% ± 4.68; $p<0.05$).

Altogether these results demonstrated a GSH increase in leukemic blasts in the presence of mesenspheres, confirming the anti-oxidant rescue provided by mesenspheres.

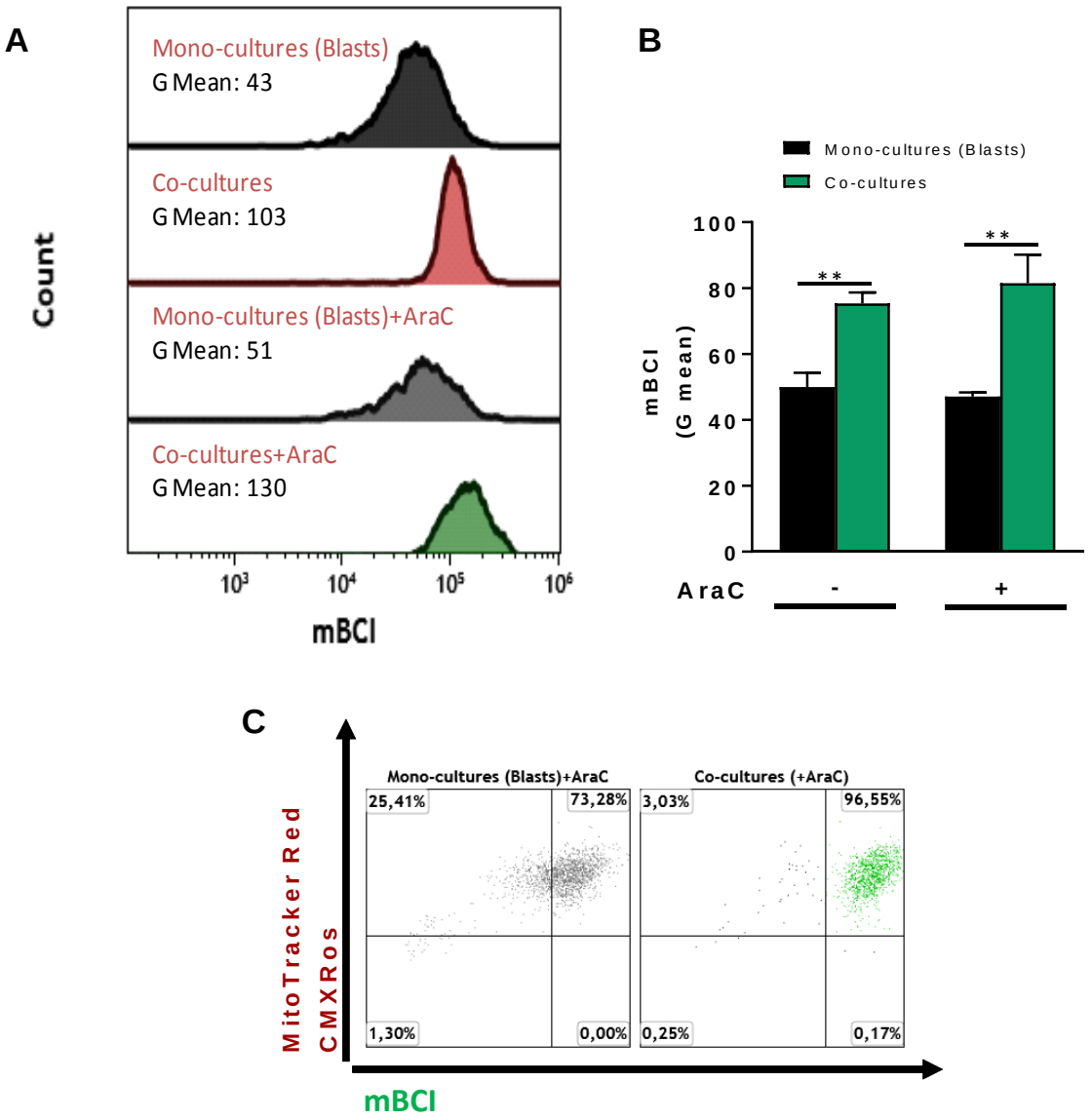

Figure 3

The presence of mesenspheres in cultures with MLL-AF9 leukemic blasts increases intracellular GSH.

Leukemic blasts and mesenspheres were co-cultured in the absence or presence of AraC (1µM) and stained with mBCI. GSH levels were monitored by flow cytometry after 24 hrs. ***A,*** *Representative histograms of GSH levels and G mean of each conditions: leukemic blasts in mono-cultures (black) or co-cultures (red) and in mono-cultures (grey) and co-cultures (green) after AraC treatment, respectively. The data shown are representative of six independent experiments.* ***B****, the fluorescence of mBCI expressed as G mean in mono-cultures (black columns) and co-cultures (green) in the absence or presence of AraC. Significant differences between mono-cultures and co-cultures in both conditions (** P <0.01). Unpaired two-tailed t test.*

C,*Leukemic blasts and mesenspheres were co-cultured in the absence or presence of AraC (1µM) and stained with mBCI and Mitotracker CMXRos red. The dot plots shown are representative of four independent experiments. Leukemic*

blasts (mono-cultures or in co-cultures) were treated with AraC and their depletion of GSH evaluated in combination with mitochondria staining (n=4).

Effects of AraC treatments in vivo using Prdx6 KO mice

We then investigated the RSL3 molecule, a GPX4 enzyme inhibitor that metabolizes lipid peroxides (including arachidonic acid metabolites) and increases lipid peroxidation.

Antioxidant Prdx6 protein rescues cells from oxidative stress.[205] To highlight a possible involvement of antioxidant molecules in leukaemia drug-resistance mechanism in vivo, we set up experiments using a Prdx6 KO mouse model.

We therefore injected CD45.1 leukemic blasts from MLL-AF9 mice into sub lethally irradiated WT mice (n=5) and Prdx6 KO (n=5) recipients and, after 13 days,we treated both groups with AraC (5 injections), as summarized by **Figure 4A**. Around 2 weeks after 5 injections of AraC, mice were sacrificed and we isolated new spheres from femur and tibia andBM cells were characterized for apoptosis, ROS and lipid peroxidation changes by flow cytometry analysis.

First, we investigated the in vivo AraC effects by measuring the blood cell counts, size of liver and spleen of WT and KO mice. When blood count was analyzed, we did not find any significant differences between WT and KO mice with the exception of a significant reduction ($p<0.05$) in WBC counts between Prdx6 KO mice ($193\pm20.74 \times 10^9$) and control mice($307.5\pm 7.5 \times 10^9$) (**Figure 4B**).

Then, we compared spleen and liver weight of WT and KO mice and we found a significant increase ($p<0.0179$) in spleen size in KO mice (mean of weight: 0.64 ± 0.032 g) as compared to the WT counterparts (mean of 0.449 ± 0.01462 g); no differences were observed in liver size (**Figure 4C-D**).

To test whether Prdx6 deficiency could alter the BM cellularity, the absolute numbers of BM cells were compared between WT and KO mice. The absolute number of total BM cells was not significantly different between WT and KO mice (mean of $21.25\pm6.25 \times 10^6$ in WT vs $13.33\pm0.2 \times 10^6$ in KO mice) (data not shown). Moreover, we demonstrated that the percentage of leukemic cells (expressing CD45.1, Lineage-negative and c-Kit-positive) did not differ between WT (68.36%±21) and KO mice(77.87%±11.27).

As shown in **Figure 4E-F-G**, we tested the apoptosis, ROS levels and lipid peroxidation in the leukemic cells of each mouseto study whether some antioxidant capacity is mediated Prdx6. For this set of experiments, BM cells were stained with anti-CD45.1 and -CD45.2 antibodies to discriminate leukemic cells (CD45.1) from normal BM cells (CD45.2) (as gated in the lineage-negative and c-Kit positive cells fraction). As regards apoptotic rate, the mean percentage of live

cells (c-kit+/Lin-) in leukemic fraction was 60.42%±25 in WT mice vs 92.09%± 0.7191 in Prdx6 KO mice (not significant). Regarding ROS staining, we found an increased, but not significant, geometric mean value of ROS levels in Prdx6-KO (Gmean of 2.727)as compared to control mice (Gmean of 1.74±0.3). Similarly, the geometric mean value of lipid peroxidation showed a slight increase in Prdx6-KO mice (mean of 260±20.6) as compared to control mice (201.8±3.175).

In summary, we found that, in vivo, the Prdx6 pathway does not seem to be critically involved in the stromal protection of leukemic blasts from ARA-C toxicity.

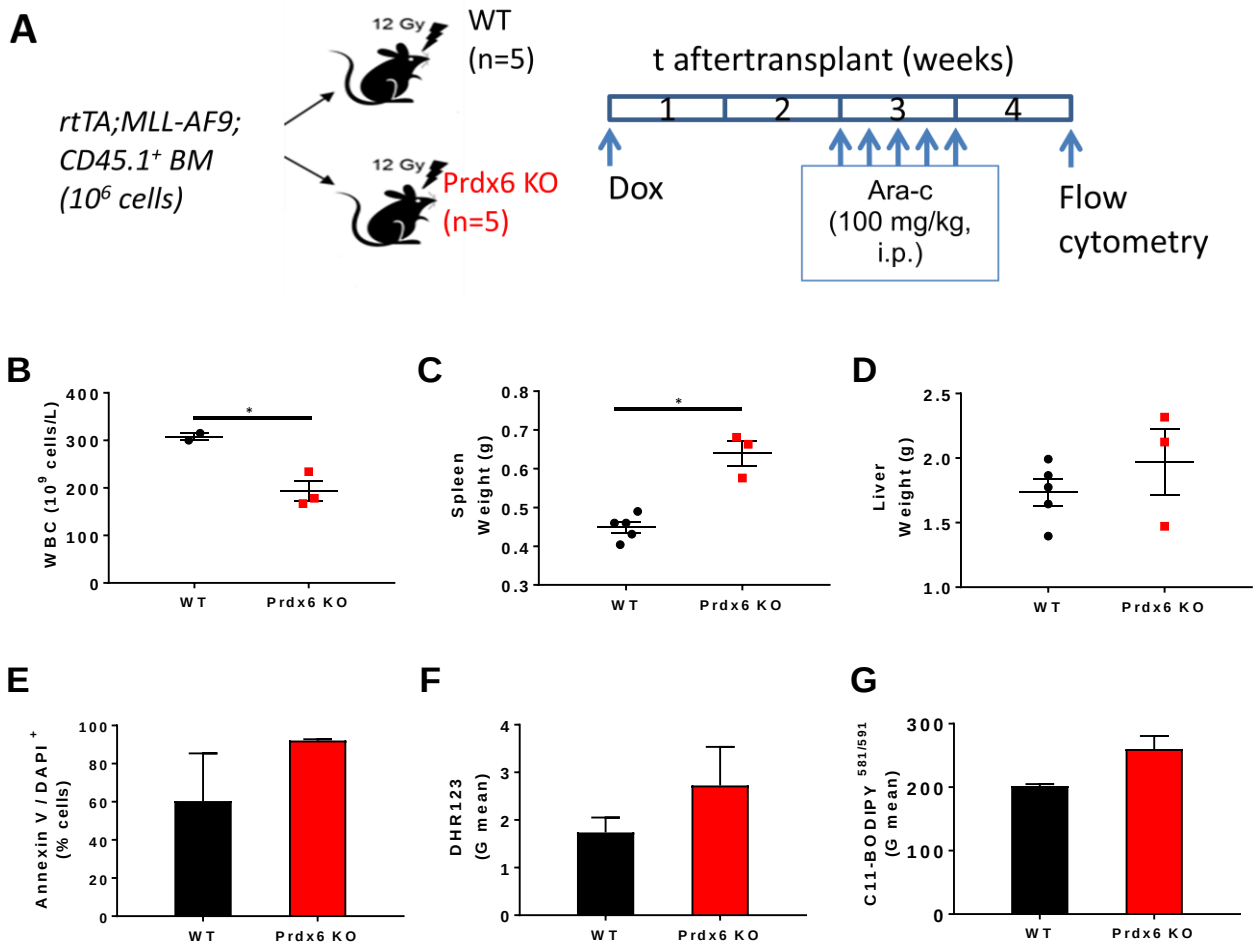

Figure 4

Differences in WT and Prdx6 KO mice and protective role of mesenspheres from Prdx6 KO mice in combination with Gpx4 inhibition.

***A**, Schematic of AraC treaments in a Prdx6 KO model. Lethally irradiated Prdx6 KO or control mice were transplanted with rtTA;MLL-AF9;CD45.1^{+} BM (10^{6} cells each). Doxycycline induction began 2 weeks post-transplant; AraC was initiated 2 weeks post-transplant and continued for 5 injections and sacrifice after 2 weeks.*

***B**, Number of WBC total cells, and spleen weight (**C**) and liver (**D**) at sacrifice. Lineage-negative cells, lin- c-kit+ cells in the leukemic fraction of the bone marrow of mice stained with Annexin V and DAPI (**E**) and ROS and lipid peroxidation using DHR123 (**F**) and C(11)-BODIPY(581/591) (**G**), respectively, by flow-cytometry. Numbers of WT and Prdx6 KO cells are represented separately. Unpaired two-tailed t-test.*

Mesenspheres from Prdx6-KO in combination with Gpx4 inhibitor did not lose their protective effects on leukemic blasts

To study *in vitro* the potential effects of inhibition of anti-oxidants molecules on our co-cultures system, we isolated mesenspheres from WT or Prdx6-KO mice from the above described experiments.

Firstly, we studied the potential effects of mesenspheres from KO mice in co-cultures with leukemic blasts. As previously reported, we set up new co-cultures experiments using WT or KO mesenspheres and leukemic blasts. Regarding the analysis of apoptosis in the presence of AraC, as expected, we found a significant ($p<0.05$) reduction in the percentage of apoptotic cells in leukemic blasts after co-cultures with WT spheres (percentage of apoptotic cells 56.48% ±6.569 in mono-cultures vs 19.41% ±5.835 in co-cultures with WT spheres) and a slight but not significant reduction of the mean apoptotic value(32.39 ± 15.5),when leukemic blasts were cultured with Prdx6 KO mice (**Figure 4H**).

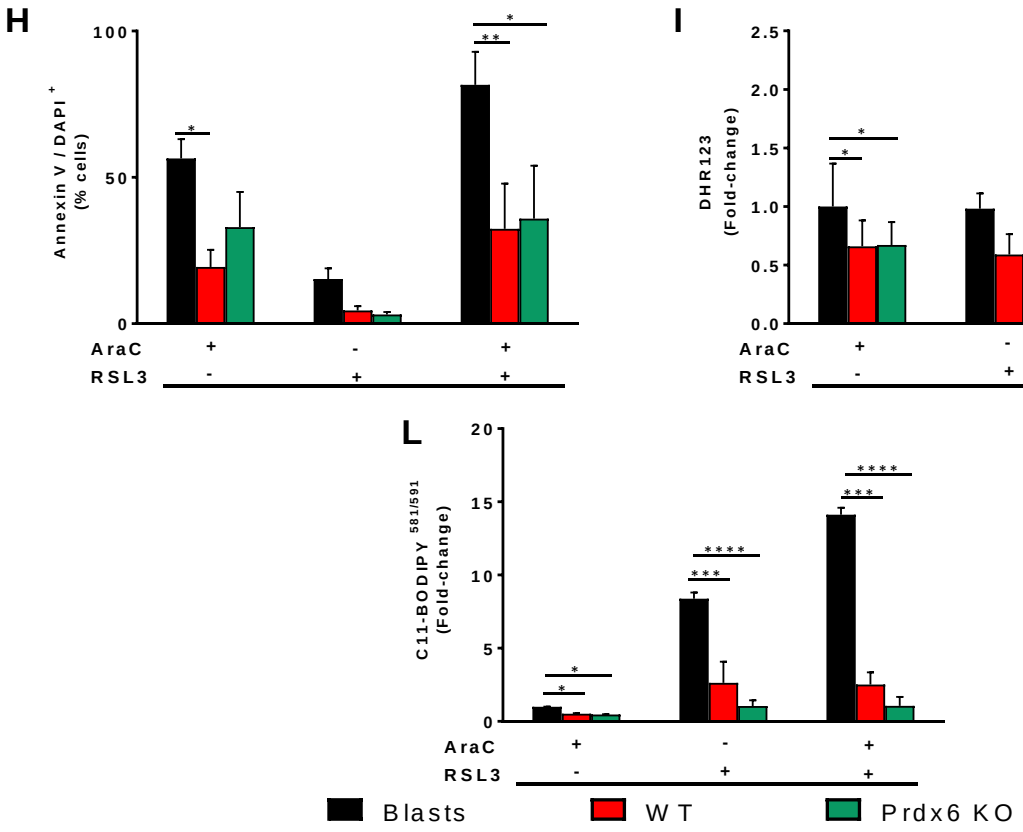

Figure 4

Potential of isolated mesenspheres by WT or Prdx6 KO mice in co-cultures with MLL-AF9 leukemic blasts after AraC treaments (first left group for each graph), RSL3 (Gpx4 inhibitor, middle group) and combination of AraC/RSL3 (right group).

***H**, Leukemic blasts (200 x 10^3 cells/ml) were cultured with WT or Prdx6 KO mice BM-derived mesenspheres (~250/ml) and the apoptotic rate was determined after 24 h by flow-cytometry following staining with Annexin V and DAPI, as described in Materials and Methods section. Significant differences of leukemic blasts in co-cultures with WT mesenspheres (red column) from the corresponding mono-cultures of leukemic blasts (black columns) in the presence of AraC(left panel, n=3; *P < 0.05) and AraC in combination with RSL3 (right panel, n=3; ** P < 0.01). Significant difference between leukemic blasts in the presence of KO mesenspheres and mono-cultures in the presence of AraC/RSL3 (n=3, *P < 0.05). One-way ANOVA followed by post-hoc multiple comparison.*

***I**, the above cultures described were also assessed by intracellular ROS production with DHR123 by flow-cytometry. Geometrical mean (G Mean) values of the fluorescence intensities normalized to Ara-induced ROS production from mono-cultures (leukemic blasts, black columns). Significant differences of leukemic blasts in co-cultures with WT spheres and KO mesenspheres from the corresponding mono-cultures of leukemic blasts in the presence of AraC(red and green columns, respectively; n=3; *P <0.05) and in the presence of AraC/Gpx4 (red and green columns, respectively; n=3; *P <0.05). One-way ANOVA followed by post-hoc multiple comparison.*

***L**, the above cultures described were also subjected to detection of lipid peroxidation using C(11)-BODIPY(581/591) by flow-cytometry. Geometrical mean (G mean) values of the fluorescence intensities normalized Ara-induced lipid peroxidation. Significant differences between leukemic blasts and leukemic blasts co-cultured with WT spheres in the presence of AraC (p< 0.05), RSL3 (p< 0.001) and RSL£/AraC (p<0.001). Significant difference also between leukemic blasts and leukemic blasts co-cultured with KO mesenspheres with AraC (p< 0.05), RSL3 (p< 0.0001) and RSL3/AraC (p<0.0001).*

Error bars represent mean values ± SEM.

As reported in our previous experiments, using a combination of inhibitors to block the protective effects of mesenspheres on leukemic blasts in co-cultures, we added RSL3 (GPX4 inhibitor) to Prdx6 KO spheres.

The survival of leukemic blasts in presence of WT or KO mesenspheres was not affected by RSL3 inhibitor alone. Surprisingly, when we added AraC in the presence of Gpx4 inhibiton, we found that the percentage of apoptotic leukemic blasts was 81.59% ±11.3 and strongly decreased in the co-cultures with WT (32.39% ±15.5; p<0.0085) and KO(35.92% ±18.09; p<0.013) spheres.

We also tested the ROS and lipid peroxidation changes and we found similar results. No differences were observed between KO and WT spheres but a strong protective effect on leukemic blasts was shown in the presence of AraC and RSL3 (**Figure 4I-L**). Specifically, when we treated cells with RSL3 alone or RSL3 with AraC, we found a significant reduction of lipid peroxidation in the presence of mesenspheres, both from WT (p<0.0001) or Prdx6 KO mice (p<0.00001) (**Figure 4L**).

In summary, these experiments demonstrate that the lack of Prdx6 only in the spheres, together with the inhibition of GPX4, is not sufficient to block the protective role of mesenspheres.

Effects of mesenspheres on MLL-AF9 leukemic cell metabolism and functional properties

We next investigated the effect of mesenspheres on leukemic cell metabolic activity. After mono-cultures and co-cultures for 24 h, the leukemic cells in different conditions were collected, counted and transferred to the SeaHorse plates for Extracellular Flux analysis.

The seeding density and concentrations of the injection compounds were optimized for our co-cultures and evaluated in measurements of oxygen consumption rates (respiration) and proton production rates (medium acidification). Oxidative phosphorylation (OXPHOS) and glycolysis activities were measured 24 h after the co-cultures and all activities were normalized to the number of leukemic cells present in the wells, as counted immediately before and after the SeaHorse measures.

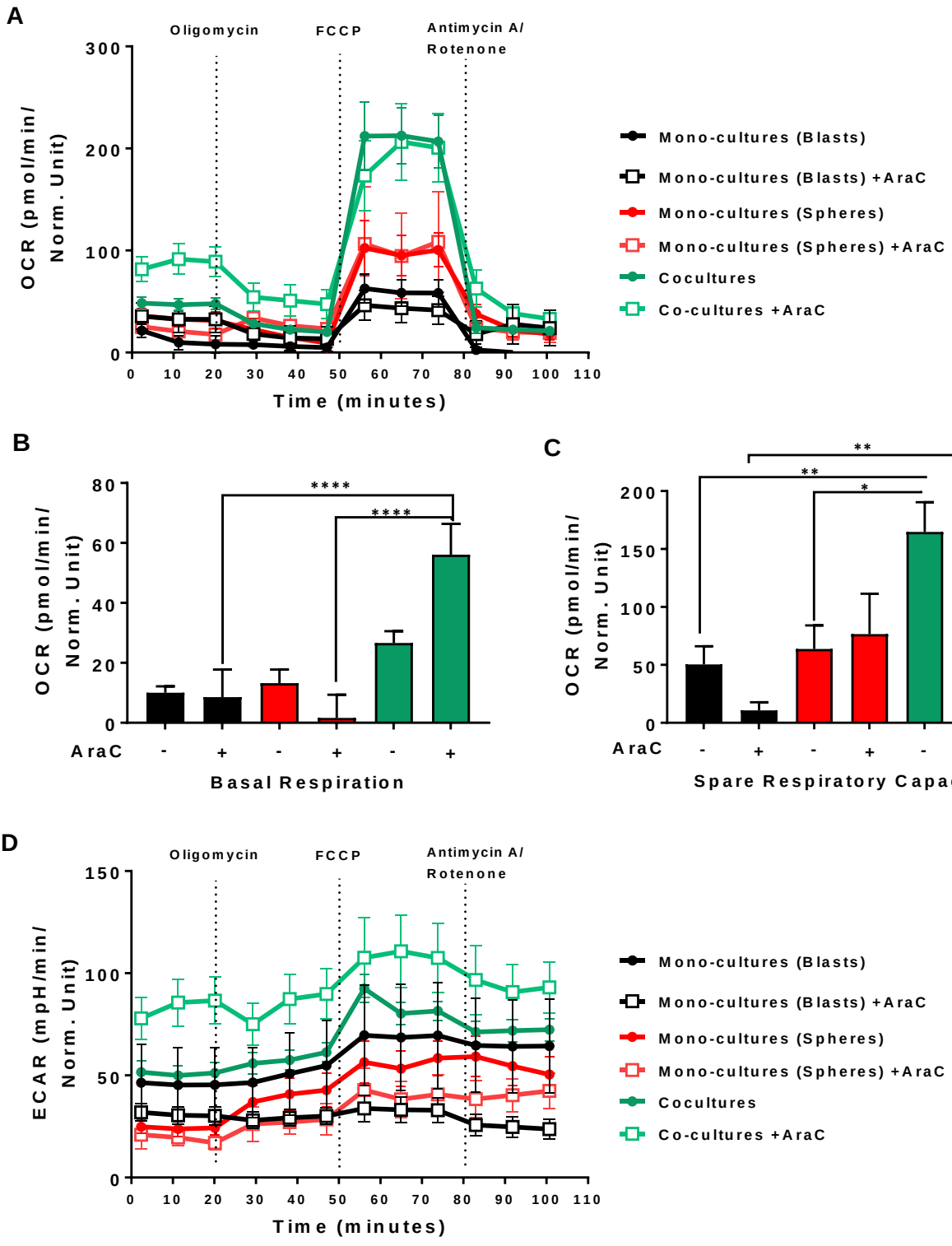
A
Oligomycin
FCCP
Antimycin A/
Rotenone
OCR (pmol/min/
Norm. Unit)
300
200
100
0
0 10 20 30 40 50 60 70 80 90 100 110
Time (minutes)
Mono-cultures (Blasts)
Mono-cultures (Blasts) +AraC
Mono-cultures (Spheres)
Mono-cultures (Spheres) +AraC
Cocultures
Co-cultures +AraC
B
OCR (pmol/min/
Norm. Unit)
80
60
40
20
0
****
****
AraC - + - + - +
Basal Respiration
C
OCR (pmol/min/
Norm. Unit)
200
150
100
50
0
**
**
*
AraC - + - + - +
Spare Respiratory Capacity
D
Oligomycin
FCCP
Antimycin A/
Rotenone
ECAR (mpH/min/
Norm. Unit)
150
100
50
0
0 10 20 30 40 50 60 70 80 90 100 110
Time (minutes)
Mono-cultures (Blasts)
Mono-cultures (Blasts) +AraC
Mono-cultures (Spheres)
Mono-cultures (Spheres) +AraC
Cocultures
Co-cultures +AraC

Figure 5

Agilent Seahorse XF Cell Mito Stress Test Profile for mitochondrial respiration in leukemic blasts, mouse BM mesenspheres and leukemic blasts co-cultured.

*Data from Mito Stress Test demonstrated absolute and baseline values of OCR (**A**, **B** and **C**) and ECAR (**D**). Leukemic blasts (200 x 10^3 cells/ml) and WT mice BM-derived mesenspheres (~250/ml) were cultured alone or in co-cultures for 24 h and then seeded on a Cell-Tak-treated XF96 cell culture plate as described in Materials and Methods section.*

***A**, Respiration (OCR) is measured under basal conditions and in response to the indicated mitochondrial inhibitors in MLL-AF9 mouse leukemic blasts (grey and black lines) and WT mouse BM mesenspheres (red lines) or in co-cultures (green lines), also in the presence of AraC. Changes after oligomycin (I.), FCCP (II.) and Antimycin A/Rotenone (III.) application are indicative for mitochondrial respiration. Individual parameters for basal respiration and spare respiratory capacity for each conditions. About basal respiration (**B**), significant differences from the corresponding mono-cultures of leukemic blasts or mesenspheres to leukamic blasts co-cultured, in the presence of AraC (n = 6 independent experiments; ****P < 0.0001). About spare respiratory capacity (**C**), significant differences from the corresponding mono-cultures of leukemic blasts or mesenspheres to leukamic blasts co-cultured, in absence of AraC (n = 6;**P < 0.01 and * P< 0.05, respectively) or between mono-cultures (leukemic blasts) vs leukemic co-cultured in the presence of AraC (**P < 0.01). One-way ANOVA followed by post-hoc multiple comparison.*

***D**, ECAR is measured under basal conditions and in response to the indicated mitochondrial inhibitors, considered as the result of anaerobic glycolysis.*

Error bars represent mean values ± SEM.

For OXPHOS, the oxygen consumption rate (OCR) was measured under basal conditions and in response to mitochondrial inhibitors. As shown in **Figure 5A-B**, the basal OCR values of the leukemic cells (OCR mean value of 10,03 ± 2.144) were increased in co-cultures(OCR mean value of 26,63 ± 3.924). Moreover, when we tested the basal respiration after AraC-treatment, we found a significantly ($p<0.0001$) enhance for the leukemic blasts in co-culture(mean value of 56,09 ± 10.25 in co-cultures vs 8,577 ± 9.19 in mono-cultures) (**Figure 5B**). This indicated that the mesenspheres could modify the metabolic activity of the leukemic cells by increasing basal respiration under AraC treatment.

Consequently, we evaluated the spare reserve capacity, that reflects the difference between basal and maximal respiratory rate. Consistent with our previous results, the spare reserve capacity were increased in co-cultures as compared to mono-cultures (OCR mean 164,8 ± 25.58 and 50,34± 15.68 for co-cultures and leukemic blasts,respectively).

We next sought the extracellular acidification rate (ECAR), indicative of the glycolytic activity. Leukemic blasts displayed a significantly higher compensatory increase of the aerobic glycolysis for meeting their energetic demands after using mitochondrial inhibitory (ECAR value after oligomycin and FCCP respectively of 46.49 ± 17.2 and 69.64 ± 24.79 in leukemic blasts vs 55.91 ±

5.242 and 92.98± 6.804 in co-culturedleukemic cells) (**Figure 5C**). Of note, when we considered AraC-treated cells, leukemic cells in co-cultures had a significant increase with a mean ECAR value of 75±10.13 and 107.6 ± 19.46 after oligomycin and FCCP as compared with 28±4.113and 33.87±6.65 in mono-cultures. The glycolytic reserve were increased in leukemic blasts in co-cultures conditions, above all in the presence of AraC.

We also checked the effect of CM from mesenspheres, leukemic blasts or co-cultures on metabolic activity. Interestingly, although both the basal respiration and spare reserve capacity of leukemic cells were increased upon normal co-cultures, these effects were not observed for CM experiments, suggesting the importance of direct contact for the leukemic cells (**Figure 6A, B, C**).

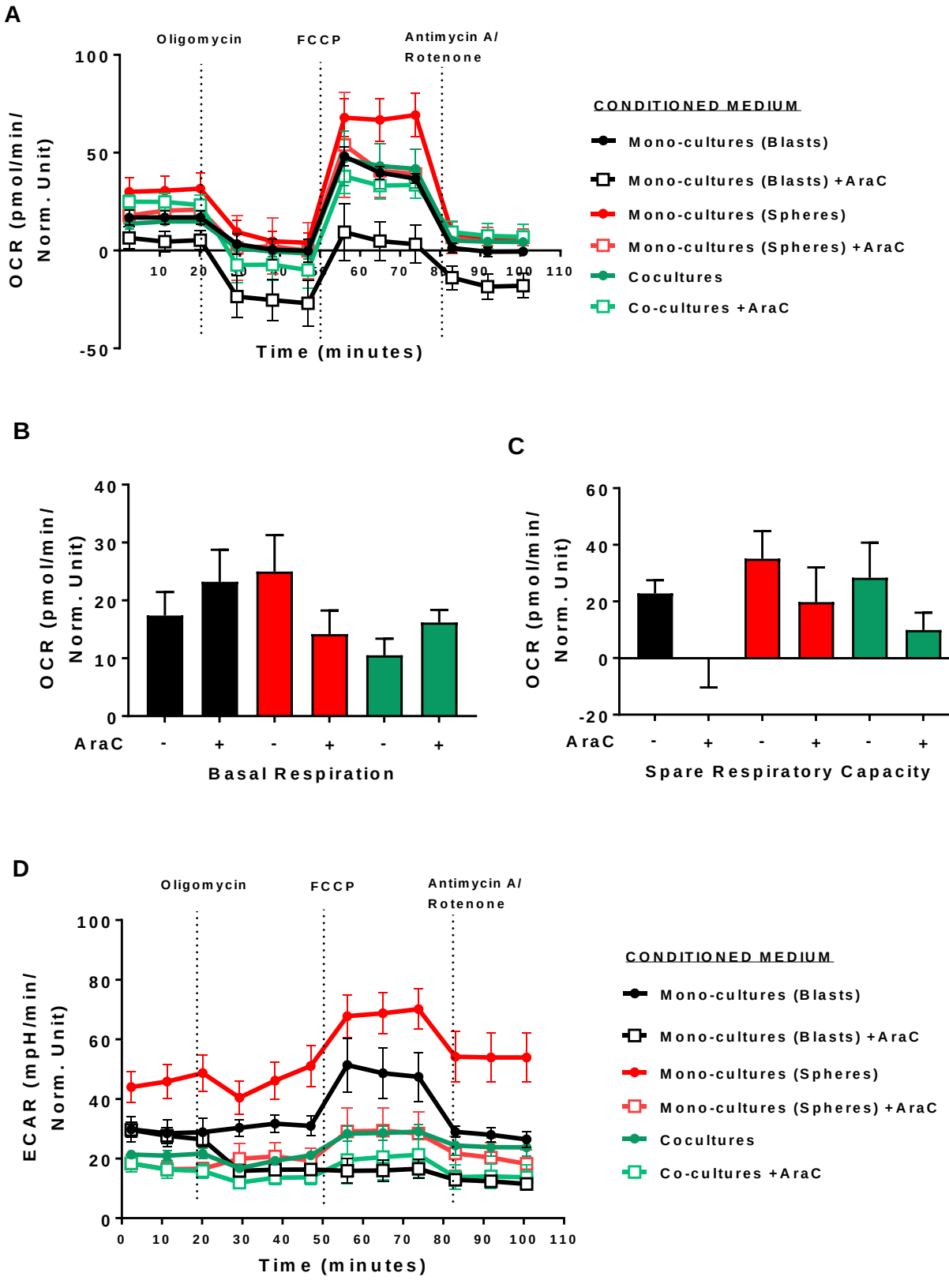
A
Oligomycin
FCCP
Antimycin A/
Rotenone
OCR (pmol/min/
Norm. Unit)
100
50
0
-50
10
20
60
70
90
100
110
Time (minutes)
CONDITIONED MEDIUM
Mono-cultures (Blasts)
Mono-cultures (Blasts) +AraC
Mono-cultures (Spheres)
Mono-cultures (Spheres) +AraC
Cocultures
Co-cultures +AraC
B
OCR (pmol/min/
Norm. Unit)
40
30
20
10
0
AraC
-
+
-
+
-
+
Basal Respiration
C
OCR (pmol/min/
Norm. Unit)
60
40
20
0
-20
AraC
-
+
-
+
-
+
Spare Respiratory Capacity
D
Oligomycin
FCCP
Antimycin A/
Rotenone
ECAR (mpH/min/
Norm. Unit)
100
80
60
40
20
0
0
10
20
30
40
50
60
70
80
90
100
110
Time (minutes)
CONDITIONED MEDIUM
Mono-cultures (Blasts)
Mono-cultures (Blasts) +AraC
Mono-cultures (Spheres)
Mono-cultures (Spheres) +AraC
Cocultures
Co-cultures +AraC

Figure 6.

Agilent Seahorse XF Cell Mito Stress Test Profile for mitochondrial respiration in leukemic blasts, mouse BM mesenspheres and co-cultures.

*Data from Mito Stress Test demonstrated absolute and baseline values of OCR (**A**, **B** and **C**) and ECAR (**D**). Leukemic blasts (200 x 10^3 cells/ml) and WT mice BM-derived mesenspheres (~250/ml) were cultured alone or in co-cultures for 24 h and then CM collected to seed new leukemic blasts (with CM from previous cultures) for 24 hrs. After that cells, counted and seeded on a Cell-Tak-treated XF96 cell culture plate as described in Materials and Methods section.*

***A**, Respiration (OCR) is measured under basal conditions and in response to the indicated mitochondrial inhibitors in MLL-AF9 mouse leukemic blasts (grey and black lines) and WT mouse BM mesenspheres (green lines) or in co-cultures (blue lines), also in the presence of AraC. Changes after oligomycin (I.), FCCP (II.) and Antimycin A/Rotenone (III.) application are indicative for mitochondrial respiration. **B**, **C** Individual parameters for basal respiration and spare respiratory capacity for each conditions. No significant differences between the corresponding mono-cultures of leukemic blasts or mesenspheres to leukemic blasts co-cultured, also in the presence of AraC (n = 4 independent experiments. **D**, ECAR is measured under basal conditions and in response to the indicated mitochondrial inhibitors, considered as the result of anaerobic glycolysis. One-way ANOVA followed by post-hoc multiple comparison.Error bars represent mean values ± SEM.*

Functional mitochondria from BM mesenspheres enter into MLL-AF9 leukemic blasts

Mitochondria serves a major source and 'a sink' of ROS cells that displayed a crucial role in cell metabolism and signaling of leukemic cells.[206] We found different amounts of intracellular ROS in leukemic blasts in co-cultures with mesenspheres. Therefore, we hypothesized that the opposite metabolic state and ROS levels of leukemic blasts, in mono-cultures vs co-cultures, was due to mitochondrial transfer between the two populations. We performed co-cultures experiments after staining of leukemic blasts and mesenspheres with Miotracker dye. To demonstrate whether mitochondria were involved in this transfer, mesenspheres were stained with a MitoTracker CMXRos Red and incubated with unlabeled or Mitotracker Green FM-stained leukemic cells for 24 hours before analysis (**Figure 7**).

To set-up our experimentsand argue against passive dye transfer, we washed stained cells several times and left in cultures alone before co-cultures,so that excess MitoTracker dye could be washed out. Moreover, we repeated experiments with transwell to exclude any possible leakage of the Mitotracker dye in the medium.

As shown in the **Figure 7A-D**, the Mitotracker labeled mitochondria transfer was checked by flow cytometry to quantify the efficiency of the mitochondria transfer. We found a percentage of leukemic blasts (around 47.15% ±8.046) positive for MitotrackerCMXRos Red from mesenspheres, previously stained. This observation led to the hypothesis that leukemic blasts acquiring mesenspheres mitochondria would display greater chemoresistance. Therefore, we repeated these

experiments in the presence of AraC treatment. To note, we found a percentage of cells stained for Mitotracker CMXRos Red around 72.2% ±12.1, with a higher ratio as compared to normal medium after drug treatment. Importanlty, Mitotracker Red CMXRos is a fluorescent dye that stains mitochondria and its accumulation is dependent upon membrane potential, suggesting a mitochondrial function evaluation.

We could also detect uptake of leukemic blasts mitochondria by mesenspheres, more difficult to evaluate for problems associated with aggregation and intrinsic morphology of spheres. Anyway, our data provided evidence for a preferential transfer of mitochondria from mesenspheres under our culture conditions (data not shown).

We also tested a transwell experiment setting to confirm the role of direct cell contact in the transfer of mitochondrian in the absence or presence of AraC (**Figure 7C**). We seeded leukemic blasts on the bottom or the top of the transwell chamber and mitotracker on the other side. In a transwell system, we calculated a percentage of Mitotracker Red CMXRos mitochondria around 0.5% ±0.092 in normal medium and 1%±0.8 with AraC treatment, significantly decreased as compared to cell-contact transfer (*P<0.001*, respectively**; Figure 7D**).

Under these conditions any Mitochondria exchanges were observed in transwell experiments, suggesting that cell-cell contact- in required for mitochondrial transfer from BMSCs to leukemic blasts.

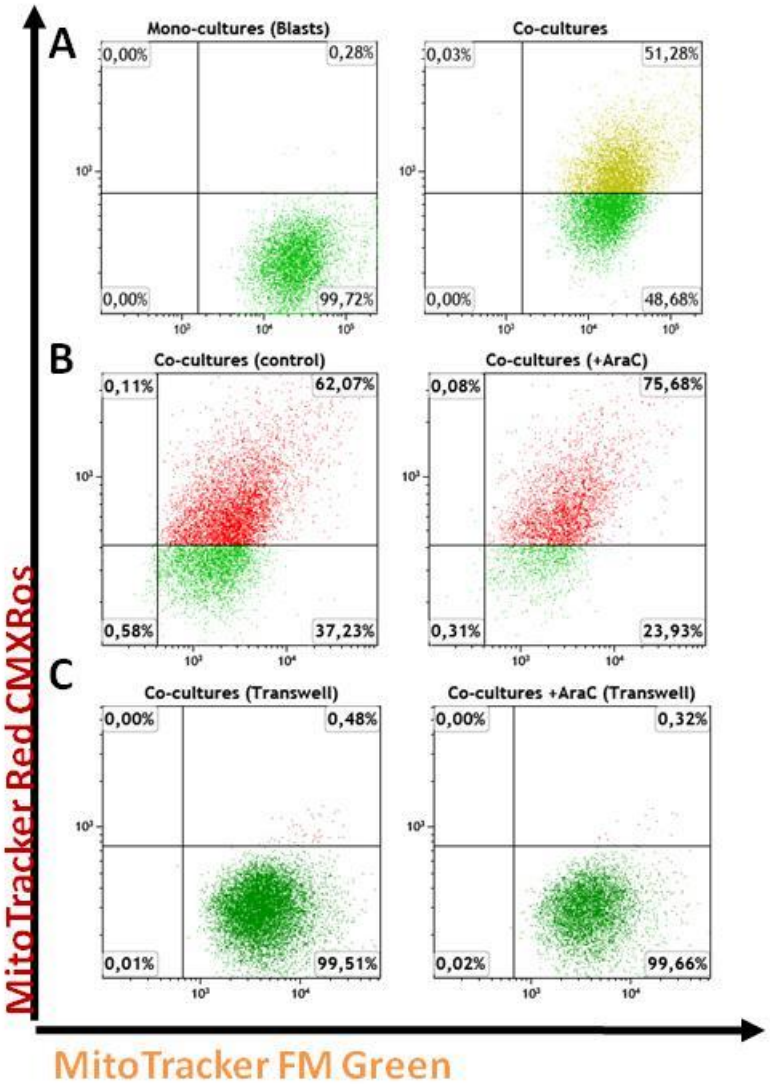
A
Mono-cultures (Blasts)
0,00%
0,28%
0,00%
99,72%
Co-cultures
0,03%
51,28%
0,00%
48,68%
B
Co-cultures (control)
0,11%
62,07%
0,58%
37,23%
Co-cultures (+AraC)
0,08%
75,68%
0,31%
23,93%
C
Co-cultures (Transwell)
0,00%
0,48%
0,01%
99,51%
Co-cultures +AraC (Transwell)
0,00%
0,32%
0,02%
99,66%
MitoTracker Red CMXRos
MitoTracker FM Green

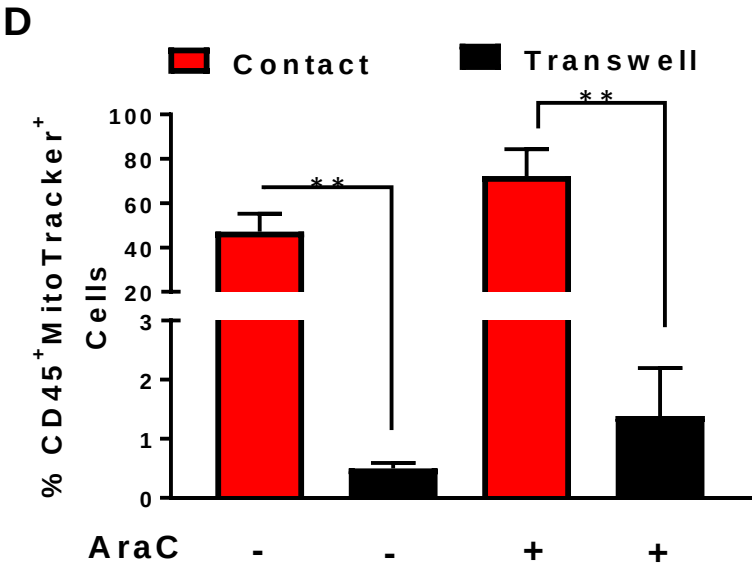
D
Contact
Transwell
% CD45+MitoTracker+ Cells
100
80
60
40
20
3
2
1
0
**
**
AraC
-
-
+
+

Figure 7

Mitochondrial transfer from WT mouse BM mesenspheres to MLL-AF9 mouse leukemic blasts. *Mesenspheres mitochondria were labeled with Mitotracker Red CMXRos (red) and leukemic blasts with Mitotracker FM Green (green).* ***A,*** *Representative flow cytometry dot plot defining the population of leukemic blasts cultured alone (mono-culture) gated on CD45^{+}, previously stained with Mitotracker FM Green (green dot plot) as described in Material and Methods section. In coculture with mesenspheres for 24 hours, co-staining of green and red (yellow), indicated robust transfer of mitochondria from mesenspheres (red) to leukemic blasts (green) (second panel).* ***B,*** *Population of leukemic blasts (stained with CD45 APC and previously with Mitotracker FM Green) cultured with mesenspheres (previously stained with Mitotracker Red CMXRos) for 24 h in control condition (left panel) compared to condition in the presence of AraC (right panel). After 24 hours in coculture with AraC, more than 75% of CD45^{+} leukemic blasts demonstrate acquisition of MitoTracker Red fluorescence as compared to more than 60% in control situation, indicating extensive mitochondrial transfer from mesenpsheres. Data representative of at least six independent experiments.*

Mitochondrial transfer from WT mouse BM mesenspheres to MLL-AF9 mouse leukemic blasts in 96-well transwell. ***C,*** *A representative dot plots defining the population of CD45-APC leukemic blasts previously stained with Mitotracker FM Green (in the lower chamber) and co-cultured for 24 h with spheres previously stained with Mitotracker Red CMXRos (in the upper chamber), left panel. Under the same conditions, CD45 APC leukemic blasts previously stained with Mitotracker FM Green (in the lower chamber) and co-cultured for 24 h, as described above, with Mitotracker Red CMXRos spheres (in the upper chamber) in the presence of AraC, right panel. Data representative of at least three independent experiments.*

D*, Percentage of leukamic blasts positive for CD45 co-cultured with Mitotracker red-mesenspheres, also positive for Mitotracker red in contact (red columns) or separated by Mitotracker red-mesenpsheres separated by transwell systems.*

Mitochondria transferred from BMSCs rescue excessive ROS levels in the leukemic blasts

The mitochondrion is a key regulator of apoptosis, and its intercellular transfer has been associated with the recovery of injured cells.[207] Therefore, we examined whether Mitotracker Red mitochondria from mesenspheres were also labelled with the specific fluorescent dyeDHR123 in leukemic blasts. We observed that DHR123-labelled mitochondria also stained for Mitotracker CMXRos Red were present in a different percentage in AraC-treated and untreated cells (**Figure 7E-F**). In particular, we found a mean of 79.17 %± 4.227 in untreated cells and a mean of 96.94%±1.279 for double positive cells. By contrast, we found a very small fraction of Mitotracker Red-positive cells, also negative for DHR123 (around 2.04%±0.67in untreated cells and around 2.4± 0.57 in AraC treated cells), totally absent in mono-cultures of leukemic blasts after 24 h in cultures (**Figure 7G**).

The fraction of DHR123-negative mitochondria were detected in both conditions, untreated and AraC-treated cells. Altogether, these results suggest that mitochondria transferred from BMSCs to

the leukemic blasts can enhance metabolism and provide antioxidant defence, decreasing excessive and damaging ROS levels.

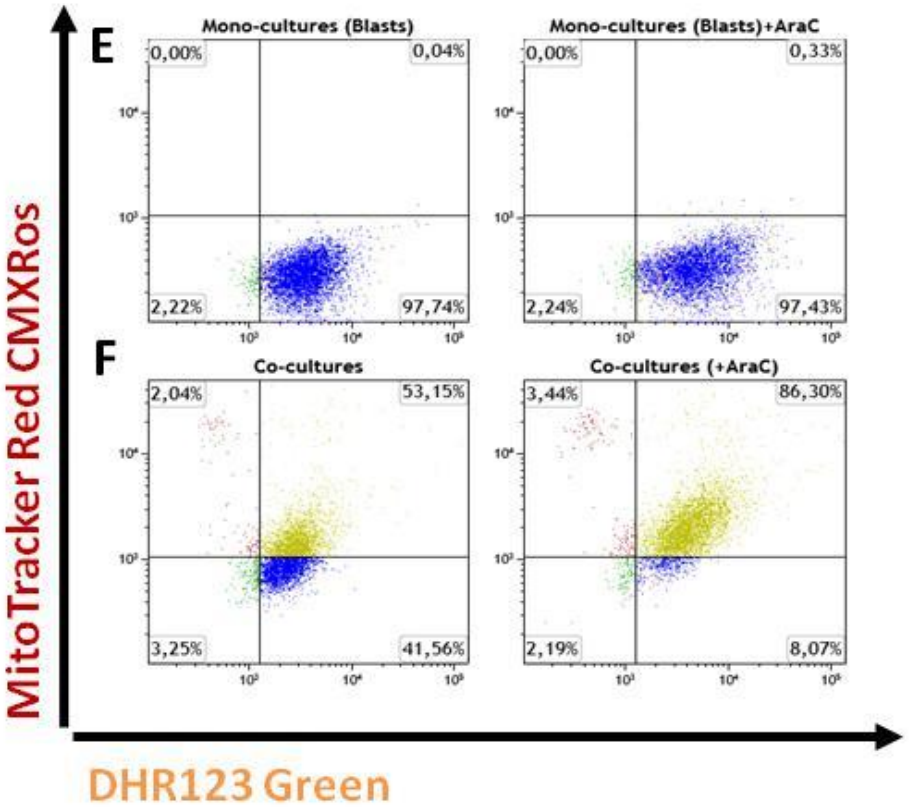

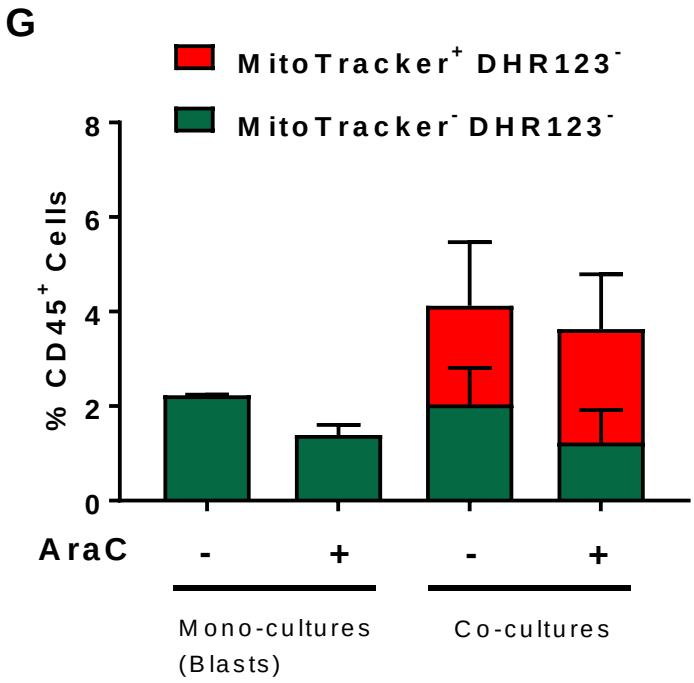

Figure 7

Mitochondrial transfer from WT mouse BM mesenspheres to MLL-AF9 mouse leukemic blasts and changes in ROS levels.

*Mesenspheres mitochondria were labeled with Mitotracker Red CMXRos (red) and leukemic blasts unstained were seeded alone or in co-cultures. After 24 h, ROS levels, using DHR123 (FITC), were assessed in leukemic blasts alone (first panels, **E**) or in co-cultures (bottom panels, **F**) to check double-staining with Mitotracker Red CMXRos, indicating changes in mitochondrial ROS production levels, also in the presence of AraC (right panels).*

***G**, Percentage of CD45 positive cells unstained for ROS dye (indicated as DHR123$^-$ cells in green). Percentage of CD45 positive cells, negative for DHR123 (DHR123$^-$) also positive for Mitotracker Red only in the presence of mesenspheres in cultures.*

Data representative of at least two independent experiments.

DISCUSSION

Here we delineate a novel method of isolating and culturing mouse BMSCs to underline the cross-talk between BMSCs as non-adherent 'mesenspheres' and leukemic blasts from a MLL-AF9 mouse model. *Ex vivo* expansion of hematopoietic progenitors is supported also by BMSCs cultured under standard adherent conditions,[194,208-210] but may be insufficient to preserve primitive HSCs.[211] Characteristics and features of 2D cultures are compromised because a highly artificial and less physiological environment. In addition, several studies have suggested that adherence to plastic promotes BMSC differentiation. Moreover, 3D cultures resembles the native configuration of cells *in vivo* with a microenvironment allowing for direct cell-cell signaling and cell-matrix interplay. In addition, BMSCs cultured as spheroids have improved cell survival, after transplantation,enhancing anti-inflammatory, angiogenic, and regenerative properties.[18,193,212]

Isern et al.[193] showed a detailed characterization ofmurine and human BM cell population that was able to form mesenspheres. Particularly, self-renewing murine mesenspheres are able to transfer hematopoietic activity to an engineered bone scaffold and human mesenspheres are capable to support cord blood HSCs.

In our current work, data demonstrate that nestin^{+} BMSCs can also support the survival of leukemic blasts MLL-AF9. We did not need to use specific surface markers to grow murine mesenspheres, because we could simply derive them from immunomagnetically enriched BM CD45^{-}/Ter119^{-}cells using a specific culture medium. Cross-talk between leukemic cells and bone marrow stromal cells favors blasts progression and drug resistance. Therefore, understanding the interaction between leukemic cells and their environment by co-culture systems is an attractive tool to find out the mechanisms mediated by these interactions, already elusive.

In a set of experiments, we investigated the effects of minimal medium in our co-cultures, mimicking the nutritional limitations encountered in the leukemic BM. Fetal bovine serum (FBS) is frequently used as supplementation to a basal medium that contains certain nutritional and macromolecular growth factors in order to promote cell growth.[213] Serum deprivation, as environmental stress, is a common model of cellular stress *in vitro* and is used to study the anti-apoptosis peculiarity of tumor cells. Surprisingly, cellular stress could be considered as one of the crucial factors responsible for initiating the carcinogenic process and treatment resistance. Serum deprivation induces apoptosis and reduces basal cellular activity in various cells.[214] Moreover, nutrient deprivation induces cell apoptosis, which is accompanied by the induction of reactive oxygen species (ROS).[215]

Tumor cells initiate and activate defence mechanisms against apoptosis under serum deprivation.[214] In this study, we observed a protective role of mesenspheres by FBS deprivation, suggesting a mesenpshere-mediated metabolic adaptation of leukemic blasts in co-culture. Indeed, leukemic blasts were more resistant to FBS starvation, as confirmed by ROS and lipid peroxidation reduction in co-cultures. Probably, mesenspheres are able to alleviate mitochondrial stress by diminishing oxidative injury of ROS in leukemic blasts.

Interestingly, CM from mesenspheres, alone and from co-cultures, were able to restore this protection only in absence of FBS. Similarly the same positive effects were found in transwell experiments. On the contrary, in our experiments with AraC treatments, neither CM from mesenspheres and co-cultures or transwell system were able to recapitulate protections from spheres in leukemic blasts. Concomitantly, further works showed that contact-mediated signals to LSCs were necessary to drug response.[150] As confirmed by our results, cell-cell contact is necessary between leukemia cells and stromal cells to provide survival signals and induce drug resistance to cytotoxic drug therapy.[216] Essentially, under FBS deprivation direct cell–cell contact mechanism and BMSC-secreted soluble factors seems to be both involved in our cultures system.

It is clearly demonstrated that cells' fate depends on the levels of ROS and a pathogenic role of ROS. Particularly, low levels of ROS provide beneficial effects, but altered ROS levels stimulate leukemogenesis.[196] Notably, in primary AML cells studies, the ROS production is characterized by heterogeneity in the bulk leukemic cell population: leukemic ROS-low cells that are quiescent cells exerting functional properties of LSCs and ROS-high cells that are more proliferating. In addition, ROS-low leukemic cells are metabolically dormant and are dependent on oxidative respiration rather than glycolysis for energy generation.[36] More primitive leukemic cells are more dependent of mitochondrial respiration than on glycolysis to sustain their energetic metabolism and survival.[36] In our novel system, after AraC treatments, we showed a supportive role by mesenspheres with a reduction of ROS level and lipid peroxidation.

For these reasons, we also evaluated the oxygen consumption rate (OCR) to study a key parameters of mitochondrial function, such as basal respiration and spare respiratory capacity. Here, we observed an increasing on mitochondrial respiration with a parallel increase in glycolytic capacity, suggesting a balance in energy metabolism in the presence of mesenpsheres. In addition, we noted an increased spare reserve capacity in leukemic blasts co-cultured with mesenspheres also after AraC treatment, suggesting a role of mesenspheres to counterbalance against increase oxidative

stress. As reported in other study under radiation,[217] in our model the cross-talk with mesenspheres could drive a re-activation or a switch preferably to mitochondrial oxidative metabolism under AraC treatment. It is noteworthy that tumor microenvironment modulates cancer cell's bioenergetics.[218] Energy metabolism is influenced by presence of mesenspheres, providing a metabolic profile in support to chemotherapy.[219]

Phospholipids are a major structural component of all cell membrane and lipid peroxidation alters the physiological functions of cell membranes. Peroxidation of cell membrane-associated phospholipids has been implicated in the pathogenesis of various disorders[220] and it also consider as marker of apoptosis,[221] as destructive process which cause leakage of cellular membranes.[222] Thus, the ability to reduce lipid peroxidation is of primary importance in the recovery of cells from oxidative stress.[220] Here, we studied the effects of AraC on lipid peroxidation. As reported in a previous study, AraC induces apoptosis and lipid peroxidation in NF-*k*B expressed cells.[221] In the present study, the reduction of lipid peroxidation could be explained by the presence of mesenspheres due to release of soluble factor or partly release of secrete cytoprotective factors as fatty acid to prevent lipid peroxidation. The surrounding stroma is known to modulate the response to chemotherapy by either direct cell-cell interactions with tumor cells, or through the release of a large spectrum of growth factors and cytokines.[223-226] Particularly, *Jeanine M. L. Roodhart et al.*[227] found that MSC-Induced Resistance is mediated by the Release of Polyunsaturated Fatty Acids. Indeed, polyunsaturated fatty acids (PUFA) are prone to oxidation by ROS and subsequent lipid peroxidation. On a speculative view, these results suggest that mesenspheres could provide more resistant PUFA to leukemic blasts and/or downregulating ROS levels.

Mitochondria are essential organelles for the survival of cells and play a crucial role in oxidative phosphorylation (OXPHOS), ATP production and diverse cell signaling pathways.[228]
When mitochondrial ROS production exceeds the capacity of the cell's antioxidant systems or when the latter systems are less active, increased ROS levels can induce cell damage, as oxidative stress.[229]To prevent the damage from ROS, cells possess several antioxidant enzymes, which are located in the mitochondria and the cytosol, respectively. One fundamental antioxidant defense mechanism is provided by nonenzymatic antioxidants such as GSH, which functions in the cellular thiol/disulfide system. Therefore, it seems reasonable to hypothesize that the presence of GSH reduced provides protection against ROS damage, as shown in our co-cultures. However, as reported by *Harris et al.*[230], the GSH antioxidant pathway is required for cancer initiation but after

cancer initiation, GSH is dispensable due to alternative antioxidant pathways. Intracellularly the majority of GSH is formed in the cytosol (90%) while mitochondria contain nearly 10 % and reticulum endplasmatic contains a very small percentage.[231] Accordingly, is described a peculiar function of the leukemia niche as metabolic support, as reflected by the selective dependence on stromal cysteine to control ROS in leukemia cells. Specifically it is showed the dependence of CLL and ALL cells on stromal cysteine supply to maintain GSH synthesis in order to mitigate oxidative stress.[66,67] Accordingly, we observed an increase level of intracellular GSH in the presence of mesenspheres, which confer protection against AraC-induced apoptosis. Interestingly, we found a correlation between mitochondria and GSH, indicating a further association with a decrease of GSH and concomitant increase in ROS only in mono-cultures.The cells in co-culture were less responsive to oxidative stress induced by AraC compared to leukemic cells alone.

However, the use of antioxidants to inhibit the ROS- inflicted damage elsewhere have so far been unsuccessful.[232] Indeed, in our in vivo experiments using Prdx6 KO mice we did not provide any important difference in terms of ROS levels and lipid peroxidation. As crucial anti-oxidant enzyme, Prdx6 is the bifunctional molecule with peroxidase and phospholipase A_2(PLA_2) activities, that are known to play a critical role in antioxidant defense of lung and other organs.[220]Both the peroxidase and PLA_2 activities are important in protecting cells against death associated with oxidant stress. Prdx6 is a thioredoxin-like protein with a 1-Cys peroxidase that utilizes GSH or ascorbate to recycle the oxidized form.[233] In particular, the cellular functions of PLA2 are responsible for phospholipid remodeling and for generation of arachidonic acid (AA) and lysophospholipid, related to multicellular functions, such as cell proliferation, apoptosis, and inflammatory events.[234]Regarding inhibition of anti-oxidant in vivo, we used a mouse model for Prdx6 KO. Specifically, our hypothesis was to find a significant increase on ROS level and lipid peroxidation in the leukemic fraction of cells transplanted in mice without protection from Prdx6 ($Prdx6^{-/-}$ mice). As described, in BM leukemic fraction (expressing CD45.1), we observed only a trend, albeit not significant toward increased ROS and peroxidation levels.These results may be the consequence of the treatment timing, which led to a massive infiltration of the BM with a shorter survival, already before treatment with AraC. Moreover, related to these problems the limited numbers of samples are not sufficient to deeply understanding of this mechanism.

In our experiments in vitro,we aimed to combine the KO for Prdx6 in the mesenspheres with the inhibiton of GPX4. Beside Prdx6, only GSH peroxidase 4 (GPx4) has been identified as another protein withsignificant PHGPx (phospholipid hydroperoxide GSH peroxidise) activity.[235] As one of

the most important mammalian redox enzymes, GPX4 has considered important of this finely tuned antioxidant defense. Recent data suggested an important role of Gpx4 for the survival of T cells and renal tubular cells by preventing ferroptosis.[236] Using mesenspheres from WT or Prdx6KO mice in vitro, we expected to block mesenspheres protection in leukemic blasts in response to oxidative stress. Notably, we set up co-cultures using WT or Prdx6$^{-/-}$ mice mesenspheres from in vivo experiments and MLL-AF9 leukemic blasts in the absence or presence of Gpx4 inhibitor, RSL3. Surprisingly, we did not observe a reverse effects on leukemic blasts mediated by mesenspheres as regard to survival and effects on ROS levels and lipid peroxidation in the presence of RSL3. In summary, this finding demonstrates that it is not sufficient to block anti-oxidant Prdx6 only in spheres (from Prdx6 KO mice) and Gpx4 in both type of cells, using inhibitor in cultures. Previous results have already shown that KO of Prdx6 has no significant effect on the expression of anti-oxidant enzymes other than Prdx6,[220] providing support to the conclusion that the described effects in our co-cultures are not sufficient to remove protection from mesenspheres. Indeed, as reported in other works,[230] if malignant transformation has already occurred, upregulation of alternative antioxidant pathways, render treatment with anti-oxidant alone ineffective.

It is relevant that mesenchymal stromal cells are capable of transferring mitochondria, rescuing cellular bioenergetics.[237] To better understand which mechanism could activate this dependence of leukemic blast by their niche, we hypothesized a new mechanism of mitochondria exchanges as fuel of bioenergetic, anti-oxidants and chemo protection for leukemic blasts.In our cell culture settings, we demonstrated transfer of mitochondria from stromal cells to leukamic cells. Our analysis demonstrated the preferential transfer of mitochondria from mesenspheres. Mitochondria transfer has already been described in different models,[238] and the mechanism of cancer cells acquiring mitochondria displaying chemoresistance is not new. However, for the first time, we demonstrated this mechanism of mitochondria transfer related to ROS in leukemia using mesenspheres by performing a novel co-cultures. Of note, we detected high percentage of leukemic mitochondria with GSH in co-cultures. Strikingly, we highlighted a proportion of mesenspheres-mitochondria with less ROS level in leukemic blasts co-cultured. This could provide another proof of a directional transfer of mitochondria as supportive for oxidative stress. Singularly, we described a heterogeneity in ROS levels of leukemic blasts mitochondria in the presence of mesenspheres. On the contrary, in terms of GSH levels, we showed a more consistent homogeneity in mitochondria of leukemic blasts co-cultured. On the other hand, mitochondrial heterogeneity emphasizes the novel level of mitochondrial complexity with an understanding mechanisms of mitochondrial function.[239]

In addition, our study demonstrates that AraC treatment could enhance intercellular mitochondria transfer between mesenspheres and leukemic blasts, in which the ROS signaling pathway is involved. Indeed, AraC treatment increased ROS levels that may subsequently increase lipid peroxidation as damage also to mitochondria. This, in turn, contributes to mitochondrial donation from mesenspheres to leukemic cells as emergency mechanism. When mitochondrial ROS production exceeds the capacity of the cell's antioxidant systems or when the latter systems are less active, increased ROS levels can induce cell damage (oxidative stress).[229] Mitochondrial energy imbalance lead to ROS production, so for this reason a donation from mesenspheres of mitochondria with decreased level of ROS could offer a unique advantage to leukemic blasts. In this instance, mitochondria, which possess powerful antioxidant systems,[229] could be donate by mesenspheres as protective and defence systems. In line of these results, the prevailing view could be explained by a cooperation between leukemic blasts and mesenspheres focused on anti-oxidant defence and source of energy mitochondria-mediated.

As microenvironmental resistance is one of the main problems for leukemia, elucidating the underlying mechanisms will be helpful to eradicate leukemia. Studies in this field will critically pave the way for novel approaches to try to improve clinical outcome. Our work highlights a new isolation and culture system to study the crosstalk of leukemic blasts with BMSCs. Although our data has uncovered that mitochondrial transfer from BMSCs endows leukemic cells with increased bioenergetics and resistance, the detailed networks and the mechanisms that drives this protection on leukemic blasts have only partially been examined. Future work will dissect specific pathways by which BMSCs boost energy availability and antioxidant defense in leukemic cells.

MATERIAL AND METHODS

Cell Isolation and Culture

Mesenspheres were cultured from mouse primary BM cells. Clean mouse bones were crushed in a mortar with 2 ml of a solution containing 0.25% type I collagenase and 20% FBS in PBS (StemCell Technologies). The suspension was incubated for 45 minutes at 37 ºC in a water bath under shaking. After addition of PBS+ 2% FBS and passage through a 40 um cell strainer, erythocytes were lysed by incubation on ice with RBS Lysis Buffer. After this, erythoid and hematopoietic cells were removed by magnetic depletion after incubation with biotin-conjugated primary antidodies against CD45 and Ter119 (BD Biosciences, 1:100) and subsequent incubation with streptavidin-conjugated magnetic beads (BD Biosciences)For sphere formation, isolated cells were plated at low density (<500,000 cells/cm^2) in ultralow-adherence 35 mm dishes (StemCell Technologies) after treatment with Poly-Hema (Sigma). The growth medium for spheres contained 0.1 mM β-mercaptoethanol; 1% nonessential amino acids (Sigma); 1% N2 and 2% B27 supplements (Invitrogen); recombinant human fibroblast growth factor (FGF)-basic, recombinant human epidermal growth factor (EGF), recombinant human platelet-derived growth factor (PDGF-AA), recombinant human oncostatin M (227 aa OSM, 20 ng/ml) and recombinant human IGF-1 (40 ng/ml; Peprotech) in Dulbecco's modified Eagle's medium (DMEM)/F12 (1:1) / human endothelial (1:2) serum-free medium (Invitrogen). Mesenspheres medium was supplemented with 15% CEE prepared as described previously.[240] The cultures were incubated at 37°C with 5% CO_2, 20% O_2 in a water-jacketed incubator and left untouched for 1 week. Afterward, half-medium changes were performed twice a week. For passage, spheres were enzymatically dissociated in 100 µl of a solution containing 0.25% type I collagenase and 20% FBS in PBS (StemCell Technologies) or Trypsin (EDTA-free) for 15 min at 37°C, with mechanical dispersion every 10 min. Cells were then washed with PBS once and replated with mesensphere medium in ultralow-adherence 35 mm dishes (StemCell Technologies) at 37°C in a water-jacketed incubator with 5% CO_2 and 20% O_2.

MLL-AF9 mouse leukemic blasts were isolated from bones of a doxycycline-inducible rtTA;MLL-AF9 mouse strain and maintained in 6 well plates in RPMI 1640 (Invitrogen) without phenol red and charcoal-depleted FBS, mouse (m)IL3, mSCF and hIL-6 (10 ng/ml), 1% Penicillin-Streptomycin, 1 ug/ml doxycycline) at 37°C in a water-jacketed incubator with 5% CO_2 and 20% O_2. Cells were split every 2 days and seeded at 500,000 cells/ml.

Co-culture experiments

We set up co-cultures systems with mesenspheres (~200 cells/ml) and leukemic blasts (250,000 cells/ml) for 24 hrs in RPMI without phenol red and without FBS or with FBS (± AraC, 1µM) in a flat-bottom 96-well low adherance tissue cultures plates (Costar) at 37 C and 5% CO2. Cultures were grown for 24 hrs before flow-cytometry staining (apoptosis, ROS levels, lipid peroxidation).
To investigate the influence of AML-derived supernatants on BMSC functionality, spheres were cultured with different dilutions of conditioned medium from AML blasts, previously cultured alone or in combination with mesenspheres.

Co-cultures in transwell systems and preparation of conditioned medium

Non-contacting co-culture transwell cell culture systems were developed to study the cross biological activity of leukemic blasts and mesenspheres which allow bidirectional diffusion of soluble factors. The non-contacting co-cultured cells were prepared as follows: leukemic blasts were plated on the bottom of the s96-well transwell cell culture system (Pore size 0.4 µm; Costar Corp. USA) using the 235µl complete media and culture environment as describe above. The mesenspheres were cultured onto the membrane of transwell cell culture inserts and allowed to grow overnight using the above mentioned condition. The next day the cells were washed with PBS and used for various experiments.

In selected experiments, the cells were seeded following the protocol with minor modifications.

We evaluated the biological activity of conditioned medium (CM) obtained from mono-cultures of leukemic blasts (as LB-CM) or mesenspheres (M-CM) and co-cultures (C-CM). Specifically, leukemic blasts were seeded as above mentioned for 24 hrs. Mono-cultures of mesenspheres were cultured also in RPMI medium used for leukemic blasts. Finally, the CM was collected and, after centrifugation at 1300 rpm for 10 min to remove cellular components or cells debris, filtered through 0.2-µm filters (Millipore, Billerica, MA) before use. Medium from dishes under normal conditions was used as a control.

Cell mitostress test assay (Seahorse)

Leukemic blasts, mono-cultured or in co-cultured, were seeded in a 24-well plate as above described. After a 24 hrs incubation, growth medium from each well was removed and cells were washed twice with 1,000 µL of pre-warmed assay medium (XF base medium supplemented with 25 mM glucose, 2 mM glutamine and 1 mM sodium pyruvate; pH 7.4) and counted. Cell were seeded

at 50,000/well in Seahorse 96-well platescoated with CellTak (BD Biosciences, San Jose, CA, USA). Then incubated in un-buffered DMEM pH 7.4 at 37 °C in a non-CO2 incubator for 40 min to allow to pre-equilibratewith the assay medium before being transferred to the XF96 analyzer. The cartridge was calibrated by the XF96 analyzer (Seahorse Bioscience, Billerica, MA, USA), and the assay continued using cell mito stress test assay protocol as described by*Nicholls et al.*[241] Load pre-warmed oligomycin, FCCP, rotenone & antimycin A were injected into the injector ports A, B and C of sensor cartridge, respectively. The final concentrations of injections were as follows: 0.25 µM oligomycin, 1 µM FCCP, 1 µM rotenone & antimycin A.

Oxygen consumption rate (OCR) and extracellular acidification rate (ECAR) were detected under basal conditions followed by the sequential addition of oligomycin, FCCP, as well as rotenone & antimycin A. This allowed for an estimation of the contribution of individual parameters for basal respiration, proton leak, maximal respiration, spare respiratory capacity, non-mitochondrial respiration and ATP production.

Flow cytometry staining and apoptosis

Leukemic blasts, mono-cultured or in co-cultured, were incubated with the appropriate dilution (2-5 µg/ml) of fluorescent antibody conjugates and werestained in PBS containing 2% FBSat 4°C, washed, and analysed on LSRFortessa flow cytometer (BD Biosciences, Franklin Lakes, NJ) equipped with FACSDiva Software (BD Biosciences)or on Gallios flow cytometer (Beckman Coulter, Miami Lakes, FL)using Kaluza (analysis software from Beckman Coulter). The following antibodies were used: fluorescent CD45.1 (A20), CD45.2 (104),c-kit (2B8) (eBioscience) and biotinylated lineage (lin) antibodies; biotinylated antibodies were detected with fluorochrome-conjugated streptavidin (BD Biosciences). 4',6-dia^{m}idino-2-phenylindole (DAPI) was used for dead cell exclusion.

Apoptosis was analyzed in leukemicblasts by flow cytometric measurement of CD45 expression in combination with annexin V binding (BD Bioscience)and DAPI.

Determination of ROS generation

Intracellular reactive oxygen species (ROS) were detected by staining cells with dihydrorhodamine 123 (DHR123, Thermo Fisher) and followed by flow cytometry analysis. DHR123 was prepared by dissolving 1 mg of the product in Dimethyl sulfoxide (DMSO) to a concentration of 1 mM. Briefly, cells were stained with DHR123 (1µM) in medium without phenol red at 37 ºC for 20 minutes, and

then finally washed with PBS and resuspended in PBS with DAPI to identify viable cells and to assess their reactive oxygen level. To discriminate between the leukemic blasts and mesenspheres in co-cultures, CD45-APC was used. For multi-parameter experiments using Mitotracker Red CMXRos (50 nm), 1µM DHR123 was added to leukemic cells and incubated for 25 min at 37 ºC as described. Cellular appearance of DHR123-Mitotracker Red fluorescence was monitored by flow cytometry.

Assessment of lipid peroxidation

The stock solution of C11-BODIPY$^{581/591}$ (Life technologies-Invitrogen, Carlsbad, USA), a fluorescent fatty acid analogue which incorporates into membranes, was prepared by dissolving 1 mg of the product in Dimethyl sulfoxide (DMSO) to a concentration of 1 mM. Upon oxidation, emission fluorescence of the dye shiftfrom red to green fluorescence emission.Regarding probe incorporation, leukemic blasts were incubated in medium without FBS at a final concentration of 5 µM C11-BODIPY$^{581/591}$ for 30 min at 37 °C and 5% CO_2,and then washed with PBS and resuspended in PBS with DAPI (1:2000) to identify viable cells and lipid peroxidation.To discriminate between the leukemic blasts and mesenspheres in co-cultures, CD45-APC was used.

Determination of intracellular GSH levels

A cell-permeant probe,monochloromobimane (mBCI, Molecular Probes)for quantifying glutathione levels in cells was used in leukemic cells, mono-cultured or co-cultured. Cells were incubated for 20 min at 37 ºC in the dark with RPMI without phenol red containing 40 µM mBCI. The cells were washed and then stained with CD45-APC.The emission of fluorescence was measured by flow cytometry. For multi-parameter experiments using Mitotracker Red CMXRos (50 nm), 40µM mBCI was added to leukemic cells and incubated for 25 min at 37 ºC as described. Cellular appearance of GSH-Mitotracker Red fluorescence was monitored.

BM cell extraction, flow cytometry in vivo experiments

For BM haematopoietic cell isolation, bones from WT and PRDX6 KO mice were crushed in a mortar, filtered through a 40-µm strainer to obtain single cell suspensions. The tissues were depleted of red blood cells by lysis in 0.15 M NH4Cl for 10 min at 4ºC. Cells were incubated with the appropriate dilution (2-5 µg/ml) of fluorescent antibody conjugates and DAPI for dead cell exclusion, and analysed on LSRFortessa flow cytometer (BD Biosciences, Franklin Lakes, NJ) equipped with FACSDiva Software (BD Biosciences). The following antibodies were used:

fluorescent CD45.1 (A20), CD45.2 (104), C-Kit (2B8) (eBioscience) and biotinylated lineage antibodies (Lineage). Biotinylated antibodies were detected with fluorochrome-conjugated streptavidin (BD Biosciences).

To isolate Nes+ cells, bones were cleaned from surrounding tissue, crushed in a mortar with a pestle, and collagenase-digested (catalog number C2674, Sigma; 0.25% collagenase in PBS supplemented with 20% fetal bovine serum) as described above.

Mitotracker staining

The transfer of mitochondria was performed using a green-fluorescent mitochondrial stain (Mitotracker Green FM)and a red-fluorescent dye (MitoTracker Red CMXRos**) (**Thermo FisherWaltham, MA USA). Briefly, leukemic blasts wereunlabeled or stained with Mitotracker Green FM (100 ng) and co-cultured with mesenspheres stained with Mitotracker Red CMXRos (50 ng) in RPMI (without phenol red) and incubated for 20 min at 37 ºC. After incubation, the unbound dyes were removed by extensively washing and then leukemic blasts and mesenspheres were seed separately in medium for many hrs at 37 ºC. Before co-cultures, both type of cells were washed twice, collected and counted. After 24 hrs of cultures, transfer of mitochondria from mesenspheres to leukemic blasts was evaluated by flow cytometry.

Mouse strains

Age and sex-matched Prdx6 KO and doxycycline-inducible rtTA;MLL-AF9 mouse strain CD45.1 and CD45.2 C57BL/6J mice (Jackson Laboratories) were used in this study.[70] Mice were housed in specific pathogen free facilities. All experiments using mice followed protocols approved by the Animal Welfare Ethical Committees and were compliant with EU recommendations. To study AraC effects on oxidative stress pathway in Prdx6 KO recipients, Prdx6KOmice and control mice were lethally irradiated (137Cs source, 9.5 Gy whole body irradiation, one dose). Then CD45.1 cells from MLL-AF9 mice wereinjected and 2 weeks after Prdx6 KOmice and control mice were treated with AraC (100 mg/kg, Intraperitoneal injection,i.p.).

Data analysis

The XF mito stress test report generator automatically calculate the XF cell mito stress test parameters from Wave data that have been exported from Excel. All parameters for Respiration and acidification rates are presented as the mean ± SEM of 4-6 independent experiments. All

experiments were performed with 2 to 4 replicate wells in the Seahorse XF96 analyzer. For experiment of energy substrates on mitochondrial respiration, significance level was determined by performing ANOVA on the complete data set with Tukey′s post-hoc testing.

– Conclusion

Like their normal counterparts, leukemic cells depend upon both cell-intrinsic and –extrinsic regulatory signals generated by their surrounding microenvironment for survival and proliferation. However, it remains unclear whether malignancy represents a cell autonomous characteristic of leukemia or is influenced also by the microenvironment. Moreover, more detailed insights into similarities and differences of the interplay between the malignant hemopoietic clone and its microenvironment are important areas to investigate into different types of leukemias (i.e. acute and chronic malignancies).

The present thesis aimed to investigate novel and unexplored mechanisms regulating the interplay between the leukemic clone and its microenvironment. Specifically, we investigated whether and to what extent the microenvironment, either as proinflammatory soluble factors or cell-mediated signals, may affect the development/maintenance of the leukemic clone in acute and chronic hemopoietic malignancies.

I) Environment-driven inflammation has long been suspected to contribute to tumor growth. MPNs are characterized by a state of chronic inflammation. Based on experimental evidences, it is argued that, besides molecular alterations, a state of chronic inflammation involving the malignant HSPCs and the non-malignant/malignant microenvironment has been indicated as main contributor in MPN initiation/clonal evolution. The driving hypothesis of this first part of my thesis was that the analysis of the *in vitro* biological effects of key pro-inflammatory mediators on the stem/progenitor cell compartments will contribute to clarify the role of inflammation in the pathogenesis of MF. Specifically, we observed potent effects of combinations of pro-inflammatory cytokines on survival and migration of $CD34^+$ cells from MF patients but not from the normal counterparts. These data demonstrate the pivotal role of the pro-inflammatory microenvironment in shaping the malignant hematopoiesis behaviour. It is however likely that in MF a combination of microenvironmental factors and intrinsic mechanisms may contribute to the generation of malignancy. In conclusion, according to first objective, we showed that in MF up-regulated production of pro-inflammatory cytokines by HSPCs and stromal cells generates a microenvironment that selects for the malignant clone. Taking into account not only the malignant clone but also the inflammatory microenvironmemt networks will likely improve the development of therapeutic strategies.

II) In addition to the well-recognized role in extracellular matrix remodelling, TIMP-1 is involved in cell proliferation and survival of normal HSCs. We therefore hypothesized that TIMP-1 might be also involved in the regulation of the functional behaviour of the leukemic clone. The second aim of this thesis was to get insight into the TIMP-1-based mechanisms underpinning the behaviour and the cross-talk between leukemic cells and MSCs, a major constituent of the of the HCS niche, in the setting of AML. We showed that this inhibitor of metalloproteinases can be considered as a 'bad actor' in the leukemic context. Specifically, we demonstrated that TIMP-1, through its receptor CD63 and PI3K/Akt/p21 pathway, modulates the survival, migration and proliferation of leukemic blasts. The dynamic interplay between leukemic cells and stromal cells is a crucial aspect in AML. It is clear that leukemic cells alter their BM microenvironment to support leukemic hematopoiesis while disrupting normal HSC homeostasis. In this context, our data support a role of TIMP-1 as a favouring factor within the leukemic microenvironment. Interestingly, AML-MSCs, but not normal MSCs, have been shown to increase AML blast proliferation and migration capacity in the presence of TIMP-1. Therefore, the combination of a pro-inflammatory factor, TIMP-1, with cellular elements of the leukemic microenvironment, the AML-MSCs, could be provide a potent device for leukemic cells in term of drug resistance. In conclusion, our findings point toward a crucial role of TIMP-1 within the leukemic microenvironment.

III) Based on a mouse model, the third aim of my thesis was focused on study of the cross-talk between the recent characterized BM stromal stem/progenitor cells, namely mesenspheres, with self-renewal ability and the leukemic clone. Specifically, we investigate whether mouse BM-derived mesenspheres show the ability to support the mouse leukemic blasts and whether their cross-talks create a protective effect where mesensheres could mediate chemoresistance. By using a novel system of co-culture, we demonstrated the supportive and protective role of BMSCs, as non-adherent cells. In this cross-talk we found a reduction of ROS levels and lipid peroxidation, in stressed conditions. Importantly, we also found that the chemoprotective role of mesenspheres is mediated by mitochondria transfer from mesenspheres to leukemic cells. This interaction could be explained as sources of anti-oxidants and nutrients. These data therefore suggest that, due to this mitochondria-driven mechanism, it will be critical to develop tools blocking this donation between cells. Importantly, this work may well substantially contribute to validate preclinical findings from mouse models in the human system.

In conclusion, this thesis provides scientific advances in the understanding of how leukemia cells modify their microenvironment and how these changes reinforce leukemic homeostasis.Therefore, in myeloid malignancies both pathogenetic hypothesis and therapeutic attempts should take into account not just the malignant clone but also the activity of the microenvironment. Indeed, the better understanding of the mechanisms underlying the interplay between the malignant clone and its microenvironment has the potential to draw therapeutic strategies based on the manipulation of key components within the leukemic microenvironment.

– Bibliography

1. Kovtonyuk LV, Fritsch K, Feng X, Manz MG, Takizawa H. Inflamm-Aging of Hematopoiesis, Hematopoietic Stem Cells, and the Bone Marrow Microenvironment. *Front Immunol*. 2016;7:502.
2. Mirantes C, Passegue E, Pietras EM. Pro-inflammatory cytokines: emerging players regulating HSC function in normal and diseased hematopoiesis. *Exp Cell Res*. 2014;329(2):248-254.
3. Lin S, Zhao R, Xiao Y, Li P. Mechanisms determining the fate of hematopoietic stem cells. *Stem Cell Investig*. 2015;2:10.
4. Ma X, Feng Y. Hypercholesterolemia Tunes Hematopoietic Stem/Progenitor Cells for Inflammation and Atherosclerosis. *Int J Mol Sci*. 2016;17(7).
5. Lapid K, Glait-Santar C, Gur-Cohen S, Canaani J, Kollet O, Lapidot T. Egress and Mobilization of Hematopoietic Stem and Progenitor Cells: A Dynamic Multi-facet Process. StemBook. Cambridge (MA): Harvard Stem Cell Institute

6. Ludin A, Gur-Cohen S, Golan K, et al. Reactive oxygen species regulate hematopoietic stem cell self-renewal, migration and development, as well as their bone marrow microenvironment. *Antioxid Redox Signal*. 2014;21(11):1605-1619.
7. Chiarini F, Lonetti A, Evangelisti C, et al. Advances in understanding the acute lymphoblastic leukemia bone marrow microenvironment: From biology to therapeutic targeting. *Biochim Biophys Acta*. 2016;1863(3):449-463.
8. Mendelson A, Frenette PS. Hematopoietic stem cell niche maintenance during homeostasis and regeneration. *Nat Med*. 2014;20(8):833-846.
9. Boulais PE, Frenette PS. Making sense of hematopoietic stem cell niches. *Blood*. 2015;125(17):2621-2629.
10. Giles AJ, Chien CD, Reid CM, et al. The functional interplay between systemic cancer and the hematopoietic stem cell niche. *Pharmacol Ther*. 2016;168:53-60.
11. Lo Celso C, Wu JW, Lin CP. In vivo imaging of hematopoietic stem cells and their microenvironment. *J Biophotonics*. 2009;2(11):619-631.
12. Grassinger J, Haylock DN, Williams B, Olsen GH, Nilsson SK. Phenotypically identical hemopoietic stem cells isolated from different regions of bone marrow have different biologic potential. *Blood*. 2010;116(17):3185-3196.
13. Hadjidakis DJ, Androulakis, II. Bone remodeling. *Ann N Y Acad Sci*. 2006;1092:385-396.
14. Coskun S, Hirschi KK. Establishment and regulation of the HSC niche: Roles of osteoblastic and vascular compartments. *Birth Defects Res C Embryo Today*. 2010;90(4):229-242.
15. Calvi LM. Osteoblastic activation in the hematopoietic stem cell niche. *Ann N Y Acad Sci*. 2006;1068:477-488.
16. Aggarwal R, Lu J, Pompili VJ, Das H. Hematopoietic stem cells: transcriptional regulation, ex vivo expansion and clinical application. *Curr Mol Med*. 2012;12(1):34-49.
17. Morrison SJ, Scadden DT. The bone marrow niche for haematopoietic stem cells. *Nature*. 2014;505(7483):327-334.
18. Mendez-Ferrer S, Michurina TV, Ferraro F, et al. Mesenchymal and haematopoietic stem cells form a unique bone marrow niche. *Nature*. 2010;466(7308):829-834.
19. Xie L, Zeng X, Hu J, Chen Q. Characterization of Nestin, a Selective Marker for Bone Marrow Derived Mesenchymal Stem Cells. *Stem Cells Int*. 2015;2015:762098.
20. Suzuki S, Namiki J, Shibata S, Mastuzaki Y, Okano H. The neural stem/progenitor cell marker nestin is expressed in proliferative endothelial cells, but not in mature vasculature. *J Histochem Cytochem*. 2010;58(8):721-730.

21. Kunisaki Y, Bruns I, Scheiermann C, et al. Arteriolar niches maintain haematopoietic stem cell quiescence. *Nature*. 2013;502(7473):637-643.
22. Kopp HG, Avecilla ST, Hooper AT, Rafii S. The bone marrow vascular niche: home of HSC differentiation and mobilization. *Physiology (Bethesda)*. 2005;20:349-356.
23. Yoon KA, Cho HS, Shin HI, Cho JY. Differential regulation of CXCL5 by FGF2 in osteoblastic and endothelial niche cells supports hematopoietic stem cell migration. *Stem Cells Dev*. 2012;21(18):3391-3402.
24. Wang LD, Wagers AJ. Dynamic niches in the origination and differentiation of haematopoietic stem cells. *Nat Rev Mol Cell Biol*. 2011;12(10):643-655.
25. Omatsu Y, Sugiyama T, Kohara H, et al. The essential functions of adipo-osteogenic progenitors as the hematopoietic stem and progenitor cell niche. *Immunity*. 2010;33(3):387-399.
26. Itkin T, Gur-Cohen S, Spencer JA, et al. Distinct bone marrow blood vessels differentially regulate haematopoiesis. *Nature*. 2016;532(7599):323-328.
27. Vukovic M, Sepulveda C, Subramani C, et al. Adult hematopoietic stem cells lacking Hif-1alpha self-renew normally. *Blood*. 2016;127(23):2841-2846.
28. Gill D, Tan PH. Induction of pathogenic cytotoxic T lymphocyte tolerance by dendritic cells: a novel therapeutic target. *Expert Opin Ther Targets*. 2010;14(8):797-824.
29. Yamazaki S, Ema H, Karlsson G, et al. Nonmyelinating Schwann cells maintain hematopoietic stem cell hibernation in the bone marrow niche. *Cell*. 2011;147(5):1146-1158.
30. Mendez-Ferrer S, Lucas D, Battista M, Frenette PS. Haematopoietic stem cell release is regulated by circadian oscillations. *Nature*. 2008;452(7186):442-447.
31. Massberg S, Schaerli P, Knezevic-Maramica I, et al. Immunosurveillance by hematopoietic progenitor cells trafficking through blood, lymph, and peripheral tissues. *Cell*. 2007;131(5):994-1008.
32. Mayadas TN, Cullere X, Lowell CA. The multifaceted functions of neutrophils. *Annu Rev Pathol*. 2014;9:181-218.
33. Chow A, Lucas D, Hidalgo A, et al. Bone marrow CD169+ macrophages promote the retention of hematopoietic stem and progenitor cells in the mesenchymal stem cell niche. *J Exp Med*. 2011;208(2):261-271.
34. Schurch CM, Riether C, Ochsenbein AF. Cytotoxic CD8+ T cells stimulate hematopoietic progenitors by promoting cytokine release from bone marrow mesenchymal stromal cells. *Cell Stem Cell*. 2014;14(4):460-472.
35. Suda T, Takubo K, Semenza GL. Metabolic regulation of hematopoietic stem cells in the hypoxic niche. *Cell Stem Cell*. 2011;9(4):298-310.
36. Lagadinou ED, Sach A, Callahan K, et al. BCL-2 inhibition targets oxidative phosphorylation and selectively eradicates quiescent human leukemia stem cells. *Cell Stem Cell*. 2013;12(3):329-341.
37. Cao X, Wu X, Frassica D, et al. Irradiation induces bone injury by damaging bone marrow microenvironment for stem cells. *Proc Natl Acad Sci U S A*. 2011;108(4):1609-1614.
38. Yahata T, Takanashi T, Muguruma Y, et al. Accumulation of oxidative DNA damage restricts the self-renewal capacity of human hematopoietic stem cells. *Blood*. 2011;118(11):2941-2950.
39. Baldridge MT, King KY, Goodell MA. Inflammatory signals regulate hematopoietic stem cells. *Trends Immunol*. 2011;32(2):57-65.
40. Nagai Y, Garrett KP, Ohta S, et al. Toll-like receptors on hematopoietic progenitor cells stimulate innate immune system replenishment. *Immunity*. 2006;24(6):801-812.
41. Glenn JD, Whartenby KA. Mesenchymal stem cells: Emerging mechanisms of immunomodulation and therapy. *World J Stem Cells*. 2014;6(5):526-539.
42. Chang AI, Schwertschkow AH, Nolta JA, Wu J. Involvement of mesenchymal stem cells in cancer progression and metastases. *Curr Cancer Drug Targets*. 2015;15(2):88-98.

43. Sun Z, Wang S, Zhao RC. The roles of mesenchymal stem cells in tumor inflammatory microenvironment. *J Hematol Oncol*. 2014;7:14.
44. Trivanovic D, Krstic J, Djordjevic IO, et al. The Roles of Mesenchymal Stromal/Stem Cells in Tumor Microenvironment Associated with Inflammation. *Mediators Inflamm*. 2016;2016:7314016.
45. Ma S, Xie N, Li W, Yuan B, Shi Y, Wang Y. Immunobiology of mesenchymal stem cells. *Cell Death Differ*. 2014;21(2):216-225.
46. Waterman RS, Tomchuck SL, Henkle SL, Betancourt AM. A new mesenchymal stem cell (MSC) paradigm: polarization into a pro-inflammatory MSC1 or an Immunosuppressive MSC2 phenotype. *PLoS One*. 2010;5(4):e10088.
47. Prockop DJ. Concise review: two negative feedback loops place mesenchymal stem/stromal cells at the center of early regulators of inflammation. *Stem Cells*. 2013;31(10):2042-2046.
48. Korn C, Mendez-Ferrer S. Myeloid malignancies and the microenvironment. *Blood*. 2017;129(7):811-822.
49. Krause DS, Scadden DT. A hostel for the hostile: the bone marrow niche in hematologic neoplasms. *Haematologica*. 2015;100(11):1376-1387.
50. Campbell PJ, Baxter EJ, Beer PA, et al. Mutation of JAK2 in the myeloproliferative disorders: timing, clonality studies, cytogenetic associations, and role in leukemic transformation. *Blood*. 2006;108(10):3548-3555.
51. Arranz L, Sanchez-Aguilera A, Martin-Perez D, et al. Neuropathy of haematopoietic stem cell niche is essential for myeloproliferative neoplasms. *Nature*. 2014;512(7512):78-81.
52. Kouvidi E, Stratigi A, Batsali A, et al. Cytogenetic evaluation of mesenchymal stem/stromal cells from patients with myelodysplastic syndromes at different time-points during ex vivo expansion. *Leuk Res*. 2016;43:24-32.
53. Krause DS, Scadden DT, Preffer FI. The hematopoietic stem cell niche--home for friend and foe? *Cytometry B Clin Cytom*. 2013;84(1):7-20.
54. Gattazzo F, Urciuolo A, Bonaldo P. Extracellular matrix: a dynamic microenvironment for stem cell niche. *Biochim Biophys Acta*. 2014;1840(8):2506-2519.
55. Hanoun M, Zhang D, Mizoguchi T, et al. Acute myelogenous leukemia-induced sympathetic neuropathy promotes malignancy in an altered hematopoietic stem cell niche. *Cell Stem Cell*. 2014;15(3):365-375.
56. Schepers K, Campbell TB, Passegue E. Normal and leukemic stem cell niches: insights and therapeutic opportunities. *Cell Stem Cell*. 2015;16(3):254-267.
57. Hatfield K, Ryningen A, Corbascio M, Bruserud O. Microvascular endothelial cells increase proliferation and inhibit apoptosis of native human acute myelogenous leukemia blasts. *Int J Cancer*. 2006;119(10):2313-2321.
58. Zhang B, Ho YW, Huang Q, et al. Altered microenvironmental regulation of leukemic and normal stem cells in chronic myelogenous leukemia. *Cancer Cell*. 2012;21(4):577-592.
59. Schmidt M, Dogan C, Birdir C, et al. Altered angiogenesis in preeclampsia: evaluation of a new test system for measuring placental growth factor. *Clin Chem Lab Med*. 2007;45(11):1504-1510.
60. Calvi LM, Link DC. The hematopoietic stem cell niche in homeostasis and disease. *Blood*. 2015;126(22):2443-2451.
61. Lee GY, Kim JA, Oh IH. Stem cell niche as a prognostic factor in leukemia. *BMB Rep*. 2015;48(8):427-428.
62. Kim JA, Shim JS, Lee GY, et al. Microenvironmental remodeling as a parameter and prognostic factor of heterogeneous leukemogenesis in acute myelogenous leukemia. *Cancer Res*. 2015;75(11):2222-2231.

63. Lopes MR, Pereira JK, de Melo Campos P, et al. De novo AML exhibits greater microenvironment dysregulation compared to AML with myelodysplasia-related changes. *Sci Rep*. 2017;7:40707.
64. Forte D, Salvestrini V, Corradi G, et al. The tissue inhibitor of metalloproteinases-1 (TIMP-1) promotes survival and migration of acute myeloid leukemia cells through CD63/PI3K/Akt/p21 signaling. *Oncotarget*. 2017;8(2):2261-2274.
65. Schepers K, Pietras EM, Reynaud D, et al. Myeloproliferative neoplasia remodels the endosteal bone marrow niche into a self-reinforcing leukemic niche. *Cell Stem Cell*. 2013;13(3):285-299.
66. Zhang W, Trachootham D, Liu J, et al. Stromal control of cystine metabolism promotes cancer cell survival in chronic lymphocytic leukaemia. *Nat Cell Biol*. 2012;14(3):276-286.
67. Boutter J, Huang Y, Marovca B, et al. Image-based RNA interference screening reveals an individual dependence of acute lymphoblastic leukemia on stromal cysteine support. *Oncotarget*. 2014;5(22):11501-11512.
68. Iwamoto S, Mihara K, Downing JR, Pui CH, Campana D. Mesenchymal cells regulate the response of acute lymphoblastic leukemia cells to asparaginase. *J Clin Invest*. 2007;117(4):1049-1057.
69. Mussai F, De Santo C, Abu-Dayyeh I, et al. Acute myeloid leukemia creates an arginase-dependent immunosuppressive microenvironment. *Blood*. 2013;122(5):749-758.
70. Stavropoulou V, Kaspar S, Brault L, et al. MLL-AF9 Expression in Hematopoietic Stem Cells Drives a Highly Invasive AML Expressing EMT-Related Genes Linked to Poor Outcome. *Cancer Cell*. 2016;30(1):43-58.
71. Kleppe M, Levine RL. New pieces of a puzzle: The current biological picture of MPN. *Biochimica et Biophysica Acta (BBA) - Reviews on Cancer*. 2012;1826(2):415-422.
72. Tefferi A, Pardanani A. Myeloproliferative Neoplasms. *JAMA Oncology*. 2015;1(1):97.
73. Cervantes F, Arellano-Rodrigo E, Alvarez-Larran A. Blood cell activation in myeloproliferative neoplasms. *Haematologica*. 2009;94(11):1484-1488.
74. James C, Ugo V, Casadevall N, Constantinescu SN, Vainchenker W. A JAK2 mutation in myeloproliferative disorders: pathogenesis and therapeutic and scientific prospects. *Trends in Molecular Medicine*. 2005;11(12):546-554.
75. Tefferi A, Vainchenker W. Myeloproliferative Neoplasms: Molecular Pathophysiology, Essential Clinical Understanding, and Treatment Strategies. *Journal of Clinical Oncology*. 2011;29(5):573-582.
76. Klampfl T, Gisslinger H, Harutyunyan AS, et al. Somatic Mutations of Calreticulin in Myeloproliferative Neoplasms. *New England Journal of Medicine*. 2013;369(25):2379-2390.
77. Chen E, Mullally A. How does JAK2V617F contribute to the pathogenesis of myeloproliferative neoplasms? *Hematology*. 2014;2014(1):268-276.
78. Rumi E, Pietra D, Pascutto C, et al. Clinical effect of driver mutations of JAK2, CALR, or MPL in primary myelofibrosis. *Blood*. 2014;124(7):1062-1069.
79. Tapper W, Jones AV, Kralovics R, et al. Genetic variation at MECOM, TERT, JAK2 and HBS1L-MYB predisposes to myeloproliferative neoplasms. *Nature Communications*. 2015;6:6691.
80. Geyer HL, Dueck AC, Scherber RM, Mesa RA. Impact of Inflammation on Myeloproliferative Neoplasm Symptom Development. *Mediators of Inflammation*. 2015;2015:1-9.
81. Hasselbalch HC. The role of cytokines in the initiation and progression of myelofibrosis. *Cytokine & Growth Factor Reviews*. 2013;24(2):133-145.
82. Le Bousse-Kerdilès MC, Martyré MC. Dual implication of fibrogenic cytokines in the pathogenesis of fibrosis and myeloproliferation in myeloid metaplasia with myelofibrosis. *Annals of Hematology*. 1999;78(10):437-444.
83. Tefferi A. Myelofibrosis with Myeloid Metaplasia. *New England Journal of Medicine*. 2000;342(17):1255-1265.

84. Tefferi A, Vaidya R, Caramazza D, Finke C, Lasho T, Pardanani A. Circulating Interleukin (IL)-8, IL-2R, IL-12, and IL-15 Levels Are Independently Prognostic in Primary Myelofibrosis: A Comprehensive Cytokine Profiling Study. *Journal of Clinical Oncology*. 2011;29(10):1356-1363.
85. Barosi G. Diagnostic and clinical relevance of the number of circulating CD34+ cells in myelofibrosis with myeloid metaplasia. *Blood*. 2001;98(12):3249-3255.
86. Xu M. Constitutive mobilization of CD34+ cells into the peripheral blood in idiopathic myelofibrosis may be due to the action of a number of proteases. *Blood*. 2005;105(11):4508-4515.
87. Migliaccio AR, Martelli F, Verrucci M, et al. Altered SDF-1/CXCR4 axis in patients with primary myelofibrosis and in the Gata1low mouse model of the disease. *Experimental Hematology*. 2008;36(2):158-171.
88. Hasselbalch HC. Perspectives on chronic inflammation in essential thrombocythemia, polycythemia vera, and myelofibrosis: is chronic inflammation a trigger and driver of clonal evolution and development of accelerated atherosclerosis and second cancer? *Blood*. 2012;119(14):3219-3225.
89. Hasselbalch HC. Chronic inflammation as a promotor of mutagenesis in essential thrombocythemia, polycythemia vera and myelofibrosis. A human inflammation model for cancer development? *Leuk Res*. 2013;37(2):214-220.
90. Lataillade JJ, Pierre-Louis O, Hasselbalch HC, et al. Does primary myelofibrosis involve a defective stem cell niche? From concept to evidence. *Blood*. 2008;112(8):3026-3035.
91. Fleischman AG. Inflammation as a Driver of Clonal Evolution in Myeloproliferative Neoplasm. *Mediators of Inflammation*. 2015;2015:1-6.
92. Le Bousse-Kerdiles MC. Primary myelofibrosis and the "bad seeds in bad soil" concept. *Fibrogenesis Tissue Repair*. 2012;5(Suppl 1):S20.
93. Rossi L, Salvestrini V, Ferrari D, Di Virgilio F, Lemoli RM. The sixth sense: hematopoietic stem cells detect danger through purinergic signaling. *Blood*. 2012;120(12):2365-2375.
94. Wang JC, Novetsky A, Chen C, Novetsky AD. Plasma matrix metalloproteinase and tissue inhibitor of metalloproteinase in patients with agnogenic myeloid metaplasia or idiopathic primary myelofibrosis. *British Journal of Haematology*. 2002;119(3):709-712.
95. Fleischman AG, Aichberger KJ, Luty SB, et al. TNF facilitates clonal expansion of JAK2V617F positive cells in myeloproliferative neoplasms. *Blood*. 2011;118(24):6392-6398.
96. Bours MJL. P2 receptors and extracellular ATP: a novel homeostatic pathway in inflammation. *Frontiers in Bioscience*. 2011;S3(1):1443.
97. Turzanski J, Grundy M, Russell NH, Pallis M. Interleukin-1β maintains an apoptosis-resistant phenotype in the blast cells of acute myeloid leukaemia via multiple pathways. *Leukemia*. 2004;18(10):1662-1670.
98. Yang J, Ikezoe T, Nishioka C, Nobumoto A, Yokoyama A. IL-1β inhibits self-renewal capacity of dormant CD34 + /CD38 − acute myelogenous leukemia cells in vitro and in vivo. *International Journal of Cancer*. 2013;133(8):1967-1981.
99. Ratajczak J, Kucia M, Reca R, Zhang J, Machalinski B, Ratajczak MZ. Quiescent CD34+early erythroid progenitors are resistant to several erythropoietic 'inhibitory' cytokines; role of FLIP. *British Journal of Haematology*. 2003;123(1):160-169.
100. Chirco R, Liu X-W, Jung K-K, Kim H-RC. Novel functions of TIMPs in cell signaling. *Cancer and Metastasis Reviews*. 2006;25(1):99-113.
101. Ries C. Cytokine functions of TIMP-1. *Cell Mol Life Sci*. 2014;71(4):659-672.
102. Lee Soo Y, Kim Jung M, Cho Soo Y, et al. TIMP-1 modulates chemotaxis of human neural stem cells through CD63 and integrin signalling. *Biochemical Journal*. 2014;459(3):565-576.
103. Stricklin GP, Welgus HG. Physiological relevance of erythroid-potentiating activity or TIMP. *Nature*. 1986;321(6070):628-628.

104. Rossi L, Forte D, Migliardi G, et al. The tissue inhibitor of metalloproteinases 1 increases the clonogenic efficiency of human hematopoietic progenitor cells through CD63/PI3K/Akt signaling. *Exp Hematol*. 2015;43(11):974-985.e971.
105. Rossi L, Salvestrini V, Ferrari D, Di Virgilio F, Lemoli RM. The sixth sense: hematopoietic stem cells detect danger through purinergic signaling. *Blood*. 2012;120(12):2365-2375.
106. Rossi L, Manfredini R, Bertolini F, et al. The extracellular nucleotide UTP is a potent inducer of hematopoietic stem cell migration. *Blood*. 2007;109(2):533-542.
107. Di Virgilio F. Nucleotide receptors: an emerging family of regulatory molecules in blood cells. *Blood*. 2001;97(3):587-600.
108. Lemoli RM. Extracellular nucleotides are potent stimulators of human hematopoietic stem cells in vitro and in vivo. *Blood*. 2004;104(6):1662-1670.
109. Salvestrini V, Zini R, Rossi L, et al. Purinergic signaling inhibits human acute myeloblastic leukemia cell proliferation, migration, and engraftment in immunodeficient mice. *Blood*. 2011;119(1):217-226.
110. Anand S, Stedham F, Beer P, et al. Effects of the JAK2 mutation on the hematopoietic stem and progenitor compartment in human myeloproliferative neoplasms. *Blood*. 2011;118(1):177-181.
111. Vainchenker W, Constantinescu SN, Plo I. Recent advances in understanding myelofibrosis and essential thrombocythemia. *F1000Research*. 2016;5:700.
112. Chachoua I, Pecquet C, El-Khoury M, et al. Thrombopoietin receptor activation by myeloproliferative neoplasm associated calreticulin mutants. *Blood*. 2015;127(10):1325-1335.
113. Bartalucci N, Tozzi L, Bogani C, et al. Co-targeting the PI3K/mTOR and JAK2 signalling pathways produces synergistic activity against myeloproliferative neoplasms. *Journal of Cellular and Molecular Medicine*. 2013;17(11):1385-1396.
114. Choong ML, Pecquet C, Pendharkar V, et al. Combination treatment for myeloproliferative neoplasms using JAK and pan-class I PI3K inhibitors. *Journal of Cellular and Molecular Medicine*. 2013;17(11):1397-1409.
115. Vardiman JW, Thiele J, Arber DA, et al. The 2008 revision of the World Health Organization (WHO) classification of myeloid neoplasms and acute leukemia: rationale and important changes. *Blood*. 2009;114(5):937-951.
116. Lemoli RM, Catani L, Talarico S, et al. Mobilization of Bone Marrow-Derived Hematopoietic and Endothelial Stem Cells After Orthotopic Liver Transplantation and Liver Resection. *Stem Cells*. 2006;24(12):2817-2825.
117. Jovanovic JV, Ivey A, Vannucchi AM, et al. Establishing optimal quantitative-polymerase chain reaction assays for routine diagnosis and tracking of minimal residual disease in JAK2-V617F-associated myeloproliferative neoplasms: a joint European LeukemiaNet/MPN&MPNr-EuroNet (COST action BM0902) study. *Leukemia*. 2013;27(10):2032-2039.
118. Kohlmann A, Klein HU, Weissmann S, et al. The Interlaboratory RObustness of Next-generation sequencing (IRON) study: a deep sequencing investigation of TET2, CBL and KRAS mutations by an international consortium involving 10 laboratories. *Leukemia*. 2011;25(12):1840-1848.
119. Willatt L, Morgan SM. Shaffer LG, Slovak ML, Campbell LJ (2009): ISCN 2009 an international system for human cytogenetic nomenclature. *Human Genetics*. 2009;126(4):603-604.
120. Gangat N, Caramazza D, Vaidya R, et al. DIPSS Plus: A Refined Dynamic International Prognostic Scoring System for Primary Myelofibrosis That Incorporates Prognostic Information From Karyotype, Platelet Count, and Transfusion Status. *Journal of Clinical Oncology*. 2011;29(4):392-397.
121. Cazzola M, Kralovics R. From Janus kinase 2 to calreticulin: the clinically relevant genomic landscape of myeloproliferative neoplasms. *Blood*. 2014;123(24):3714-3719.

122. Rampal R, Al-Shahrour F, Abdel-Wahab O, et al. Integrated genomic analysis illustrates the central role of JAK-STAT pathway activation in myeloproliferative neoplasm pathogenesis. *Blood*. 2014;123(22):e123-e133.
123. Hasselbalch HC, Bjørn ME. MPNs as Inflammatory Diseases: The Evidence, Consequences, and Perspectives. *Mediators of Inflammation*. 2015;2015:1-16.
124. Hermouet S, Bigot-Corbel E, Gardie B. Pathogenesis of Myeloproliferative Neoplasms: Role and Mechanisms of Chronic Inflammation. *Mediators of Inflammation*. 2015;2015:1-16.
125. Wang W-A, Groenendyk J, Michalak M. Calreticulin signaling in health and disease. *The International Journal of Biochemistry & Cell Biology*. 2012;44(6):842-846.
126. Tosato G, Yao L, Pike SE. Calreticulin and Tumor Suppression. Calreticulin: Springer Nature; 2003:162-179.
127. Cheng W-F, Hung C-F, Chai C-Y, et al. Tumor-specific immunity and antiangiogenesis generated by a DNA vaccine encoding calreticulin linked to a tumor antigen. *Journal of Clinical Investigation*. 2001;108(5):669-678.
128. Gold L, Williams D, Groenendyk J, Michalak M, Eggleton P. Unfolding the complexities of ER chaperones in health and disease: report on the 11th international calreticulin workshop. *Cell Stress and Chaperones*. 2015;20(6):875-883.
129. Lu Y-C, Weng W-C, Lee H. Functional Roles of Calreticulin in Cancer Biology. *BioMed Research International*. 2015;2015:1-9.
130. Eggleton P, Bremer E, Dudek E, Michalak M. Calreticulin, a therapeutic target? *Expert Opinion on Therapeutic Targets*. 2016;20(9):1137-1147.
131. Araki M, Yang Y, Masubuchi N, et al. Activation of the thrombopoietin receptor by mutant calreticulin in CALR-mutant myeloproliferative neoplasms. *Blood*. 2016;127(10):1307-1316.
132. Vannucchi AM, Rotunno G, Bartalucci N, et al. Calreticulin mutation-specific immunostaining in myeloproliferative neoplasms: pathogenetic insight and diagnostic value. *Leukemia*. 2014;28(9):1811-1818.
133. Panteli KE, Hatzimichael EC, Bouranta PK, et al. Serum interleukin (IL)-1, IL-2, sIL-2Ra, IL-6 and thrombopoietin levels in patients with chronic myeloproliferative diseases. *British Journal of Haematology*. 2005;130(5):709-715.
134. Duo C-C, Gong F-Y, He X-Y, et al. Soluble Calreticulin Induces Tumor Necrosis Factor-α (TNF-α) and Interleukin (IL)-6 Production by Macrophages through Mitogen-Activated Protein Kinase (MAPK) and NFκB Signaling Pathways. *International Journal of Molecular Sciences*. 2014;15(2):2916-2928.
135. Garbati MR, Welgan CA, Landefeld SH, et al. Mutant calreticulin-expressing cells induce monocyte hyperreactivity through a paracrine mechanism. *American Journal of Hematology*. 2016;91(2):211-219.
136. Vig S, Pandey AK, Verma G, Datta M. C/EBPα mediates the transcriptional suppression of human calreticulin gene expression by TNFα. *The International Journal of Biochemistry & Cell Biology*. 2012;44(1):113-122.
137. Blank U, Karlsson S. TGF- signaling in the control of hematopoietic stem cells. *Blood*. 2015;125(23):3542-3550.
138. Palandri F, Latagliata R, Polverelli N, et al. Mutations and long-term outcome of 217 young patients with essential thrombocythemia or early primary myelofibrosis. *Leukemia*. 2015;29(6):1344-1349.
139. Passamonti F, Cervantes F, Vannucchi AM, et al. A dynamic prognostic model to predict survival in primary myelofibrosis: a study by the IWG-MRT (International Working Group for Myeloproliferative Neoplasms Research and Treatment). *Blood*. 2009;115(9):1703-1708.
140. Dohner H, Weisdorf DJ, Bloomfield CD. Acute Myeloid Leukemia. *N Engl J Med*. 2015;373(12):1136-1152.

141. Konopleva MY, Jordan CT. Leukemia stem cells and microenvironment: biology and therapeutic targeting. *J Clin Oncol*. 2011;29(5):591-599.
142. Horton SJ, Huntly BJ. Recent advances in acute myeloid leukemia stem cell biology. *Haematologica*. 2012;97(7):966-974.
143. Hasselbalch HC. Chronic inflammation as a promotor of mutagenesis in essential thrombocythemia, polycythemia vera and myelofibrosis. A human inflammation model for cancer development? *Leukemia Research*. 2013;37(2):214-220.
144. Tili E, Chiabai M, Palmieri D, et al. Quaking and miR-155 interactions in inflammation and leukemogenesis. *Oncotarget*. 2015;6(28):24599-24610.
145. Grivennikov SI, Karin M. Inflammation and oncogenesis: a vicious connection. *Curr Opin Genet Dev*. 2010;20(1):65-71.
146. Takizawa H, Boettcher S, Manz MG. Demand-adapted regulation of early hematopoiesis in infection and inflammation. *Blood*. 2012;119(13):2991-3002.
147. King KY, Goodell MA. Inflammatory modulation of HSCs: viewing the HSC as a foundation for the immune response. *Nat Rev Immunol*. 2011;11(10):685-692.
148. Mendez-Ferrer S, Garcia-Fernandez M, de Castillejo CL. Convert and conquer: the strategy of chronic myelogenous leukemic cells. *Cancer Cell*. 2015;27(5):611-613.
149. Bakker E, Qattan M, Mutti L, Demonacos C, Krstic-Demonacos M. The role of microenvironment and immunity in drug response in leukemia. *Biochim Biophys Acta*. 2015.
150. Raaijmakers MH. Niche contributions to oncogenesis: emerging concepts and implications for the hematopoietic system. *Haematologica*. 2011;96(7):1041-1048.
151. Moore CS, Crocker SJ. An alternate perspective on the roles of TIMPs and MMPs in pathology. *Am J Pathol*. 2012;180(1):12-16.
152. Hatfield KJ, Reikvam H, Bruserud O. The crosstalk between the matrix metalloprotease system and the chemokine network in acute myeloid leukemia. *Curr Med Chem*. 2010;17(36):4448-4461.
153. Jung KK, Liu XW, Chirco R, Fridman R, Kim HR. Identification of CD63 as a tissue inhibitor of metalloproteinase-1 interacting cell surface protein. *Embo j*. 2006;25(17):3934-3942.
154. Pols MS, Klumperman J. Trafficking and function of the tetraspanin CD63. *Exp Cell Res*. 2009;315(9):1584-1592.
155. Ridnour LA, Barasch KM, Windhausen AN, et al. Nitric oxide synthase and breast cancer: role of TIMP-1 in NO-mediated Akt activation. *PLoS One*. 2012;7(9):e44081.
156. Seubert B, Cui H, Simonavicius N, et al. Tetraspanin CD63 acts as a pro-metastatic factor via beta-catenin stabilization. *Int J Cancer*. 2015;136(10):2304-2315.
157. Schelter F, Grandl M, Seubert B, et al. Tumor cell-derived Timp-1 is necessary for maintaining metastasis-promoting Met-signaling via inhibition of Adam-10. *Clin Exp Metastasis*. 2011;28(8):793-802.
158. Kobuch J, Cui H, Grunwald B, Saftig P, Knolle PA, Kruger A. TIMP-1 signaling via CD63 triggers granulopoiesis and neutrophilia in mice. *Haematologica*. 2015;100(8):1005-1013.
159. Seubert B, Grunwald B, Kobuch J, et al. Tissue inhibitor of metalloproteinases (TIMP)-1 creates a premetastatic niche in the liver through SDF-1/CXCR4-dependent neutrophil recruitment in mice. *Hepatology*. 2015;61(1):238-248.
160. Wurtz SO, Schrohl AS, Mouridsen H, Brunner N. TIMP-1 as a tumor marker in breast cancer--an update. *Acta Oncol*. 2008;47(4):580-590.
161. Pesta M, Kulda V, Kucera R, et al. Prognostic significance of TIMP-1 in non-small cell lung cancer. *Anticancer Res*. 2011;31(11):4031-4038.
162. Holten-Andersen MN, Stephens RW, Nielsen HJ, et al. High preoperative plasma tissue inhibitor of metalloproteinase-1 levels are associated with short survival of patients with colorectal cancer. *Clin Cancer Res*. 2000;6(11):4292-4299.

163. Dasse E, Bridoux L, Baranek T, et al. Tissue inhibitor of metalloproteinase-1 promotes hematopoietic differentiation via caspase-3 upstream the MEKK1/MEK6/p38alpha pathway. *Leukemia*. 2007;21(4):595-603.
164. Pennanen H, Kuittinen O, Soini Y, Turpeenniemi-Hujanen T. Clinicopathological correlations of TIMP-1 and TIMP-2 in Hodgkin's lymphoma. *Eur J Haematol*. 2004;72(1):1-9.
165. Guedez L, Martinez A, Zhao S, et al. Tissue inhibitor of metalloproteinase 1 (TIMP-1) promotes plasmablastic differentiation of a Burkitt lymphoma cell line: implications in the pathogenesis of plasmacytic/plasmablastic tumors. *Blood*. 2005;105(4):1660-1668.
166. Guedez L, Stetler-Stevenson WG. The prognostic value of TIMP-1 in multiple myeloma. Leuk Res. Vol. 34. England; 2010:576-577.
167. Kovac M, Vaskova M, Petrackova D, et al. Cytokines, growth, and environment factors in bone marrow plasma of acute lymphoblastic leukemia pediatric patients. *Eur Cytokine Netw*. 2014;25(1):8-13.
168. Zhang X, Ma W, Cui J, et al. Regulation of p21 by TWIST2 contributes to its tumor-suppressor function in human acute myeloid leukemia. *Oncogene*. 2015;34(23):3000-3010.
169. Sison EA, Brown P. The bone marrow microenvironment and leukemia: biology and therapeutic targeting. *Expert Rev Hematol*. 2011;4(3):271-283.
170. Peled A, Tavor S. Role of CXCR4 in the pathogenesis of acute myeloid leukemia. *Theranostics*. 2013;3(1):34-39.
171. Bertacchini J, Heidari N, Mediani L, et al. Targeting PI3K/AKT/mTOR network for treatment of leukemia. *Cell Mol Life Sci*. 2015;72(12):2337-2347.
172. Schubert M, Herbert N, Taubert I, et al. Differential survival of AML subpopulations in NOD/SCID mice. *Exp Hematol*. 2011;39(2):250-263.e254.
173. Cui H, Grosso S, Schelter F, Mari B, Kruger A. On the Pro-Metastatic Stress Response to Cancer Therapies: Evidence for a Positive Co-Operation between TIMP-1, HIF-1alpha, and miR-210. *Front Pharmacol*. 2012;3:134.
174. Schelter F, Halbgewachs B, Baumler P, et al. Tissue inhibitor of metalloproteinases-1-induced scattered liver metastasis is mediated by hypoxia-inducible factor-1alpha. *Clin Exp Metastasis*. 2011;28(2):91-99.
175. Wang Y, Liu Y, Malek SN, Zheng P. Targeting HIF1alpha eliminates cancer stem cells in hematological malignancies. *Cell Stem Cell*. 2011;8(4):399-411.
176. Dommange F, Cartron G, Espanel C, et al. CXCL12 polymorphism and malignant cell dissemination/tissue infiltration in acute myeloid leukemia. *Faseb j*. 2006;20(11):1913-1915.
177. Roboz GJ, Guzman M. Acute myeloid leukemia stem cells: seek and destroy. *Expert Rev Hematol*. 2009;2(6):663-672.
178. Agarwal P, Bhatia R. Influence of Bone Marrow Microenvironment on Leukemic Stem Cells: Breaking Up an Intimate Relationship. *Adv Cancer Res*. 2015;127:227-252.
179. Tabe Y, Konopleva M. Role of Microenvironment in Resistance to Therapy in AML. *Curr Hematol Malig Rep*. 2015;10(2):96-103.
180. Egea V, Zahler S, Rieth N, et al. Tissue inhibitor of metalloproteinase-1 (TIMP-1) regulates mesenchymal stem cells through let-7f microRNA and Wnt/beta-catenin signaling. *Proc Natl Acad Sci U S A*. 2012;109(6):E309-316.
181. Marquez-Curtis LA, Dobrowsky A, Montano J, et al. Matrix metalloproteinase and tissue inhibitors of metalloproteinase secretion by haematopoietic and stromal precursors and their production in normal and leukemic long-term marrow cultures. Br J Haematol. Vol. 115. England; 2001:595-604.
182. Ciciarello M, Zini R, Rossi L, et al. Extracellular purines promote the differentiation of human bone marrow-derived mesenchymal stem cells to the osteogenic and adipogenic lineages. *Stem Cells Dev*. 2013;22(7):1097-1111.

183. Krivtsov AV, Armstrong SA. MLL translocations, histone modifications and leukaemia stem-cell development. *Nat Rev Cancer*. 2007;7(11):823-833.
184. Muntean AG, Hess JL. The pathogenesis of mixed-lineage leukemia. *Annu Rev Pathol*. 2012;7:283-301.
185. Bonnet D, Dick JE. Human acute myeloid leukemia is organized as a hierarchy that originates from a primitive hematopoietic cell. *Nat Med*. 1997;3(7):730-737.
186. Huntly BJ, Gilliland DG. Cancer biology: summing up cancer stem cells. Nature. Vol. 435. England; 2005:1169-1170.
187. Kreso A, Dick JE. Evolution of the cancer stem cell model. *Cell Stem Cell*. 2014;14(3):275-291.
188. Lapidot T, Sirard C, Vormoor J, et al. A cell initiating human acute myeloid leukaemia after transplantation into SCID mice. *Nature*. 1994;367(6464):645-648.
189. Pollyea DA, Jordan CT. Therapeutic targeting of acute myeloid leukemia stem cells. *Blood*. 2017.
190. Wang Y, He QY, Chiu JF. Dioscin induced activation of p38 MAPK and JNK via mitochondrial pathway in HL-60 cell line. *Eur J Pharmacol*. 2014;735:52-58.
191. Ishikawa F, Yoshida S, Saito Y, et al. Chemotherapy-resistant human AML stem cells home to and engraft within the bone-marrow endosteal region. *Nat Biotechnol*. 2007;25(11):1315-1321.
192. Nombela-Arrieta C, Pivarnik G, Winkel B, et al. Quantitative imaging of haematopoietic stem and progenitor cell localization and hypoxic status in the bone marrow microenvironment. *Nat Cell Biol*. 2013;15(5):533-543.
193. Isern J, Martín-Antonio B, Ghazanfari R, et al. Self-renewing human bone marrow mesenspheres promote hematopoietic stem cell expansion. *Cell Rep*. 2013;3(5):1714-1724.
194. Sharma MB, Limaye LS, Kale VP. Mimicking the functional hematopoietic stem cell niche in vitro: recapitulation of marrow physiology by hydrogel-based three-dimensional cultures of mesenchymal stromal cells. *Haematologica*. 2012;97(5):651-660.
195. Schmitt-Graeff AH, Nitschke R, Zeiser R. The Hematopoietic Niche in Myeloproliferative Neoplasms. *Mediators Inflamm*. 2015;2015:347270.
196. Zhou FL, Zhang WG, Wei YC, et al. Involvement of oxidative stress in the relapse of acute myeloid leukemia. *J Biol Chem*. 2010;285(20):15010-15015.
197. Li L, Li M, Sun C, et al. Altered hematopoietic cell gene expression precedes development of therapy-related myelodysplasia/acute myeloid leukemia and identifies patients at risk. *Cancer Cell*. 2011;20(5):591-605.
198. Testa U, Labbaye C, Castelli G, Pelosi E. Oxidative stress and hypoxia in normal and leukemic stem cells. *Exp Hematol*. 2016;44(7):540-560.
199. Moschoi R, Imbert V, Nebout M, et al. Protective mitochondrial transfer from bone marrow stromal cells to acute myeloid leukemic cells during chemotherapy. *Blood*. 2016;128(2):253-264.
200. Manesia JK, Xu Z, Broekaert D, et al. Highly proliferative primitive fetal liver hematopoietic stem cells are fueled by oxidative metabolic pathways. *Stem Cell Res*. 2015;15(3):715-721.
201. Momparler RL. Optimization of cytarabine (ARA-C) therapy for acute myeloid leukemia. *Exp Hematol Oncol*. 2013;2:20.
202. Sawayama Y, Miyazaki Y, Ando K, et al. Expression of myeloperoxidase enhances the chemosensitivity of leukemia cells through the generation of reactive oxygen species and the nitration of protein. *Leukemia*. 2008;22(5):956-964.
203. Barrera G. Oxidative stress and lipid peroxidation products in cancer progression and therapy. *ISRN Oncol*. 2012;2012:137289.
204. Aon MA, Cortassa S, Maack C, O'Rourke B. Sequential opening of mitochondrial ion channels as a function of glutathione redox thiol status. *J Biol Chem*. 2007;282(30):21889-21900.

205. Asuni AA, Guridi M, Sanchez S, Sadowski MJ. Antioxidant peroxiredoxin 6 protein rescues toxicity due to oxidative stress and cellular hypoxia in vitro, and attenuates prion-related pathology in vivo. *Neurochem Int*. 2015;90:152-165.
206. Starkov AA. Expression of myeloperoxidase enhances the chemosensitivity of leukemia cells through the generation of reactive oxygen species and the nitration of protein. *Ann N Y Acad Sci*. 2008;22(5):956-964.
207. Wang X, Gerdes HH. Transfer of mitochondria via tunneling nanotubes rescues apoptotic PC12 cells. *Cell Death Differ*. 2015;22(7):1181-1191.
208. Breems DA, Blokland EA, Ploemacher RE. Stroma-conditioned media improve expansion of human primitive hematopoietic stem cells and progenitor cells. *Leukemia*. 1997;11(1):142-150.
209. Harvey K, Dzierzak E. Cell-cell contact and anatomical compatibility in stromal cell-mediated HSC support during development. *Stem Cells*. 2004;22(3):253-258.
210. Verfaillie CM. Direct contact between human primitive hematopoietic progenitors and bone marrow stroma is not required for long-term in vitro hematopoiesis. *Blood*. 1992;79(11):2821-2826.
211. de Lima M, McNiece I, Robinson SN, et al. Cord-blood engraftment with ex vivo mesenchymal-cell coculture. *N Engl J Med*. 2012;367(24):2305-2315.
212. Cesarz Z, Tamama K. Spheroid Culture of Mesenchymal Stem Cells. *Stem Cells Int*. 2016;2016:9176357.
213. Basso FG, Turrioni AP, Almeida LF, et al. Nutritional deprivation and LPS exposure as feasible methods for induction of cellular - A methodology to validate for vitro photobiomodulation studies. *J Photochem Photobiol B*. 2016;159:205-210.
214. Sun L, Wang HX, Zhu XJ, et al. Serum deprivation elevates the levels of microvesicles with different size distributions and selectively enriched proteins in human myeloma cells in vitro. *Acta Pharmacol Sin*. 2014;35(3):381-393.
215. Wu CA, Chao Y, Shiah SG, Lin WW. Nutrient deprivation induces the Warburg effect through ROS/AMPK-dependent activation of pyruvate dehydrogenase kinase. *Biochim Biophys Acta*. 2013;1833(5):1147-1156.
216. Xia B, Tian C, Guo S, et al. c-Myc plays part in drug resistance mediated by bone marrow stromal cells in acute myeloid leukemia. *Leuk Res*. 2015;39(1):92-99.
217. Lu CL, Qin L, Liu HC, Candas D, Fan M, Li JJ. Tumor cells switch to mitochondrial oxidative phosphorylation under radiation via mTOR-mediated hexokinase II inhibition--a Warburg-reversing effect. *PLoS One*. 2015;10(3):e0121046.
218. Anastasiou D. Tumour microenvironment factors shaping the cancer metabolism landscape. *Br J Cancer*. 2017;116(3):277-286.
219. Jose C, Bellance N, Rossignol R. Choosing between glycolysis and oxidative phosphorylation: a tumor's dilemma? *Biochim Biophys Acta*. 2011;1807(6):552-561.
220. Li H, Benipal B, Zhou S, et al. Critical role of peroxiredoxin 6 in the repair of peroxidized cell membranes following oxidative stress. *Free Radic Biol Med*. 2015;87:356-365.
221. Sreenivasan Y, Sarkar A, Manna SK. Mechanism of cytosine arabinoside-mediated apoptosis: role of Rel A (p65) dephosphorylation. *Oncogene*. 2003;22(28):4356-4369.
222. Dingjan I, Verboogen DR, Paardekooper LM, et al. Lipid peroxidation causes endosomal antigen release for cross-presentation. *Sci Rep*. 2016;6:22064.
223. Weaver VM, Lelievre S, Lakins JN, et al. beta4 integrin-dependent formation of polarized three-dimensional architecture confers resistance to apoptosis in normal and malignant mammary epithelium. *Cancer Cell*. 2002;2(3):205-216.
224. Shekhar MP, Pauley R, Heppner G. Host microenvironment in breast cancer development: extracellular matrix-stromal cell contribution to neoplastic phenotype of epithelial cells in the breast. *Breast Cancer Res*. 2003;5(3):130-135.

225. Hazlehurst LA, Landowski TH, Dalton WS. Role of the tumor microenvironment in mediating de novo resistance to drugs and physiological mediators of cell death. *Oncogene*. 2003;22(47):7396-7402.
226. Muerkoster S, Wegehenkel K, Arlt A, et al. Tumor stroma interactions induce chemoresistance in pancreatic ductal carcinoma cells involving increased secretion and paracrine effects of nitric oxide and interleukin-1beta. *Cancer Res*. 2004;64(4):1331-1337.
227. Roodhart JM, Daenen LG, Stigter EC, et al. Mesenchymal stem cells induce resistance to chemotherapy through the release of platinum-induced fatty acids. *Cancer Cell*. 2011;20(3):370-383.
228. Chandel NS. Evolution of Mitochondria as Signaling Organelles. *Cell Metab*. 2015;22(2):204-206.
229. Liemburg-Apers DC, Willems PH, Koopman WJ, Grefte S. Interactions between mitochondrial reactive oxygen species and cellular glucose metabolism. *Arch Toxicol*. 2015;89(8):1209-1226.
230. Harris IS, Treloar AE, Inoue S, et al. Glutathione and thioredoxin antioxidant pathways synergize to drive cancer initiation and progression. *Cancer Cell*. 2015;27(2):211-222.
231. Mari M, Morales A, Colell A, Garcia-Ruiz C, Fernandez-Checa JC. Mitochondrial glutathione, a key survival antioxidant. *Antioxid Redox Signal*. 2009;11(11):2685-2700.
232. Halliwell B. Free radicals and antioxidants - quo vadis? *Trends Pharmacol Sci*. 2011;32(3):125-130.
233. Kwon J, Wang A, Burke DJ, et al. Peroxiredoxin 6 (Prdx6) supports NADPH oxidase1 (Nox1)-based superoxide generation and cell migration. *Free Radic Biol Med*. 2016;96:99-115.
234. Kim SY, Chun E, Lee KY. Phospholipase A(2) of peroxiredoxin 6 has a critical role in tumor necrosis factor-induced apoptosis. *Cell Death Differ*. 2011;18(10):1573-1583.
235. Savaskan NE, Ufer C, Kuhn H, Borchert A. Molecular biology of glutathione peroxidase 4: from genomic structure to developmental expression and neural function. *Biol Chem*. 2007;388(10):1007-1017.
236. Matsushita M, Freigang S, Schneider C, Conrad M, Bornkamm GW, Kopf M. T cell lipid peroxidation induces ferroptosis and prevents immunity to infection. *J Exp Med*. 2015;212(4):555-568.
237. Lin HY, Liou CW, Chen SD, et al. Mitochondrial transfer from Wharton's jelly-derived mesenchymal stem cells to mitochondria-defective cells recaptures impaired mitochondrial function. *Mitochondrion*. 2015;22:31-44.
238. Pasquier J, Guerrouahen BS, Al Thawadi H, et al. Preferential transfer of mitochondria from endothelial to cancer cells through tunneling nanotubes modulates chemoresistance. *J Transl Med*. 2013;11:94.
239. Kuznetsov AV, Troppmair J, Sucher R, Hermann M, Saks V, Margreiter R. Mitochondrial subpopulations and heterogeneity revealed by confocal imaging: possible physiological role? *Biochim Biophys Acta*. 2006;1757(5-6):686-691.
240. Pajtler K, Bohrer A, Maurer J, et al. Production of chick embryo extract for the cultivation of murine neural crest stem cells. *J Vis Exp*. 2010(45).
241. Nicholls DG, Darley-Usmar VM, Wu M, Jensen PB, Rogers GW, Ferrick DA. Bioenergetic profile experiment using C2C12 myoblast cells. *J Vis Exp*. 2010(46).